TOXICITY EVALUATION OF PLASTIC NANOPARTICLES ON AQUATIC ORGANISMS

Done is better than perfect!

Abstract

Plastics are an immense family of unique and versatile materials which play an essential role in modern society and are an indispensable part of our daily lives. With a global production of nearly 440 million tons in 2019, plastic waste has been described to accumulate virtually in any environment, from marine to freshwater ecosystems. The irreversibility and global ubiquity of marine plastic pollution has turned plastics into a potential planetary boundary threat. Nanoplastics (NPs) represent the smallest fraction of plastic litter and can result in the environment as the degradation products of larger plastic items. Nevertheless, only recently such particles have been detected in real environments, albeit not yet accurately quantified. As evidenced in Chapter 1, although today there is still a lack of clarity as regards their toxicological effects, the high exposure potential, together with the physical and chemical heterogeneity of NPs, the likely significant diffusive release of plastic additives and adsorbed substances, combined with their small size and enhanced accessibility to biological tissues, potentially make NPs highly hazardous pollutants. Ecological risk assessment of nanoplastics is urgently needed. In the absence of reliable environmental exposure estimates to date, ecotoxicological research has focused on defining a hazard assessment of NPs. This thesis aimed at investigating the mechanism of toxicity of NPs, taking advantage of high-throughput sequencing technologies. In an initial experiment, described in Chapter 2, adult specimens of the freshwater benthic crayfish *Procambarus clarkii* were exposed to 100 μg of 100 nm carboxylated polystyrene nanoparticles (PS NPs) in a 72h dietary exposure experiment. The cosmopolitan red swamp crayfish *P. clarkii* is widely used as bioindicator of environmental pollution and was selected here as a representative non-model decapod of the freshwater ecosystem. An integrated approach was conceived to assess the biological effects of polystyrene NPs, by analyzing both transcriptomic and physiological responses. Total hemocyte counts, basal and total phenoloxidase activities, glycemia and total protein concentration were investigated in crayfish hemolymph at 0h, 24h, 48h and 72h to evaluate general stress response over time. Transcriptomes of hemocytes and hepatopancreas were analyzed after 72h. At the physiological level, crayfish were able to compensate for the induced stress by not exceeding the generic stress thresholds. The RNA-Sequencing analysis revealed the altered expression of few genes involved in immune response, oxidative stress, gene transcription and translation, protein degradation, lipid metabolism, oxygen demand, and reproduction in *P. clarkii* exposed to NPs. Activation of oxidative stress pathways and inflammatory responses has been widely recognized as primary molecular mechanisms of NP-induced toxicity, in agreement with our

findings. In particular, we noted an alteration of several genes related to the ubiquitin-proteasome system, one of the major degradation pathways for maintaining cellular protein homeostasis, which has not been described before. Moreover, a rather clear transcriptomic response to NPs emerged as a strong downregulation of vitellogenin expression in the hepatopancreas of female crayfish, which may indicate a shift in energy allocation induced by plastic exposure from reproduction to organism maintenance, as previously advocated. This finding may provide the basis for a deeper exploration of the potential population-level effects of nanosized polystyrene particles. Overall, this study suggests that a low concentration of PS NPs may induce mild stress in crayfish, and sheds light on molecular pathways possibly involved in nanoplastic toxicity. In Chapter 3 we examined the underlying mechanism of NPs toxicity in a sensitive early developmental stage of a key marine invertebrate species, the bivalve *Mytilus galloprovincialis*. The Mediterranean mussel is a widely used species in ecotoxicological studies. This work integrated and complemented a previous study by Balbi and colleagues from the University of Genova. *M. galloprovincialis* fertilized eggs were exposed for 24h to 50 nm amino-modified polystyrene nanoplastics at concentration close to EC50 (0.150 mg/L), to investigate their expression profiles during early embryo development. Illumina RNA-sequencing was applied to assemble the first *de novo* transcriptome for *M. galloprovincialis* in the trocophora larval stage (24 hours post fertilization). The transcriptome shows high quality and a good proportion of accurately functionally annotated sequences, thus providing a valuable scientific resource for future studies on the early larval stages of this bivalve species. Nevertheless, exposure to amino-modified PS NPs did not cause noticeable shifts in the overall gene expression profile of the exposed larvae, as shown by differential gene expression analysis. A possible explanation for this result is a dilution effect of the transcriptomic responses due to the pooling of more than 7000 individual larvae in each analyzed sample. Otherwise, the early life stage of trocophora may not represent the most sensitive phase of mussel larval development, but the transition from the trocophora stage to the first D-shelled larva might represent a more sensitive step to abiotic stressors. In conclusion, we report that after the exposure to relatively low concentrations of NPs, crayfish were able to compensate the induced stress not exceeding generic stress thresholds. At a transcriptomic level, mussel larvae and crayfish did not show substantial changes in the gene expression profiles. Still some specific biological pathways related to NPs stress response in crayfish have been identified. The work done in this thesis furthers the current understanding of the toxicological hazard posed by NPs. RNA-Sequencing has proven to be a powerful tool to better elucidate the molecular pathways underlying nanoplastic toxicity.

Table of contents

Abstract ..... **I**

Chapter 1. General Introduction **1**

1.1 Plastic pollution 1

1.2 Plastic fate in the environment 2

1.3 A focus on nanoplastics: an emerging field of research 5

1.4 Plastic toxicity 7

1.5 NGS technology 9

1.6 Thesis aims and structure 10

Chapter 2. Physiological and transcriptomic responses of red swamp crayfish (*Procambarus clarkii*) to orally administered nano-sized polystyrene **12**

2.1 Introduction 12

2.2 Materials and methods 15

2.2.1. Animal collection and housing conditions 15

2.2.2. Polystyrene nanoplastics characterization 15

2.2.3. Nanoplastic Supplemented Food 16

2.2.4. Feeding assay 17

2.2.5. Sample collection 17

2.2.6. General stress parameters 17

2.2.7. Transcriptomic analysis 18

2.2.8. Statistical analysis 21

2.3 Results 22

2.3.1. Particle characterization 23

2.3.2. Physiological biomarkers 23

2.3.3. Transcriptomic response of *P clarkii* to nanoplastic exposure 26

2.4 Discussion 29

2.4.1. Physiological biomarkers 29

2.4.2. Transcriptomic analysis 31

2.5 Conclusions 41

Chapter 3. Evaluation of nanoplastic toxicity on Mediterranean mussel (*Mytilus galloprovincialis*) larvae: an RNA Sequencing approach **43**

3.1 Introduction 43

3.2 Materials and methods 45

3.2.1. Embryotoxicity test 45

3.2.2. Library generation and Illumina de novo sequencing 46
3.2.3. Bioinformatic analysis 47
3.3 Results 51
3.3.1. RNA sequencing results 51
3.3.2. *De novo* transcriptome assembly annotation, and refinement 51
3.3.3. Analysis of differentially expressed genes (DEGs) 53
3.4 Discussion 55
3.5 Conclusions 57
Chapter 4. Concluding remarks and future outlooks 59

References 62
List of Figures 97
List of Tables 98
Acknowledgements 99
List of scientific publications 100

Appendix 101

Chapter 1
General Introduction

1.1. Plastic pollution

About 100 years ago, the german scientist and Nobel Prize laureate Hermann Staudinger laid the foundation for modern polymer science with his paper "Über Polymerisation" (Staudinger, 1920). Since then, the world has witnessed a rapid growth of the plastics industry, so that today it directly employs more than 1.56 million people in Europe and generates a turnover of more than 350 billion euros in 2019, bringing undeniable societal benefits (PlasticsEurope, 2020). By far the largest end-use markets in Europe are packaging and building and construction, followed by automotive (PlasticsEurope, 2020). It is therefore evident that plastic products play an essential role in modern society and are an indispensable part of our daily lives. With a steadily growing trend, global plastics production reached nearly 440 million tonnes (Mt) in 2019, including 370 Mt of polymer resins (PlasticsEurope, 2020) and 70 Mt of synthetic fibers, which accounted for about 63% of the global fiber production in 2019 (Textile Exchanges, 2020). While much attention has been paid in recent years to promoting a more circular and sustainable plastics system in terms of reuse, recycling, proper waste management and the use of renewable raw materials, there are still environmental and climate challenges associated with the production, use and disposal of the different types of plastics (Fogh Mortensen et al., 2021; Lau et al., 2020; PlasticsEurope, 2020). Among others, the leakage of plastics into the environment is undoubtedly a global problem (EFSA CONTAM Panel, 2016; GESAMP, 2016, 2015; Koelmans et al., 2017a; Lusher et al., 2017; SAPEA, 2019). Plastics are an immense family of unique and versatile materials. Overall, thermoplastic polymers are the most commonly produced polymers, with polyolefins (polyethylene, PE, and polypropylene, PP) mainly used for food packaging, reusable bags, trays and containers, accounting for almost 50% of total plastics demand in Europe (PlasticsEurope, 2020). Thermoplastics, which include polystyrene (PS), polyvinyl chloride (PVC), polyethylene terephthalate (PET) and polyurethane (PU), in addition to PE and PP (SAPEA, 2019), were among the most common types of plastics polluting the aquatic and terrestrial environments (Erni-Cassola et al., 2019; Horton et al., 2017a; Klein et al., 2015; Llorca et al., 2021; Mani et al., 2015; Piehl et al., 2019; Suaria et al., 2016; Ter Halle et al., 2017; Yang et al., 2021). It is estimated that globally, approximately 4.8 – 12.7 Mt of macroplastic are released into the oceans each year through mismanaged waste

from coastal populations (Jambeck et al., 2015), while an additional plastic input of 0.79 – 1.52 Mt per year flows into the ocean from inland areas via rivers (Lebreton et al., 2017). Losses of primary microplastics into the natural environment are in the order of 1.8 – 5.0 Mt per year, with 0.8 – 2.5 Mt entering the oceans (Boucher and Friot, 2017). The irreversibility and global ubiquity of marine plastic pollution make plastics a potential planetary boundary threat (Nash et al., 2017; Rockström et al., 2009; Villarrubia-Gómez et al., 2018). However, as land-based sources are considered the primary input of plastics to the oceans (Boucher and Friot, 2017; GESAMP, 2015), both terrestrial and freshwater environments are in turn exposed to extensive plastic pollution, resulting from agricultural practices (sewage sludge application, plastic mulching, irrigation and flooding), wastewater discharges from households (synthetic fibers from clothes washing and microparticles from personal care products), urban runoff (including car tires abrasion), industrial origins in the form of spilled plastic resin powders or pellets, atmospheric deposition, and fragmentation of larger plastic debris from general littering (Bläsing and Amelung, 2018; Boucher and Friot, 2017; Eerkes-Medrano et al., 2015; González-Fernández et al., 2021; Horton et al., 2017b; Hurley and Nizzetto, 2018). At the global scale, the annual rate of plastics entering aquatic systems from land is estimated to increase 2.6-fold from 2016 to 2040, while the rate of plastic waste retained in terrestrial systems is estimated to increase 2.8-fold (Lau et al., 2020), ultimately leading to potentially about 12,000 Mt of plastic waste accumulating in landfills or the natural environment by 2050 (Geyer et al., 2017). Immediate and concerted action based on current knowledge and technologies could reverse the increasing trend of plastic pollution and reduce it by more than 75% in 2040 compared to a business-as-usual scenario (Finnegan and Gouramanis, 2021; Lau et al., 2020). However, given the long degradation times of this material, even such a significant reduction in pollution rates is expected to result in a cumulative 710 Mt of plastic waste entering aquatic and terrestrial ecosystems over the same period (Lau et al., 2020). This amount cannot be avoided unless circular business models, changing consumption patterns and policies are adopted and further innovations are implemented (Fogh Mortensen et al., 2021; González-Fernández et al., 2021).

1.2. Plastic fate in the environment

Plastics comprise any polymeric material composed by hundreds or thousands of monomeric subunits linked by covalent bonds. Additional substances such as plasticizers, flame retardants, fillers, light and heat stabilizers, or pigments may be added, accounting for about 7% of non-fiber plastics by mass (Geyer, 2020), to achieve the desired strength, permeability, and color and/or to reduce cost (Vert et al., 2012). The highly desirable properties of plastics, i.e.,

durability, flexibility, and resistance to degradation, make these materials highly threatening from an environmental perspective. Once intentionally or accidentally released into the environment, plastics tend to accumulate. Plastic items of various shapes and sizes have been found virtually in every habitat. Plastics have been observed in many different domains of the marine system (Erni-Cassola et al., 2019), including near the surface (Suaria et al., 2016; Ter Halle et al., 2017), with particular attention to the so-called ocean garbage patches in the subtropical gyres (Cózar et al., 2014; Lebreton et al., 2012), and in the underlying water column (Baini et al., 2018; Egger et al., 2020; Kooi et al., 2016). It is estimated that in the Great Pacific Garbage Patch alone, at least 79 thousand tonnes of plastic are floating in an area of 1.6 million km^2 (Lebreton et al., 2018). Plastic has been described to accumulate both in deep-sea sediments (Jamieson et al., 2019; Kane et al., 2020; Krause et al., 2020; Sanchez-Vidal et al., 2018; Taylor et al., 2016; Van Cauwenberghe et al., 2013; Woodall et al., 2014) and nearshore sandy beaches (Browne et al., 2011; Vlachogianni et al., 2020). In freshwater environments, plastic pollution has been reported in surface waters (Atwood et al., 2019; González-Fernández et al., 2021; Horton et al., 2017b; Klein et al., 2018; Lechner et al., 2014; Llorca et al., 2021; Mani et al., 2015; Sighicelli et al., 2018) and sediments of rivers and lakes (Boyle and Örmeci, 2020; Horton et al., 2017a; Hurley et al., 2018; Klein et al., 2015; Leslie et al., 2017; Piehl et al., 2019). Recently, scientific attention has turned to terrestrial systems, where soil appears to be an important long-term sink for plastic debris (Wahl et al., 2021; Yang et al., 2021) and the presence of airborne microplastic pollution, both indoors and outdoors, has been noted (Vianello et al., 2019; Wright et al., 2020). Finally, plastic pollution also affects remote and supposedly pristine areas, such as polar ecosystems (Obbard, 2018; Rowlands et al., 2021) and alpine snow (Bergmann et al., 2019). The occurrence of plastic particles has been reported in the water column (Cincinelli et al., 2017; Cózar et al., 2017; Isobe et al., 2017; Jones-Williams et al., 2020; Lacerda et al., 2019; Lusher et al., 2015), seafloor (Bergmann et al., 2017; Munari et al., 2017; Reed et al., 2018) and sea-ice (Kelly et al., 2020; Peeken et al., 2018) in both the Arctic and Antarctic, which is of particular concern due to the specificity and sensitivity of these ecosystems. With prolonged exposure to environmental factors, such as mechanical abrasion, moisture, elevated temperature, UV radiation, or microbial activity, they can undergo weathering through abiotic and/or biotic processes. The former include physical degradation, which refers to changes in bulk structure, such as cracking, embrittlement and flaking, or chemical degradation, namely changes at the molecular level (Chamas et al., 2020). Photodegradation and photo-initiated oxidation by solar UV radiation are the main mechanisms of initialization of polymer degradation under environmental conditions. Less commonly, the

molecular breakdown can also be initiated thermally or hydrolytically (Gabbott et al., 2020). Photooxidation leads to the cleavage of carbon-hydrogen bonds, followed by the formation of free radicals along the polymer chains. These radicals can react with oxygen to form peroxy radicals, which catalyze the process and promote autoxidation (Gewert et al., 2015). The photo-initiated oxidative degradation leads to a decrease in the molecular weight of the polymers and increases the hydrophilicity of the chain due to the formation of oxygen-containing functional groups at the chain ends (Gewert et al., 2015). The resulting smaller polymer fragments are more susceptible to microbial biodegradation by extracellular and intracellular depolymerases (Gabbott et al., 2020). Currently, over 400 microbial species, belonging to five bacterial and three fungal phyla, have been reported to have plastic-degrading capabilities (Gambarini et al., 2021). However, for most of the conventional high molecular weight polymers, including PP, PS, PE, nylon, and PVC, evidence of microbial degradation remains limited and extensive further data are required (Jacquin et al., 2019; Lear et al., 2021). Even when evidence is provided, such as for PET (Danso et al., 2019; Yoshida et al., 2016), it is currently controversial whether and to what extent such microbial mineralization processes function in real natural environments and/or contribute significantly to plastic removal (Andrady A. L., 2015; Gabbott et al., 2020; Gambarini et al., 2021; Lear et al., 2021). In general, the degradation rates of plastics are extremely low and the effectiveness of these biotic and abiotic processes depends on several factors involving both the properties of the polymer and the environment (Andrady A. L., 2015). Important intrinsic characteristics include the nature of the polymer backbone - i.e., homo- (e.g., PE, PP, PS) and or hetero- (e.g., PET, PU) chain -, the presence and nature of functional groups, crystallinity, molecular weight, and surface- to- volume ratio. For example, long polyolefins such as PE, PP and PS, characterized by high molecular weight and absence of functional groups, are considered inert and exhibit limited degradation (Gewert et al., 2015). Moreover, antioxidants and stabilizers used as additives in commercial plastics, enhance resistance towards degradation (Chamas et al., 2020). Besides, environmental factors that may accelerate or inhibit the degradation processes need to be considered. In landfill or soil environments, plastics may be buried in anoxic sediments in the absence of UV light and oxygen, resulting in a drastic reduction in the rate of degradation. In other situations, plastics exposed to sunlight on land may experience “heat buildup”, reaching higher temperatures than ambient air, resulting in accelerated degradation (Andrady A. L., 2015; Chamas et al., 2020). In aquatic environments, biofouling can hinder the rate of photodegradation by reducing sunlight penetration, and also increase the overall density of plastic pieces, causing them to sink (Chamas et al., 2020; Koelmans et al., 2017b; Kooi et al., 2017).

1.3. A focus on nanoplastics: an emerging field of research

Plastics in the environment are commonly classified as macro-, meso-, micro-, and nanoplastics, although these terms are not yet uniformly defined and used. Macroplastics are generally defined as plastic particles larger than 2.5 cm, while mesoplastics fall in the range between 5 mm and 2.5 cm (González-Fernández et al., 2021). Particles smaller than 5 mm are addressed as microplastics (MPs) (Arthur et al., 2009; Frias and Nash, 2019; MSFD Technical Subgroup on Marine Litter, 2013; Thompson et al., 2004). Nanoplastics (NPs) represent the smallest fraction of plastic litter and are referred to as particles under 1 µm (Gigault et al., 2018; Pinto da Costa et al., 2016) or 100 nm (Alimi et al., 2018; Besseling et al., 2019; EFSA CONTAM Panel, 2016; Koelmans et al., 2015) in size. Recently, scientists agreed on the need to rely on particle properties to define a nanoplastic, rather than arbitrary size cutoffs as in engineered nanomaterials (ENMs), and provided specific defining characteristics for NPs (Gigault et al., 2021; Mitrano et al., 2021). ENMs are intentionally designed and manufactured for specific applications, processes or products with particle sizes between 1 and 100 nm in at least one dimension (European Commission, 2011). Therefore, they usually have a uniform composition and their properties are known (Gigault et al., 2021). On the other hand, NPs can enter the environment directly from household products (Hernandez et al., 2019, 2017) but are most likely to be formed incidentally during the degradation of larger plastic items (Ekvall et al., 2019; Gigault et al., 2016; Lambert and Wagner, 2016; Wahl et al., 2021). In laboratory conditions, secondary plastic nanoparticles have been shown to be released from mechanical breakdown of disposable polystyrene coffee cup lids (Ekvall et al., 2019; Lambert and Wagner, 2016), UV degradation of recovered marine microplastic litter (Gigault et al., 2016) and from shear stress exposure of MPs extracted from a commercial facial scrub (Enfrin et al., 2020). Additionally, these particulates may be unintentionally discharged in the environment by manufacturing processes (Stephens et al., 2013; H. Zhang et al., 2012). Noteworthy, a recent article demonstrated for the first time the natural occurring formation of 20-150 nm particles of common plastic polymers (PE, PS and PVC) in the soil matrix of a contaminated agricultural field, as a result of the breakdown of larger plastic items (Wahl et al., 2021). Thereby, nanoplastics are highly heterogeneous in their composition and physical properties depending on both the origin of the material and the pathway to its formation (Gigault et al., 2016; Lambert and Wagner, 2016; Ter Halle et al., 2017; Wahl et al., 2021), making tracking and quantifying these particles in complex environments challenging. Nanoplastics own some peculiar characteristics that distinguish them from MPs . The breakup of original bulk plastic into NPs

increases the exposed surface area, which leads to an increased sorption capacity of inorganic and organic contaminants (Alimi et al., 2018; Liu et al., 2016; Mitrano et al., 2021). In addition, the leaching rates of additives from NPs are predicted to be much larger than the leaching rate from MPs due to their smaller dimensions (Gigault et al., 2021). Moreover, the higher surface-to-volume ratio of NPs compared to MPs results in the higher relative importance of surface interactions compared to physical interactions (Gigault et al., 2021; Song et al., 2019; Tallec et al., 2019). Unlike at the macro- and micro- scales, where the dispersion of particles in a suspension medium is mainly regulated by buoyancy and sedimentation properties directly correlated to their density and shape, at the nanoscale, colloidal particles diffuse in the solution, in a constant random motion called Brownian motion (Hassan et al., 2015). At this scale, interactions and collisions with other particles and molecules prevail and can prevent particles' sedimentation (Gigault et al., 2018). Although our understanding of the behavior of nanoplastics in natural systems is still in its infancy, it is reasonable to assume that NPs, like other colloids, commonly form heteroaggregates with other natural and/or anthropogenic materials (Frehland et al., 2020; Hüffer et al., 2017; Singh et al., 2019). MPs have been referred to as plastisphere and described as a new man-made ecosystem capable of harboring a community of microorganisms while developing complex biofilms (Amaral-Zettler et al., 2020; Zettler et al., 2013). Although biofouling can influence environmental fate by altering the hydrophobicity and density of the microplastic (Kooi et al., 2017), the plastic core still makes up the largest portion of the total particle (Gigault et al., 2021). On the other hand, since NPs are smaller than most microorganisms, they might ultimately represent smaller components of a larger complex consisting of the NP coated with biomolecules from the surrounding environment – i.e. the protein corona – and sorbed microorganisms (Cedervall et al., 2007; Fadare et al., 2020). The fate of these heteroaggregates might not have a strong dependence on the intrinsic properties of the plastic (Gigault et al., 2021).

Recent works indicated the presence of nanoplastics in seawater of the North Atlantic subtropical gyre (Ter Halle et al., 2017) and agricultural soil enriched with plastic waste (Wahl et al., 2021). Nevertheless, nanoplastics in natural environmental samples remain largely unquantified due to methodological limitations (Pinto da Costa et al., 2019; Renner et al., 2018). The numerical abundance of NPs is predicted to potentially reach concentrations 17 orders of magnitude higher than microplastic particle concentrations (Besseling et al., 2019). These estimates raised concerns about the potential impact of plastic particles on biota, especially considering that NPs approaching the size of natural proteins may be small enough to be

uptaken, translocated and transported across biological membranes (Al-Sid-Cheikh et al., 2018; Gigault et al., 2021). The high exposure potential, along with the physical and chemical heterogeneity of NPs compared to ENMs, the likely consistent diffusive release of plastic additives and adsorbed substances, combined with the increased bioavailability of NPs and enhanced accessibility to tissues, present us with unique considerations and challenges and raise further concerns about the potential hazard posed by NPs (Gigault et al., 2021; Mitrano et al., 2021).

1.4. Plastic toxicity

Social and scientific awareness of plastic pollution has developed over the past decade as research on the issue boomed and policy makers recognized it as a primary environmental problem (Rochman et al., 2013). Most importantly, the persistence and pervasiveness of plastic pollution have attracted scientific attention, such that marine plastics have recently been identified as a potential planetary boundary threat (Villarrubia-Gómez et al., 2018). The crucial question, still unanswered, is whether ocean plastic concentration today or in the future reaches a level capable of causing shifts in Earth-system functioning (Villarrubia-Gómez et al., 2018). Although there is considerable evidence of the induced effects of plastic litter at organismic and sub-organismic levels, ecological risk assessments are still challenging as the pathway and spatial and temporal patterns of exposure of organisms and habitats in nature remain poorly understood (Browne et al., 2015; Koelmans et al., 2017a; Rochman et al., 2016). Available preliminary risk assessments found no immediate risk to the freshwater or marine environment from MPs (Adam et al., 2019; Everaert et al., 2018). Nevertheless, the authors point out that negative ecological impacts are to be expected in highly polluted areas and when considering future scenarios with increasing MP concentrations, and call for further research and improved analytical methods to quantify MPs and NPs in nature.

There is a growing body of peer-reviewed literature addressing the question of whether MP and NP cause toxicity to organisms and, if so, what are the main causes of that toxicity. To date, over 900 marine species have been observed interacting with plastic pollution (Gall and Thompson, 2015; Kühn and van Franeker, 2020), from marine megafauna to fish and invertebrates. Marine organisms may eventually suffer lethal and sub-lethal harm, including drowning, starvation, physical injury, reduced mobility, and physiological stress due to entanglement or ingestion (Browne et al., 2015; Senko et al., 2020). Under laboratory conditions, MPs and NPs caused mortality (Gray and Weinstein, 2017; Jemec et al., 2016),

reduced feeding capacity (Cole et al., 2019, 2015; Coppock et al., 2019; Watts et al., 2015; Welden and Cowie, 2016; Wright et al., 2013), reduced growth (Besseling et al., 2014; Redondo-Hasselerharm et al., 2018), behavioral and histopathological changes (Brun et al., 2019; Cedervall et al., 2012; Chae et al., 2018; Limonta et al., 2019) and impaired reproduction (Jeong et al., 2016; Sussarellu et al., 2016; W. Zhang et al., 2020). However, the hazard assessment outcomes from different studies are variable and sometimes contradictory, which is likely due to the lack of a standardized research methodology, the use of different research models including marine, freshwater, and terrestrial vertebrates and invertebrates, and last but not least, the high heterogeneity of the particles themselves (different size, shape, surface charge, and polymer type) (Hu and Palić, 2020). To address the limitation of MP and NP toxicology research, the implementation of a mechanism-based approach, such as Adverse Outcome Pathway (AOP), may be useful in an effort to organize and link information about detected effects from the molecular level of a biological system to an apical endpoint of perturbation, (Ankley et al., 2010; Galloway et al., 2017). An AOP primarily support hazard identification and is defined as a sequence of events linking a molecular initiating event (MIE) to one or more adverse outcomes (AO), i.e., the classic organismic or population level apical endpoints used for hazard evaluation and risk assessment, progressing through a series of key events (KE) occurring at more complex levels of biological organization (Leist et al., 2017). Recently, several authors have tried to define MP and NP AOPs (Galloway and Lewis, 2016; Hu and Palić, 2020; Jeong and Choi, 2019; Liu et al., 2021b). The constructed AOP based on literature analysis revealed that MPs and NPs both share the formation of reactive oxygen species (ROS) as their MIE. The MPs most prominent AOs were identified in increasing mortality, decreasing rates of growth, and reproduction failure (Jeong and Choi, 2019). On the other side, the NPs AOP indicate that at the ecosystem level, NPs could cause toxicity through the activation of oxidative stress pathways, followed by inflammatory responses (cytokine production), mitochondrial dysfunction, lysosome disruption, lipid peroxidation and acetylcholinesterase inhibition, that in turn would further induce inflammation and neuronal dysfunction leading to behavior alterations and impaired development and growth (Hu and Palić, 2020). In a recent paper, the AOP approach was applied to whole-body proteomics data obtained from the exposure of the cladoceran *Daphnia pulex* to polystyrene nanoplastics (0.1 – 2 mg/L) for 21 days, which were further confirmed at the molecular and biochemical levels (Liu et al., 2021b). The obtained AOP scheme confirmed ROS production as a molecular initiating event and identified growth inhibition and decrease in reproductive output as AOs. In addition, alterations in specific signaling pathways, changes in the metabolism of glutathione,

protein, lipids and molting proteins are proposed as intermediate KE (Liu et al., 2021b). This study highlights the potential of omic-based data in the establishment of AOPs. In this respect, compared to other omic areas, such as proteomics and metabolomics, transcriptomics allows to gather a wealth of data in a high-throughput, user-friendly, and relatively cheap way and can therefore play an important role in the application of the AOP (Vinken, 2019). Transcriptomic data can play a dual role in the field of AOP: (i) they can define molecular initiating events and key events; (ii) and they can provide a set of biomarkers eligible for toxicity testing and hazard identification (Vinken, 2019). Transcriptomic profiles thereby serve as first-level identifiers of chemical hazard and can be followed up by more specific single-target tests (Vinken, 2019). In line with that, a rapidly growing body of omic data on MPs and NPs is available in literature, aiming at providing a detailed description of the cellular pathways underlying plastic particles toxicity and detoxification (Gu et al., 2020; W. Liu et al., 2020; Liu et al., 2021a; Magni et al., 2019; W. Zhang et al., 2020).

1.5. NGS technology

Ecotoxicogenomics represents a relatively new field of research, which is based on the application of classical toxicogenomics – that is, the study of gene, protein or metabolite expression profiles of organisms, tissues or cells in response to a chemical or physical stressor – to organisms representative of ecosystems and is used to study the adverse effects of chemicals on individuals and on their ecosystems (Snape et al., 2004). Ecotoxicogenomics thus integrate omic technologies (transcriptomics, proteomics, and metabolomics) and ecotoxicology and is defined as “the study of gene and protein expression in non-target organisms that is important in responses to environmental toxicant exposures” (Snape et al., 2004). The most powerful application of ecotoxicogenomic tools is ecological risk assessment, where they can provide us with a better mechanistic understanding of the molecular mechanisms triggered by toxic substances (Prat and Degli-Esposti, 2019). The use of Next Generation Sequencing (NGS) in environmental science has enormous potential but is still in its infancy (Prat and Degli-Esposti, 2019). NGS is a collective term for various sequencing technologies such as Illumina/Solexa, Roche 454, or Ion Torrent, which are able to produce an enormous amount of DNA and RNA (more precisely cDNA) sequencing data much more efficiently than the older Sanger sequencing technology (Goodwin et al., 2016; Metzker, 2010). Sequencing of short cDNA molecules (RNA sequencing, RNA-Seq) has been shown to be a rapid and reliable method for qualitatively and quantitatively determining RNA expression levels and is a powerful tool for deciphering the molecular mechanisms triggered by exposure

to one or more stressors behind the physiological disturbances observed by classical methods (Wang et al., 2009). RNA-Seq is particularly useful when considering non-model species with environmental relevance. Indeed, it allows differential gene expression and evolutionary studies without the need for prior suitable genomic resources, as RNA-Seq data can be used to reconstruct and quantify entire transcriptomes simultaneously (Prat and Degli-Esposti, 2019). As discussed in paragraph 1.4, RNA-Seq, or transcriptomics, can provide valuable information on the mechanisms of toxicity of one or more compounds in the frame of the AOP approach (Prat and Degli-Esposti, 2019). Omic sciences, an in particular RNA-Seq analysis, has recently gained much attention in the field of MPs and NPs. In a series of recent publications, transcriptomic analyses have been performed to integrate phenotypic responses, such as physiological and behavioral changes, in model (Coady et al., 2020; Limonta et al., 2019; Liu et al., 2021a; Pang et al., 2021; Pedersen et al., 2020b; Veneman et al., 2017; W. Zhang et al., 2020; Zhao et al., 2020) and non-model species (Gardon et al., 2020; Jeong et al., 2021). These initial investigations highlighted the potential of multidimensional characterization of NP impacts on human and animal health by the use of an integrated approach at different levels of biological organization.

1.6. Thesis aims and structure

At the time of the beginning of this thesis, the research field of nanoplastics was still in its infancy and since then the science has advanced rapidly. However, it is still unclear to what extent micro- and especially nanoplastic particles pose a risk to terrestrial and aquatic life (Chapter 1). Among the many uncertainties related to the toxicology of MP and NP, this work aimed to investigate the toxicity of NPs at molecular level by using a high-throughput sequencing approach. Indeed, linking the effects of contaminants from lower to higher levels of biological organization is critical for integrating, assessing, interpreting, and predicting effects on populations and ecosystems. In particular, the aim of this work was to evaluate the efficacy of using the reliable, rapid, and cost-effective approach of transcriptomics, also in combination with other phenotypic endpoints, to study the toxicity of plastic nanoparticles.

To address this goal, two case studies are presented in Chapters 2 and 3 of this thesis. Two different invertebrate species were selected for these studies: the red swamp crayfish (*Procambarus clarkii*, Girard, 1852), a benthic freshwater decapod crustacean, and a key marine bivalve species, the Mediterranean mussel (*Mytilus galloprovincialis*, Lamarck, 1819). These two species have long been used as bioindicators of pollution in freshwater and marine

ecosystems, respectively, given their widespread distribution, high tolerance to polluted environments, sedentary lifestyles, and ecological and economic importance. Invertebrates share with mammals general mechanisms of innate immunity, which makes them relevant test organisms for studying common biological responses to environmental contaminants, including NPs (Canesi and Procházková, 2013). In addition, the heterogeneity of invertebrate species and their crucial role in different environments, as well as the potential transfer of nanoparticles through the food chain, increase the significance of using these organisms for obtaining reproducible and reliable data on the environmental effects of nanoparticles (Baun et al., 2008; Canesi and Procházková, 2013). Most of the current literature on MP and NP focuses on assessing the threat of plastic pollution to the marine environment, while freshwater systems receive little attention. Actually, it has been documented that MPs are ubiquitous in waters and sediments of rivers and lakes around the world and that riverine systems can act as a primary influx of MPs into the oceans as well as long-term storage for plastics. Furthermore, the available ecotoxicological data, particularly those from ecotoxicogenomics, are mainly representative of model species, while ecologically relevant species, such as freshwater decapods, have received less attention. Within this framework, Chapter 2 addresses the toxicological response to NPs in a freshwater non-model species. The red swamp crayfish, an invasive species capable of tolerating highly perturbed environments and potentially highly exposed to plastic particle ingestion in light of its generalist and opportunistic feeding habits (Gherardi, 2006; Lv et al., 2019; Zhang et al., 2020), was exposed to a relatively low concentration of NPs in a 72 hours dietary experiment. An integrated approach was conceived to assess the biological effects of PS NPs, by analyzing both transcriptomic and physiological responses. In Chapter 3 the underlying mechanisms of toxicity of NPs were investigated in the sensitive early developmental stage of the bivalve *M. galloprovincialis*. Indeed, several studies on the biological impact of NPs on marine invertebrates have recognized larvae as valid tools for studies on developmental disorders induced by different types of nanoparticles or environmental perturbations. In the final chapter of the thesis, a summary and general discussion of the main results of the work are given.

Chapter 2

Physiological and transcriptomic responses of red swamp crayfish (*Procambarus clarkii*) to orally administered nano-sized polystyrene

This chapter is adapted from: Capanni, F., Greco, S., Tomasi, N., Giulianini, P.G., Manfrin, C., 2021. Orally administered nano-polystyrene caused vitellogenin alteration and oxidative stress in the red swamp crayfish (*Procambarus clarkii*). Sci. Total Environ. 791, 147984. https://doi.org/10.1016/j.scitotenv.2021.147984

2.1. Introduction

Plastic pollution has been recognized as a severe human pressure on aquatic ecosystems and a major water quality problem (Koelmans et al., 2015; Rochman et al., 2013; Wagner et al., 2014). With the growing global population and without waste management infrastructure improvements, the cumulative amount of plastic waste possibly discharged in the ocean from land is predicted to increase in the future (Jambeck et al., 2015). To date, the bulk of MP and NP research efforts have been focused on the marine environment, with global oceans considered as the ultimate sink for contamination (Eerkes-Medrano et al., 2015; Lambert and Wagner, 2018; Wagner et al., 2014). Nevertheless, given that most of the plastic is used and disposed of on land, both terrestrial and freshwater environments can be subject to plastic pollution, including then act as long-term reservoirs (Horton et al., 2017b). Horton and colleagues assessed that in the EU between 473,000 and 910,000 metric tons of plastic waste are released and retained annually within continental environments, which is 4 to 23 times the amount estimated to be released to the ocean (Horton et al., 2017b). Several recent monitoring studies have established that MPs are ubiquitously found in waters and shore sediments of rivers and lakes all over the world (Atwood et al., 2019; Hurley et al., 2018; Lambert and Wagner, 2018; Lebreton et al., 2017; Leslie et al., 2017; Mani et al., 2015; Piehl et al., 2019; Sighicelli et al., 2018). MPs and NPs have been described to reach terrestrial soils as a result of agricultural practices, urban runoff, atmospheric deposition and local fragmentation of larger plastic debris (e.g. plastic mulch) (Bläsing and Amelung, 2018; Hurley and Nizzetto, 2018; Ng

et al., 2018). Therefore, understanding MPs and NPs dynamics in terrestrial and freshwater systems seems of critical importance to allow for a more comprehensive assessment of hazards and risks posed by these pollutants to ecosystems (Hurley and Nizzetto, 2018; Ter Halle et al., 2017). Ecological effects of NPs on freshwater organisms have been evaluated across several levels of organization, from infra-organismic responses, such as oxidative stress (Jeong et al., 2016), altered lipid metabolism (Cedervall et al., 2012; Y. Li et al., 2020a), and mobilization (Auclair et al., 2020) and glucose metabolism (Brun et al., 2019), to organismic endpoints like mortality, impaired reproductive capacity (Jeong et al., 2016; W. Zhang et al., 2020), histopathological and behavioral changes (Brun et al., 2019; Cedervall et al., 2012; Chae et al., 2018), which then potentially affect population dynamics. A rapidly growing body of omic data on MPs and NPs is available in the literature, aiming at providing a detailed description of the cellular pathways underlying plastic particles detoxification (Gu et al., 2020; W. Liu et al., 2020; Liu et al., 2021a; Magni et al., 2019; W. Zhang et al., 2020). Currently, little is still known about the effects of NPs on decapod crustaceans despite their ecological and economic relevance. Due to their detritivorous behavior and feeding habits, benthic and epibenthic decapod crustaceans ingest various types of inorganic particles from the sediment in which they live or from their prey. Alongside, they also readily ingest plastic fragments or fibers (Cau et al., 2019; Devriese et al., 2015; Lv et al., 2019; Murray and Cowie, 2011; Taylor et al., 2016; D. Zhang et al., 2020). Plastic fibers have been reported to become knotted in the stomach of Crustacea such as *Nephrops norvegicus* and *Carcinus maenas*, likely due to the action of gastric mills (Murray and Cowie, 2011; Watts et al., 2015). Interestingly, in the shrimp *Palaemonetes varians*, long ingested fibers were regurgitated rather than expelled like shorter fibers or beads (Saborowski et al., 2019). Furthermore, in some crustacean species, such as crab, krill and Norway lobster, a digestive mechanical breakdown of larger plastic particles into much smaller fragments has been observed, identifying a new pathway of secondary MPs and NPs generation (Cau et al., 2020; Dawson et al., 2018; Watts et al., 2015). It has been outlined that the approximate size retention of the fine-mesh chitinous filtration system - i.e. the gastric sieve - of crustaceans is typically around 1 μm, preventing the passage of larger particles to the midgut gland, the main site of nutrient absorption in crustaceans (Dawson et al., 2018; Hämer et al., 2014; Korez et al., 2020; Pattarayingsakul et al., 2019). Therefore, a growing body of evidence highlights NP effects on survival, growth, molting, nutritional values and energy metabolism, immunity, and antioxidant defenses (Bergami et al., 2020; Y. Li et al., 2020a, 2020b; Redondo-Hasselerharm et al., 2018; P. Yu et al., 2018).

The red swamp crayfish *P. clarkii* is a benthic freshwater crustacean widely distributed all over the world. Native to Mexico and South-Central America, this species has been extensively harvested since the 1950s and successfully translocated all over the world for aquaculture purposes (Gherardi, 2006; Hobbs et al., 2008; Manfrin et al., 2019). As a result of these translocations, today *P. clarkii* is the most cosmopolitan crayfish, occurring in natural habitats of all continents except Australia and Antarctica (Gherardi, 2006). In Europe, the red swamp crayfish is considered the most plastic ecologically invasive decapod (Souty-Grosset et al., 2016). Because of its high environmental tolerance, this species has been used for a long time as a bioindicator of environmental pollution from heavy metals (Fernández-Cisnal et al., 2018, 2017; Gherardi et al., 2002; Goretti et al., 2016; Osuna-Jiménez et al., 2014; Zhang et al., 2019), cyanotoxins (Tricarico et al., 2008) and organic compounds (Vioque-Fernández et al., 2007a). Being a benthic opportunistic feeder, showing a pronounced burrowing activity this species may be susceptible to plastic ingestion from sediment (Lv et al., 2019; D. Zhang et al., 2020). As an invertebrate, *P. clarkii* lacks an adaptive immune system and must rely on innate immunity. The innate immune system of crustaceans consists of three main components: physical barriers, humoral defenses, and cellular responses (Manfrin et al., 2016). When physical barriers are not sufficient to prevent damage, internal mechanisms are activated. Hyperglycemia, mediated by the crustacean hyperglycemic hormone (CHH), is a common stress response of crustaceans (Manfrin et al., 2016). In addition to satisfying the increasing energy demand, CHH release can trigger the phenoloxidase (PO) activity. PO is controlled by the prophenoloxidase system (proPO), which represents a major humoral defense in invertebrates, ultimately leading to clotting and melanization of hemolymph (Cerenius and Söderhäll, 2004). Cellular responses, such as recognition of foreign particles, phagocytosis, encapsulation and nodule formation, mainly rely on hemocytes (Giulianini et al., 2007). As changes in total circulating hemocytes count (THC) have been reported following stress in several crustacean species, THC has long been used as a biomarker of health status (Coates and Söderhäll, 2020).

In this study, common biochemical and cellular measures of crustacean condition, including hemolymph glycemia (Lorenzon, 2005; Manfrin et al., 2016) and total protein content, total hemocyte count (THC, Giulianini et al., 2007), as well as immune-related enzymes (proPO, and PO) activities (Cerenius and Söderhäll, 2004) were assayed to estimate the immunological toxicity of polystyrene (PS) NPs on *P. clarkii*. Furthermore, transcriptome sequencing was performed on crayfish hemocyte and hepatopancreas samples following NP exposure for 72

hours. This integrated approach allowed us to figure out at the same time if crayfish were able to maintain homeostasis and which specific pathways were involved in the compensatory mechanisms. This study will be useful to shed light on the potential effects of plastic nanoparticles on crayfish.

2.2. Materials and methods

2.2.1. Animal collection and housing conditions

Adult crayfish *P. clarkii* (wet weight: 32.2 ± 15.5 g; total length, from the tip of the rostrum to the tip of telson: 102.2 ± 13.9 mm, N = 38) were sampled in Brancolo Channel ("Brancolo's reclamation area", 45°46'N, 13°30'E, GO, Italy) in October 2018. They were acclimatized for one month in three 120 L glass aquaria (120 x 40 x 50 cm) provided with closed-circuit filtered and thoroughly aerated tap water (pH 8.35 ± 0.1, electric conductivity 305 ± 2.1 µS, and temperature 21.0 ± 1.0 °C). Polyvinyl chloride tubings were placed within each tank as shelters. The photoperiod was set to 12:12 (L:D) and individuals were fed daily ad libitum with commercial food (Sera granular, Heisenberg, Germany). Water was completely changed twice a week. Only apparently healthy crayfish were selected for the experiment. Before the experiment, crayfish were weighted and the total length from the tip of the rostrum to the tip of the telson was determined to a precision of ± 0.1 mm. The reproductive stage of males was determined according to Taketomi (Taketomi et al., 1996). Sexually mature males were staged E, based on the presence of reversed spines on the ischia of the third and fourth pereiopods, while sexually immature males were collectively staged D (pooling Taketomi's A – D stages). Females individuals were sexed after dissection at the end of the experiment. Ovary maturation stages were established according to color and aspect, and the gonadosomatic index (GSI = ovary wet weight (g) / female total wet weight (g) *100) was determined (Alcorlo et al., 2009). Specimens were starved for 24h prior to the start of the experiment to empty their digestive systems.

2.2.2. Polystyrene nanoplastics characterization

Yellow-Green fluorescent polystyrene nanoparticles (Fluoresbrite® YG Carboxylate Microspheres, 0.10 µm) with a density of 1.05 g/cm^3 were purchased from Polysciences (Polysciences Inc, Warrington, PA), supplied as a 2.5% aqueous suspension with a concentration of 4.55 x 10^{13} particles/mL. For particle characterization, a 2 mg/L solution in MilliQ water was prepared. Primary particle diameter identification was achieved by

transmission electron microscopy (TEM, EM 208, Philips, Eindhoven, The Netherlands). Intensity-weighted size distribution and hydrodynamic diameter (Z-average), as well as polydispersity index (PdI), were acquired by Dynamic Light Scattering (DLS) using a Malvern Zetasizer nano ZS (Malvern Instruments Ltd., Worcestershire, UK). Measurements were conducted at 26.5 °C and performed in triplicate.

2.2.3. Nanoplastic-Supplemented Food

Artificial agar-based food was prepared with a specified amount of artificial food (Sera granular, Heisenberg, Germany) and a supplement of nanoparticles. The standard food preparation contained one regular granule (6.3 ± 0.7 mg) of artificial food, which was suspended in 400 µL of MilliQ water in a 1.5 Eppendorf tube. After vortexing, the supernatant was removed. 4 µL of nanoplastic solution 2.5% solids ($1.82e^{11}$ particles) were added to the rehydrated granules, which correspond to 100 µg PS NPs accounting for a 1.6 ± 0.2 % of food dry weight (the agar content was not considered part of the diet). A solution of agar 3X (25-30 µL for each feeding unit, Amresco, Solon, OH, USA) was added as a thickener. The mixture was then dried at room temperature overnight to obtain small pellets. One single artificial granule was administered to each exposed crayfish at the beginning of the experiment. The dose of 100 µg (equivalent to 1.4×10^{11} particles/L) was selected considering a polluted freshwater environment scenario, that possibly record microplastic concentrations up to 10^2 particles/L (Triebskorn et al., 2019). As suggested by Besseling and coworkers (2019), nanofragmentation of MPs can ultimately result in nanoparticle concentrations of 14 orders of magnitude higher. Additionally, the relatively low tested dose of 100 µg was chosen to evaluate the sub-lethal effects of PS NPs on *P. clarkii*, based on acute toxicity thresholds available in literature on other crustacean species (Heinlaan et al., 2020; Li et al., 2020a; Liu et al., 2019b).

2.2.4. Feeding assay

A total of 24 intact *P. clarkii* (12 females and 12 males) were randomly divided into exposed (N = 12) and control (N = 12) groups, taking care to assign an equal number of males and females to each group. Two custom-made glass tanks filled with 4 L tap water were used for the experiment, one for each group (Figure S1). Aquaria were provided with three almost entirely separated cells (12 x 14 x 15 cm) to keep individuals isolated and prevent aggressive behaviors. During the 72h experiment, water was recirculated in a closed loop but was not replaced, and the experimental conditions were kept stable with a photoperiod of 12:12 (L:D) and a temperature of 21 °C. Crayfish were fed once at T0 (0h) with one pellet of normal (control

group) or nanoplastic spiked (exposed group) food, with no additional feeding provided for the rest of the trial. After 72h crayfish were anesthetized by hypothermia and sacrificed. Four replicates of the experiment were conducted. One control animal from the first replica died at day 2. Four individuals (2 control and 2 exposed animals) from the fourth replica were excluded from subsequent analysis, as they escaped from exposure tanks.

2.2.5. Sample collection

Hemolymph was withdrawn from exposed and control animals by pericardial cavity puncture with a 1-ml syringe (26-gauge needle) before the exposure (as baseline sample, T0) and also at 24 (T1), 48 (T2), 72 (T3) hours after the food pellets provision. Hemolymph samples were taken between 10 and 12 AM at about the same time each day to compare the same circadian status for all the experimental crayfish. Approximately 200 µL of hemolymph from each animal were collected in a sterile Eppendorf tube without using anticoagulant and promptly placed on ice. Plasma was isolated from hemolymph through centrifugation (10,000 x g for 1 minute at 4°C) and immediately stored at -20°C for subsequent analysis. For transcriptomic analysis, the remaining hemocyte pellet after plasma isolation at T3 sampling time was saved and stored at −80 °C in 200-500 µL of TRIzol RNA isolation solution (Invitrogen, Thermo Fisher Scientific, Inc.). At the end of the experiment, crayfish were dissected, hepatopancreas samples were collected and immediately stored in 300 µL of TRIzol at −80 °C for RNA extraction.

2.2.6. General stress parameters

2.2.6.1 Glycemia

Plasma glucose was determined using the Glucose Colorimetric Assay Kit (Catalog No. 10009582; Cayman Chemical, Ann Arbor, MI, USA). Standard curves were prepared at concentrations of 0, 2.5, 5, 7.5, 10, 15, 20 and 25 mg/dL of glucose following manufacturer's instructions. Standard curves R^2 values were 0.9985 or greater. Standard and sample absorbances were measured at 510 nm in an Infinite® 200 PRO micro-plate reader (Tecan, Männedorf, Switzerland) equipped with the software Tecan i-control (version 1.7.1.12). Absorbance values were corrected by subtracting measurements from control reactions without samples. Glucose levels were interpolated from standard curves and reported as mg/dL. All standards and samples were assayed in duplicate.

2.2.6.2 Total hemocyte count

After collection, a drop of hemolymph was immediately placed on a hemocytometer for the total hemocyte count (THC) assay. For each time point (0, 24h, 48h, 72h), all crayfish were

checked. The number of hemocytes was determined using a Bürker counting chamber placed under an Olympus BX50 microscope (Olympus, Tokyo, Japan). Each sample was photographed at 10X magnification using an Olympus DP12 camera (Olympus, Tokyo, Japan). The pictures were then uploaded in the free software ImageJ (more information available at http://rsb.info.nih.gov/ij/) implemented with the Cell Counter plug-in allowing for the manual cell counting and hemocyte quantification.

2.2.6.3 Basal and total plasmatic phenoloxidase activities

Phenoloxidase (PO) activity was monitored spectrophotometrically as the formation of dopachrome from 3,4-dihydroxyDL-phenylalanine (DL-DOPA, Sigma-Aldrich) as reported previously by Giglio et al. (2018), with minor modifications. Briefly, 20 µL of plasma were mixed with either 180 µL of DL-DOPA (3 mg/mL in PBS) or 180 µL of a solution of DL-DOPA (3 mg/mL in PBS) and SDS (1 mg/mL) in a microtiter plate (Biorad), for the determination of basal and total plasmatic PO (proPO) enzyme activity, respectively. SDS has been described as a good chemical activator of PO from its inactive zymogen, prophenoloxidase (proPO, Radha et al., 2013). Absorbance was measured kinetically at 25°C at 492 nm over 60 min at 5-min intervals in an Infinite® 200 PRO micro-plate reader (Tecan, Männedorf, Switzerland) equipped with the software Tecan i-control (version 1.7.1.12). Four technical repetitions were performed for each plasma sample. The enzyme activity was measured as the slope (absorbance vs time) of the reaction curve during the linear phase of the reaction. Absorbance values were blank (reagents) subtracted. The slope of the reaction curve at V_{max} was plotted as absorbance per µL of hemolymph per min.

2.2.6.4 Hemolymph protein concentration

Total Protein content was assessed in plasma samples. The analysis was performed by measuring sample absorbance at 280 nm following the Protein A280 method for NanoDrop™ 2000 (Thermo Fisher Scientific, Wilmington, DE, USA).

2.2.7. Transcriptomic analysis

2.2.7.1 Total RNA isolation

Total RNA was extracted from *P. clarkii* hemocytes and hepatopancreas. Tissues in TRIzol were mechanically homogenized using a Dremel homogenizer (Dremel® 300-1/55, USA) for about 2-3 min or a Mini-Beadbeater (BioSpec Products, Bartlesville, Oklahoma) using glass beads (0.5 mm diameter, Scientific Industries Inc., Bohemia, New York) for hepatopancreas and hemocyte samples, respectively. RNA purification was performed using a Direct-zol™

RNA MiniPrep (Catalog No. R2052; Zymo Research, Irvine, CA, USA) spin column system according to the manufacturer instructions with minor modifications. RNA quality and concentration were assessed with NanoDrop™ 2000 Spectrophotometer (Thermo Scientific; Thermo Fisher Scientific Inc.), agarose gel electrophoresis, Qubit® 2.0 Fluorometer (Life Technologies, Carlsbad, CA, USA) using the Qubit® RNA HS Assay Kit (Catalog No. Q32852; Invitrogen; Thermo Fisher Scientific, Inc.) and an Agilent RNA 6000 Nano Kit (Catalog No. 5067-1511; Agilent Technologies, Palo Alto, CA, USA) for the 2100 Bioanalyzer System. The Bioanalyzer RNA integrity number (RIN) is not reported here because it is not an appropriate measure of RNA quality for non-model invertebrate organisms. Indeed, invertebrate 28S ribosomal RNA has a strong tendency to denature and break into two smaller fragments, resulting in an apparently "degraded" RNA profile in which both 18S and 28S overlap in a single band (DeLeo et al., 2018). RNA was successfully extracted from 18 out of 19 hepatopancreas samples (18 digestive glands from 7 males and 11 females). However, extracted RNA from female hemocytes showed inadequate quality standards for library preparation, therefore only male hemocyte samples were used (N = 7).

2.2.7.2 Library generation, Illumina de novo sequencing

Illumina libraries were constructed from 25 (18 hepatopancreas and 7 hemocyte) samples using QuantSeq™ 3′ mRNA-Seq Library Prep Kit FWD (Catalog No. 15; Lexogen GmbH, Vienna, Austria) according to the manufacturer's instructions using 65-525 ng of total RNA for each sample as input. The quality of purified libraries was evaluated by examining the size distribution and the absence of primer species using an Agilent High Sensitivity DNA Kit (Catalog No. 5067-4626 and 5067-4627; Agilent Technologies, Palo Alto, CA, USA) for the 2100 Bioanalyzer System. Libraries concentrations ranged from 1.9 to 8.2 ng/ μL, with a typical size of 200-600 base pairs (bp). High-throughput sequencing was performed as single-end 100 bp sequencing using a NovaSeq™ 6000 platform (Illumina, San Diego, CA, USA) at CBM S.c.r.l. (Area Science Park, Trieste, Italy) based on standard protocols. The RNA sequencing data are available online at the NCBI sequence read archive (SRA) under the BioProject ID: PRJNA691574.

2.2.7.3 Raw data analysis

Raw demultiplexed reads in FASTQ format provided by the sequencing center were quality assessed and trimmed using CLC Genomics Workbench software (v. 20.0.03), developed by QIAGEN (Hilden, Germany). The trimming procedure included removal of adaptor sequences, low-quality bases (quality score threshold = 0.05), ambiguous nucleotides, poly(A) and poly(G)

sequence stretches and short reads (read length < 75 nucleotides). In addition, 2 and 15 nucleotides were discarded at the 3' and 5' terminus of the reads, respectively, to remove a bias in nucleotide composition observed in a preliminary screening. Quality assessment of the trimmed reads and preliminary mapping on RNA-seq data from a previous transcriptome study (unpublished results) (see chapter 2.2.7.4) revealed the presence of outlier transcripts characterized by both high expression levels and high fluctuation within samples from the same experimental group. The latter were identified as mitochondrial RNA (mtRNA) and ribosomal RNA (rRNA), indicated here as *non*-mRNA contamination that was not completely removed by the previously illustrated poly(A) selection method. The complete mitochondrial genome (NC_016926.1) and ribosomal RNA sequences of *P. clarkii* were retrieved from the National Center for Biotechnology Information (NCBI) (http://www.ncbi.nlm.nih.gov/taxonomy). *P. clarkii* rRNA sequences were blasted (E-value = 1e-50) against the reference transcriptome using the tool BLAST provided by CLC Genomics Workbench, resulting in a final set of 90 rRNA sequences. Therefore, reads that showed significant similarity to mtRNA and rRNA sequences were removed by creating an *ad hoc* workflow using the tool provided by CLC Genomics Workbench. Briefly, the trimmed reads were first filtered by mapping against the mitochondrial complete genome using the following mapping settings: mismatch cost = 2, insertion cost = 3, deletion cost = 3, length fraction = 0.8, similarity fraction = 0.9, using the tool *Map Reads to Reference* provided by CLC Genomics Workbench. Subsequently, unmapped reads on mitochondrial sequence were automatically mapped against rRNA sequences (mapping settings: mismatch cost = 2, insertion cost = 3, deletion cost = 3, length fraction = 0.9, similarity fraction = 0.9). Mapping reads were discarded, while unmapped, i.e., filtered, reads were used for subsequent analysis.

2.2.7.4 Differential gene expression analysis

Clean reads from each library were aligned to a reference transcriptome previously assembled in our laboratory, the Laboratory of Applied and Comparative Genomics at the University of Trieste, from Illumina RNA-sequencing data (depth 2×100 bp) from 12 tissues of *P. clarkii* (brain, eyestalk, green glands, ventral ganglia, heart, hepatopancreas, gills, hemocytes, muscle, Y-organ and epidermis, ovary and testis) (Unpublished results), with the *RNA-seq analysis* tool included in the CLC Genomics Workbench. The mapping parameters were set as follows: mismatch cost = 2, insertion cost = 3, deletion cost = 3, length fraction = 0.5, similarity fraction = 0.9. Mapping outcomes, as read counts per gene per sequencing library, were analyzed via the *Differential expression for RNA-seq* tool (CLC Genomics Workbench), considering three

separated groups of samples (i.e., hemocytes, male hepatopancreas and female hepatopancreas) and thus comparing each experimental condition with the paired control. To identify significant differentially expressed genes (DEGs) the adjusted *p*-value (false discovery rate - FDR) and absolute fold change cutoffs were set at 0.05 and 2, respectively. Finally, a functional gene ontology (GO) enrichment analysis of DEGs was performed through a hypergeometric test to identify significantly enriched features.

2.2.8. Statistical analysis

All statistical data analyses were performed using R version 4.0.2 software (R Core Team, 2020). The significance of treatment effects was assessed for each physiological variable (hemolymph plasmatic PO and proPO activity, glucose concentration, protein concentration, THC) using Linear Mixed effects Models (LMM). LMM assuming Gaussian distributions of residual error were fitted using lmer function from the lmerTest package (v. 3.1.2, Kuznetsova et al., 2017) in R. The analysis tested 3 fixed factors: "Sex" (2 levels, males and females), "Treatment'' (2 levels, exposed and control) and "Time" (4 levels, T0, T24h, T48h, T72h). To avoid pseudo-replication due to repeated sampling of crayfish from different trials over time, "Individual" (19 levels) was incorporated as a random factor (random intercept) nested in "Trial" (Replicate 1, 2, 3, or 4) in the model designs. Fully models comprising all fixed effects, together with their interactions and random effects, were first tested. The goodness-of-fit of all the models was assessed using maximum likelihood for model fits (Zuur et al., 2009). Final models were obtained by backward elimination of non-significant variables from the full model using the step function from the lmerTest package (Kuznetsova et al., 2017) and were presented using REML estimation (Zuur et al., 2009). Model assumptions, in terms of linearity, normality, and homogeneity of variances, were evaluated by visual inspection of residuals' plots, and verified by Shapiro and Fligner-Killeen's tests. Hypotheses testing was conducted by performing a type III Wald chi-squared test using the Anova function from the car package (v. 3.0.9, Fox and Weisberg, 2019). Post-hoc Tukey tests for pairwise comparisons were conducted using the function pairs, after the least-square means were calculated using the function lsmeans (from the R package lsmeans v. 2.30.0, Lenth, 2016). The conditional coefficients of determination were calculated for all the models using the function r.squaredGLMM implemented in the package MuMIn (v. 1.43.17, Barton, 2020). An alpha level of .05 was used for all statistical tests.

2.3. Results

Biometric data, sex and reproductive stage of crayfish analyzed are reported in Table 1. The average body weight was 32.2 ± 11.0 g and the mean total length was 106 ± 10.5 mm. All males were sexually mature or close to maturity. As for the female individuals, there are no tools to assess the reproductive status before the dissection of the crayfish. At the end of the experiment, based on the analysis of the color and appearance of the ovaries, it was possible to determine that most females were ovigerous individuals. These findings were consistent with previous data describing the presence of ovigerous females and stage E males in the Brancolo Channel during autumn (Peruzza et al., 2015). However, it was possible to highlight some small differences in ovarian maturation stage between control and exposed female individuals, with controls showing a slightly more advanced stage of development (GSI mean ± SD: control 2.33 ± 1.03; exposed 1.04 ± 0.86). This difference was not expected as all individuals were collected at the same location and during the same period.

Table 1: Biometric data of P. clarkii *individuals are presented as total wet weight and total length (TL). In addition, sex and reproductive stage of female (ovarian wet weight, gonadosomatic index (GSI) and ovarian maturation stage) and male individuals (developmental stage) are indicated Abbreviations are as follows: NP, nanoplastic-exposed; C: control.*

Individual	Weight (g)	TL (mm)	Sex	Ovarian wet weight (g)	GSI	Ovarian maturation stage*	Developmental stage**
NP1	27.1	104.3	F	0.54	2.01	5-6	
NP2	35.3	110.6	F	0.20	0.58	2	
NP3	25.3	98.3	F	0.09	0.35	2	
C1	35.5	109.3	F	1.29	3.64	6	
C3	34.2	111.3	F	0.55	1.60	5	
NP4	60.1	121.9	M				E
NP5	31.4	107.4	M				E
NP6	16.8	93.8	M				E
C4	33.3	114.8	M				E
C5	41.2	110.5	M				E
C6	13.8	83.3	M				D
NP7	22.8	100.9	F	0.08	0.33	2	
NP8	39.6	114.1	F	0.28	0.72	4	
NP9	44.5	119.2	F	0.99	2.24	6	
C7	22.6	98.8	F	0.64	2.83	6	
C8	44.9	115.2	F	1.16	2.57	6	
C9	36.1	111.3	F	0.37	1.04	4	
NP12	25.4	92.2	M				E
C12	19.7	91.1	M				E

* Ovarian maturation stage determined according to Alcorlo et al. (2009) ** Developmental stage determined according to Taketomi et al. (1996)

2.3.1. Particle characterization

TEM images showed well-distributed particles with uniform size and spherical morphology (Figure S2). Primary particles' nominal size of 100 nm was confirmed by TEM imaging with an average diameter of 103 ± 3.18 nm (average ± S.D., N = 440). PS NP particle hydrodynamic diameter (D_h), and heterogeneity (polydispersity index, pdi) were characterized by Dynamic Light Scattering (DLS) at a concentration of 2 mg/L in MilliQ water, resulting in a Z-average diameter size (± S.D.) of 113.9 ± 0.91 nm (Figure S2) and an average polydispersity index (± S.D.) of 0.02 ± 0.01.

2.3.2. Physiological biomarkers

2.3.2.1 Glycemia

The best-fit model for plasma glucose included Treatment and Time as fixed explanatory variables and id nested in Trail as a random intercept. Glycemia levels did not differ between treatments (χ^2 = 0.97, df = 1, 69, P > 0.05; Table A3), neither was found a significant interaction between treatment and exposure time when comparing glucose concentrations over all time points (i.e., T0, T24h, T48h, and T72h post-exposure) among control and exposed groups. The model revealed only a significant main effect of time (χ^2 = 11.25, df = 3, 69, P = 0.01; Table A3), with a general reduction of glycemia from T0 to T72h and a significant decline between T0 and T24h (Mean ± S.D; T0: 11.7 ± 7.13 mg/dL; T24h: 7.95 ± 5.57 mg/dL; post-hoc test P = 0.027, Figure 1A). A full description of the results can be found in the Appendix (Tables A1, A2, and A3).

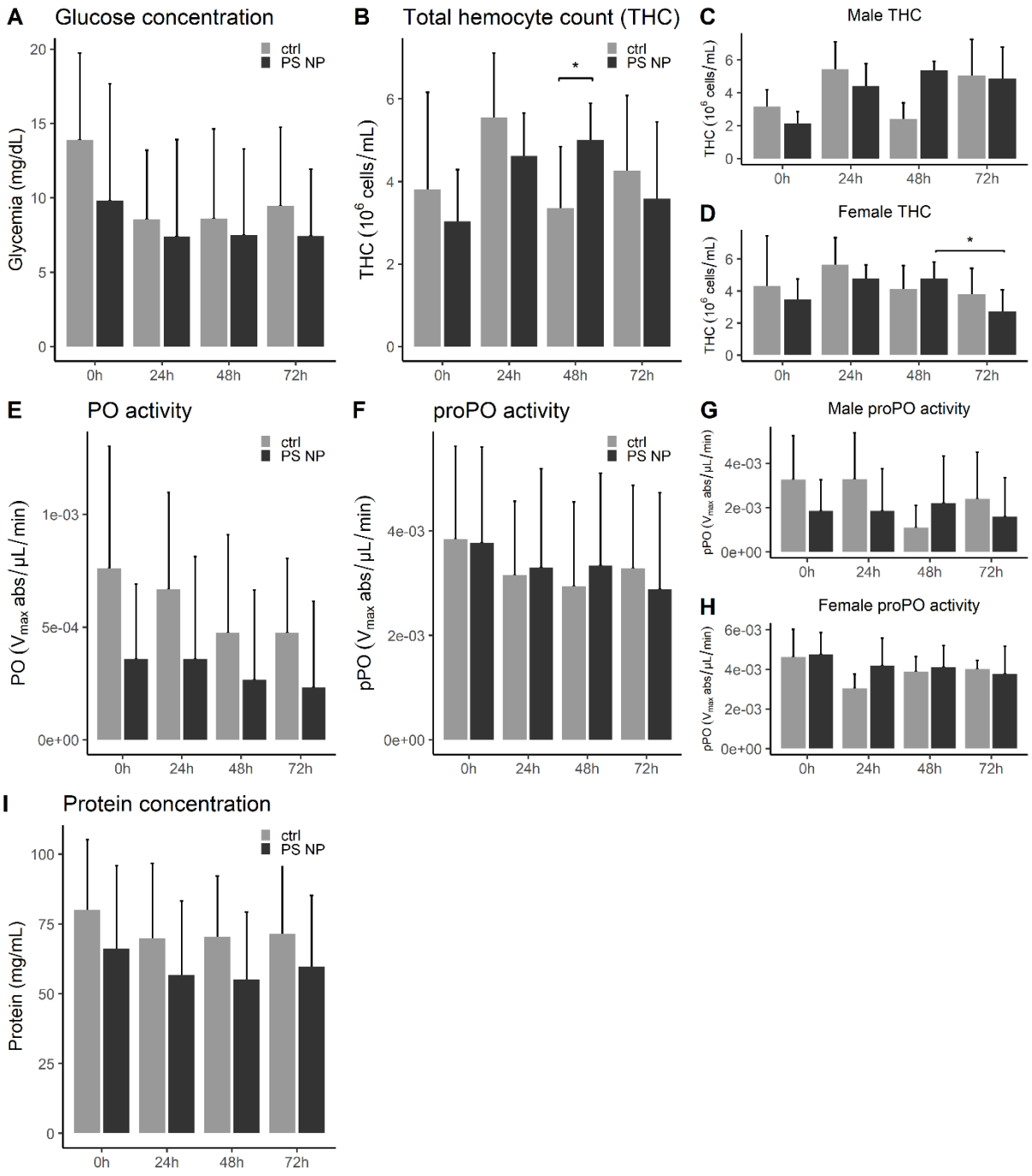

Figure 1:Effects of PS NP exposure on physiological parameters of P. clarkii. *Data are presented for all individuals (N = 19) as mean + S.D., over all time points (T0, T24h, T48h, and T72h post-exposure). When mixed models revealed a statistical significance for sex, data are also showed for males (N=8) and females (N=11) separately. Asterisks represent significant differences between groups (*P<0.05).*

2.3.2.2 Total hemocyte counts

The final mixed model for THC comprised Treatment, Time and Sex as fixed effects, and included Treatment:Time and Time:Sex as significant interactions (χ^2 = 9.77, df = 3, 72, P = 0.021; χ^2 = 9.53, df = 3, 72, P = 0.023; Table A6). A random intercept for id was also taken into account. Despite a moderate inter-individual variability, PS NP exposure was followed by an increase of THC (Figure 1B). At 48h, exposed crayfish showed statistically significant higher THC levels compared to controls (Mean ± S.D; ctrl: 3.34 ± 1.5 $\times 10^6$ cells/mL; exposed: 5.01 ± 0.89 $\times 10^6$ cells/mL; post-hoc test P = 0.023; Table A4, Figure 1B). At 72h, PS NP exposed individuals demonstrated a different behavior based on sex: free hemocytes' concentration remained stable in males, while markedly decrease in females (post-hoc test P = 0.021, Figure 1D). Thence, 3 days post-administration males showed statistically higher THC levels than females (Mean ± S.D; females: 2.71 ± 1.35 $\times 10^6$ cells/mL; males: 4.87 ± 1.90 $\times 10^6$ cells/mL; post-hoc test P = 0.020, Figure 1C, D). Total hemocyte count mean values for control and exposed individuals are summarized in Table A4; model estimates, 95% confidence intervals, and p-values, as well as the outputs of the analysis of deviance, are reported in Tables A5 and A6.

2.3.2.3 Basal and total plasmatic phenoloxidase activities

The results showed no significant differences in either basal PO (χ^2 = 2.70, df = 1, 65, P > 0.05; Table A9) or total plasmatic PO (χ^2 = 0.11, df = 1, 64, P > 0.05; Table A12) activities among control and exposed groups, despite significant overall variation over time was found for both phenoloxidase (χ^2 = 16.2, df = 3, 65, P = 0.001, Table A9) and prophenoloxidase (χ^2 = 23.2, df = 3, 64, P < 0.001, Table A12) activities. Although a high inter-individual variability was observed, PO activity appeared to slightly decrease in all specimens over time (Figure 1E). Meanwhile, total phenoloxidase activity was significantly determined by sex (χ^2 = 6.95, df = 1, 64, P = 0.008; Table A12), with an enzyme activity higher in females than in males (Mean ± S.D; females: 4.93 ± 4.29 $\times 10^{-4}$ abs/µL/min; males: 3.26 ± 4.05 $\times 10^{-4}$ abs/µL/min; post-hoc test P = 0.018, Figure 1G, H). Although non-significant, a minor proPO activity increase after 48h was recorded both in males and in females. Phenoloxidase and prophenoloxidase enzyme activity summary statistics can be found in Tables A7 and A10, while mixed models and ANOVAsummaries are reported in Tables A8, A9 and A11, A12, respectively.

2.3.2.4 Hemolymph protein concentration

As with glycemia and phenoloxidase enzyme activity, no clear effect of Treatment was found in protein concentration after 72h of exposure ($\chi^2 = 1.25$, df = 1, 73, $P > 0.05$; Table A15, Figure 1I). A full description of protein concentration statistics is given in the Appendix (Tables A13, A14, A15).

2.3.3. Transcriptomic response of *P. clarkii* to nanoplastic exposure

2.3.3.1 Illumina *sequencing*

A total of 126,179,823 raw reads were obtained from Illumina-based RNA-seq (Table 2), with a mean of 5,047,193 raw reads per sample and an average length of 97.5 ± 1.23 bp (Mean ± S.D.).

Table 2: General information on RNA-Seq output and mapping rates for hemocytes and hepatopancreas libraries.

Terms	Hemocytes	Hepatopancreas males	Hepatopancreas females	All
Number of libraries	7	7	11	25
Number of raw sequencing reads	43,763,356	32,742,172	49,674,295	126,179,823
Number of clean sequencing reads	19,895,749	16,021,331	24,550,051	60,467,131
% GC content	39.7	41.0	41.3	40.8
Q20	100	100	100	100
Q30	97.8	98.4	98.3	98.2
Mapping rate (%)	67.4	86.6	84.3	80.2

After trimming, 1,078,492 to 6,572,996 clean reads per sample (mean length of 83.1 ± 0.07 bp) were generated. The Q30 (Q score ≥ 30) was 98.2% and the mean GC content was 40.8% (Table 2). Clean reads were mapped back to the reference transcriptome and the read counts for each gene were obtained from the mapping results. A total of 48 million reads (80.2%) mapped to the reference transcriptome (Table 2). Detailed information on sequencing outputs and mapping results are available in the Appendix (Table A16).

2.3.3.2 Analysis of differentially expressed genes (DEGs)

A preliminary Multidimensional Scaling (MDS) analysis was performed to visualize the level of similarity between samples based on gene expression profiles (Figure 2).

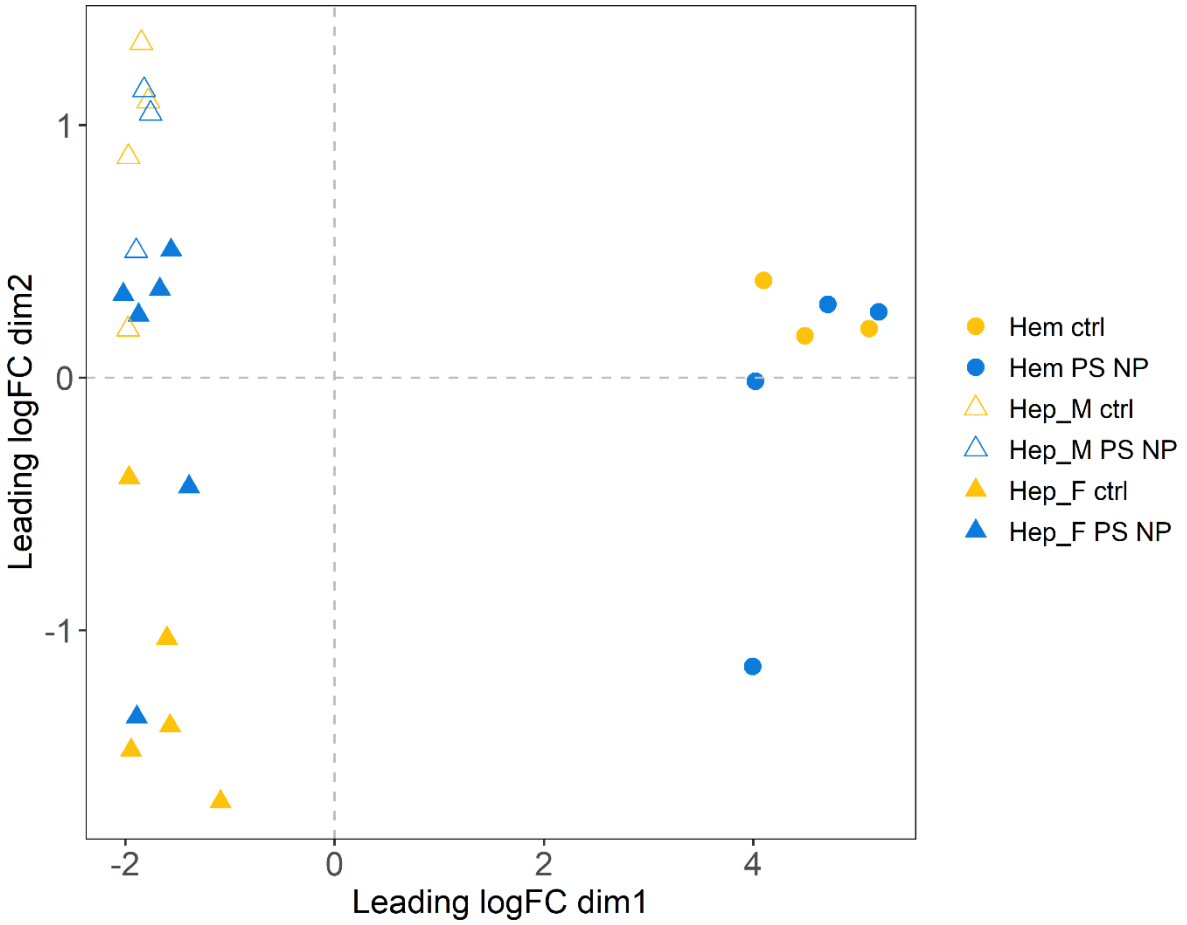

Figure 2: Multidimensional scaling (MDS) plot of P. clarkii *samples with total counts used as an expression value parameter. Distances correspond to leading log-fold-changes, i.e., the average (root-mean-square) of the largest absolute log-fold-changes, between each pair of samples. Different colors correspond to different experimental groups (Control, yellow; PS NP exposed, blue). Shapes define different groups of samples: hemocytes (Hem, circle), hepatopancreas of male specimens (Hep_M, empty triangle), and hepatopancreas of female specimens (Hep_F, full triangle).*

MDS revealed a clear separation of samples by tissue type along the first dimension (Dim1), as expected. Although not as clearly marked, further segregation between the two sexes in hepatopancreas samples was visible along the second dimension (Dim2). A weak clustering effect due to treatment was observable for females in the hepatopancreas, while no evident segregation by treatment was observable within other groups of samples (Figure 2). Differential expression analysis was performed between PS NP exposed crayfish and control counterparts in hemocytes (Hem, N = 7) and hepatopancreas samples according to sex (Hep_F, N = 10; Hep_M, N = 7). One sample, belonging to the female hepatopancreas group (R3T3), was excluded from DEG analysis because it was considered an outlier as its gene expression pattern greatly differs from other specimens of the same group, possibly because of an undetermined

individual peculiarity. In general, the alterations induced by PS NPs were of a limited entity, both in terms of up- and down-regulation, even though a tissue-dependent effect was detectable. DEG analysis highlighted a total of 12, 98, and 32 DEGs in Hem, Hep_F, and Hep_M groups, respectively. Overall, the NP treatment mostly resulted in upregulation, as evidenced by the disproportion between positively and negatively regulated genes (8 vs 4 in Hem, 65 vs 33 in Hep_F, and 25 vs 7 in Hep_M). A complete list of DEGs, including the fold ratio, the adjusted p-value, and annotation information can be found in the Appendix (Table A17), while they are visually displayed by volcano plots and heatmaps in Figure 3.

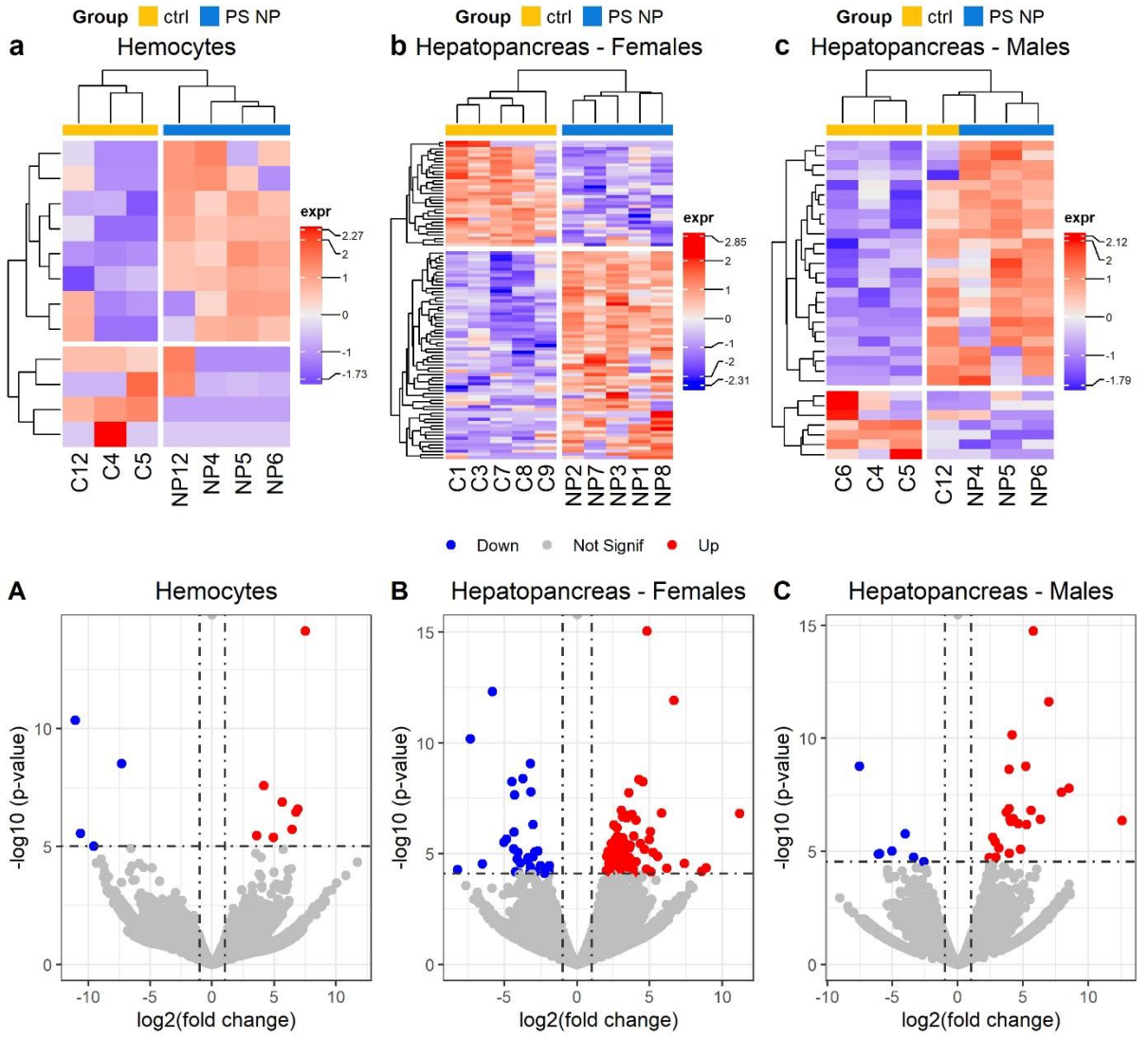

Figure 3: Visual identification of DEGs (FDR ≤ 0.05 and |fold change| > 2) identified in P. clarkii *exposed to PS NPs, relative to the controls, for each sample group analyzed: hemocytes (A, a), female hepatopancreas (B, b), and male hepatopancreas (C, c). The hierarchical clustering is based on Euclidean distance and complete linkage of normalized expression values (log CPM - counts per million -). Clustering indicates similar expression patterns among the samples of the control group (C, yellow) or nanoplastic-exposed group (NP, blue) (columns) and among genes (rows). Colors represent the normalized gene expression levels from light blue (low) to red (high). In the volcano plots, red (upregulation) and blue (downregulation) dots indicate DEG transcripts in the nanoplastic-exposed group, respectively, and dots in grey color show no significant differential expression.*

Only 3 transcripts, c*ytochrome P450 49a1* alongside two unknown genes, were differentially expressed in both sexes in the hepatopancreas, even though their regulation patterns differed between sexes (Figure S3). A functional Gene Ontology (GO) enrichment analysis was performed by hypergeometric test for all different groups of DEGs but was inconclusive, likely due to the low number of genes and relatively low rate of annotated genes as a consequence of dealing with a non-model organism.

2.4. Discussion

2.4.1. Physiological biomarkers

Numerous studies have reported hyperglycemia mediated by CHH release following exposure to several stressors in crustaceans (Bonvillain et al., 2012; Celi et al., 2013; El-Bakary and Sayed, 2011; Lorenzon et al., 2004; Manfrin et al., 2016), although to the best of our knowledge, the effects of NPs have never been investigated in this species. MPs and NPs have been described to induce different glycemic responses in fish. Brun and colleagues reported a significant reduction in whole-body glucose levels in zebrafish (*Danio rerio*) larvae following a 2-day exposure to 20 mg/L of PS NPs (Brun et al., 2019). Differently, a significant hyperglycemic response was recorded in Nile tilapia (*Oreochromis niloticus*) after exposure to microplastics (1-100 mg/L) for 15 days in a dose-dependent manner (Hamed et al., 2019). In this study, the lack of a significant glycemic response to plastic exposure could either be due to the moderate physiologic stress induced by the relatively low dose (100 µg) of PS NPs administered or to the recovery of the animals to glycemia homeostatic levels within 24h after ingestion (Lorenzon et al., 2004).

Crustaceans' hemocytes are crucial players in the host immune response. THC is sensitive to various environmental pressures, and a reduction in circulating hemocytes, termed hemocytopenia, has been reported in several crustacean species under stress conditions (Celi et al., 2013; Johnson et al., 2011; Lorenzon et al., 2008; Wei et al., 2020). In this study, PS NP exposure did not cause hemocytopenia but conversely was followed by a significant increase of THC 48h after exposure. A similar increase in total hemocyte count was previously observed in *Pontastacus leptodactylus* injected with 200 µL of 0.9 µm carboxylated polystyrene latex beads after 24h (Giulianini et al., 2007). The authors reported that maximum THC increases were registered at 1-2h after injection and clearly showed phagocytic activity of crayfish hemocytes against exogenous particles. Nanoparticles, particularly metal-based NPs, have recently gained great interest as antimicrobials, drug delivery vehicles, and immunostimulants

in aquaculture (Shaalan et al., 2016; Swain et al., 2014). Several peer-reviewed papers have reported the enhancement of crayfish and shrimp immune responses as a result of nanoparticles mediated supplementary diets (Ishwarya et al., 2019, 2018; Juarez-Moreno et al., 2017; Kandasamy et al., 2013; Muralisankar et al., 2016, 2014; Sivaramasamy et al., 2016; Sun et al., 2016; Tello-Olea et al., 2019). Authors addressed that Au, Cu, Zn and Ag-based and chitosan NPs, within a certain range of doses, were all able to increase THC, phenoloxidase enzyme activity, nutritional indices, and development and to raise survival rate after virus infection in decapod species, without causing toxicity in terms of mortality, antioxidant and metabolic enzymes activity or lipid peroxidation. Even though this study relied on a relatively small sample number, these results may suggest that a low dose of PS NPs promotes immune stimulation but does not cause toxicity in crayfish after 72h of exposure, with minor differences between sexes.

Phenoloxidase, primary involved in the melanization cascade, is one of the most common measures of invertebrate immunity. Overall, elevated PO levels identify a stress response, while low levels are associated with immunocompromised animals (Coates and Söderhäll, 2020). To cope with MP and NP-induced stress, PO activity initially increased under a short time and low concentration exposure in decapod crustaceans (Y. Li et al., 2020a; Liu et al., 2019a). Prophenoloxidase expression was also enhanced by low doses of NPs (Y. Li et al., 2020a). However, higher concentrations of particles over a long time exposure caused a decrease in PO activity and proPO expression, showing an exceed capacity of the immune defense system (Y. Li et al., 2020a; Liu et al., 2019a). The lack of a clear enzyme response in *P. clarkii* may be due to the lower exposure time and dose of PS NPs administered to crayfish, compared to the mentioned studies (5-40 mg/L for 28d, Li et al., 2020a; 0.04-40 mg/L for 21d, Liu et al., 2019a).

The assessment of hemolymph protein levels is a useful tool for monitoring the physiological status of crustaceans exposed to different environmental conditions or stressors (Coates and Söderhäll, 2020; Lorenzon et al., 2011). We did not find significant alterations of total protein content in *P. clarkii* after PS NP exposure. Our findings agree with other laboratory studies that tested acute stress on crustaceans (Celi et al., 2013; El-Bakary and Sayed, 2011), and may confirm the idea that hemolymph protein concentration can be considered a chronic, rather than an acute response, biomarker as previously reported by Bonvillain et al. (2012), who evidenced that fluctuations in protein concentrations in *P. clarkii* were associated with chronic stress in different laboratory and field studies (Bonvillain et al., 2012).

This poor response could be explained in the light of the relatively low concentration of PS NPs (100 µg) used for this study in comparison to PS NP toxicity thresholds available in the literature for crustacean species. Indeed, a 96h half-lethal concentration (LC50) value of 396 mg/L (95% CI, 26.0–638 mg/L) was calculated for 75 nm PS NPs in juvenile shrimp *Macrobrachium nipponense* (Y. Li et al., 2020a). In *Daphnia* species, Liu and colleagues reported a 48h LC50 of approximately 77 mg/L for 75 nm PS NPs (95% CI, 32.4-127 mg/L, Liu et al., 2019b). Moreover, Heinlaan et al. determined an effective concentration for 50% immobilization (EC50) of 22.0 ± 0.7 mg/L and 13 ± 1.4 mg/L for 26 nm and 100 nm non dialyzed carboxylated PS NPs, respectively, which further rose to >100 mg/L for dialyzed (removal of antimicrobial additive sodium azide) particles (Heinlaan et al., 2020).

2.4.2. Transcriptomic analysis

2.4.2.1 Hemocytes

The differential gene expression analysis in hemocyte samples revealed that just a little number of genes underwent significant expression shifts in response to PS NP exposure. Three out of 8 upregulated DEGs in hemocytes (i.e., *transcription factor btf3*, *pre-mRNA-splicing factor ATP-dependent RNA helicase PRP16*, and *putative ribosomal protein S23e*) were involved in gene transcription and translation (Table A17). The basic transcription factor 3 (BTF3) is involved in the initiation of transcription by RNA polymerase and in cell-cycle regulation and apoptosis (Jamil et al., 2015). PRP16 is required for the catalytic steps of the splicing pathway and mediate structural rearrangement of the spliceosome (Wang and Guthrie, 1998). The ribosomal protein S23 is a component of the 40S small ribosomal subunit, which is involved in the initiation phase of translation and, in association with other initiation factors, is thought to scan the 5′ untranslated region (UTR) until it recognizes the initiation codon AUG (Holcik and Sonenberg, 2005). Since proteins catalyzed most cellular processes, the regulation of their levels through changes in gene expression is fundamental to respond to stress stimuli (Holcik and Sonenberg, 2005).

In previous studies, MP exposure induced upregulation of genes associated with translation, ribosomal and spliceosomal functions in the marine copepod *Tigriopus japonicus* (6 µm PS MPs; 0.23 mg/L for two-generation exposure, Zhang et al., 2019) and in developing zebrafish (10-45 µm PE MPs; 5 mg/L for 48h, LeMoine et al., 2018). Besides, proteomic analysis of the zebra mussel (*Dreissena polymorpha*) gills revealed an upregulation of protein involved in ribosomal structure and function (including 40S ribosomal protein S23) after 6 days of MP

exposure (1-10 µm; 4×10^6 MP/L, Magni et al., 2019). Interestingly, the authors related the over-production of this class of proteins with their involvement in the formation of stress granules (SG), given the concurrent alteration of other RNA-binding proteins (i.e., eukaryotic translation initiation factors). Here, as we did not find a significant difference in the expression of other specific proteins involved in the formation of SG, (e.g., eukaryotic translation initiation factors, translational silencers, polysome-associated proteins, and cytoplasmic polyadenylation element-binding protein, Anderson and Kedersha, 2009) we assumed that the upregulation of these genes must be traced back to an overall higher protein biosynthesis.

In response to PS NP toxicity, two cytoskeleton-associated DEGs were also identified in hemocytes. The genes annotated as *dystonin-like* and *integrin beta-4-like* were upregulated in PS NP exposed crayfish, suggesting a primary involvement of hemocytes in the immune response (Table A17). Dystonins, also known as bullous pemphigoid antigen 1 (BPAG1), are cytoskeletal actin-binding protein (Brown et al., 1995) which can interact with the hemidesmosomal transmembrane β-integrins to form cell-extracellular matrix junctions (Jefferson et al., 2004; Koster et al., 2003). In turn, integrins are part of a largely conserved superfamily of cell adhesion receptors (Giancotti and Ruoslahti, 1999). Hemocyte-surface associated integrins, and specifically the integrin β subunit, have been suggested to have a role in many cell-mediated innate immune responses, such as microbial agglutination (Huang et al., 2015; Y. Zhang et al., 2012), hemocytes degranulation, activation of proPO activating system and phagocytosis (Chai et al., 2018; Lin et al., 2013; Wang et al., 2014; Xu et al., 2018). In accordance with these results, Gu and colleagues observed an alteration of phagosome processes and integrin-mediated signaling pathway in phagocytes of zebrafish exposed to nano-sized polystyrene (Gu et al., 2020). Furthermore, altered cytoskeletal dynamics have been previously revealed by proteomic analysis in gills of the zebra mussel (Magni et al., 2019) and oocytes of female oysters (*Crassostrea gigas*) (Sussarellu et al., 2016) after MP exposure.

2.4.2.2 Hepatopancreas

2.4.2.2.1 Acute phase and inflammation-related genes

In the hepatopancreas of *P. clarkii*, a group of DEGs coding for acute phase and inflammatory response proteins was identified. Specifically, the expression of *serum amyloid A-5 protein-like*, *activating transcription factor 4*, *hemocyte homeostasis-associated protein*, and the antimicrobial peptide *anti-lipopolysaccharide factor ALF9* were significantly upregulated after PS NP exposure in females (Table A17). Similarly, *C-type lectin-2*, *macrophage mannose receptor 1-like,* and the *anti-lipopolysaccharide factor ALF4* were over-expressed in males

(Table A17). Serum amyloid A (SAA) is a major acute-phase protein that is reported to be involved in the modulation of numerous immunological responses during the inflammatory response to infection, trauma or stress (Jensen and Whitehead, 1998; Qu et al., 2014). The hemocyte homeostasis protein (HHAP) has been previously described in shrimps, even though its function has still to be further clarified. In *Penaeus monodon* and *Litopenaeus vannamei* HHAP is essential for shrimp survival, being primarily involved in regulating hemocyte numbers and apoptosis (Apitanyasai et al., 2015; Charoensapsri et al., 2015; Prapavorarat et al., 2010). Differently, in *Pacifastacus leniusculus* an HHAP-like protein was involved in the control of bacterial number in the intestine but did not affect hemocytes homeostasis (Apitanyasai et al., 2016). C-type lectins (CTLs), including mannose receptors (Man et al., 2018), are pattern recognition receptors (PRRs) responsible for pathogen detection and immune system activation (Cerenius and Söderhäll, 2018). In *P. clarkii*, CTLs have been described to mediate hemocyte binding (opsonization), to promote encapsulation (Zhang et al., 2011) and phagocytosis of bacteria (Chen et al., 2013; Zhang et al., 2016, 2013) and to trigger the proPO activating system (Wang et al., 2011). CTLs have been also reported to influence the expression of antimicrobial peptides (Bi et al., 2020; Sun et al., 2017) and other immune effector genes (Luo et al., 2019). Among the major crustacean AMPs protein families, anti-lipopolysaccharide factors (ALFs) exhibit potent antimicrobial activity against a broad range of microorganisms, from Gram-positive and Gram-negative bacteria, to filamentous fungi and enveloped viruses (Rosa et al., 2013; Smith and Dyrynda, 2015). Here, an up-regulation of ALF4 and ALF9 AMPs was observed in PS NP group. The promoted expression of AMPs by carboxy-modified PS NPs has been earlier described by Bergami and colleagues in Antarctic sea urchin (*Sterechinus neumayeri*) coelomocytes, under *in vitro* conditions (Bergami et al., 2019). AMPs are regulated by Toll-like receptors (TLR) signaling pathway and may involve ATF4, a member of the ATF/CREB (activating transcription factor/cyclic AMP response element binding protein) transcription factor family (Huang et al., 2017; Lan et al., 2016). Previous proteomic analysis revealed that CTLs were significantly upregulated by MP exposure in *T. japonicus* (Zhang et al., 2019) and *L vannamei* (Duan et al., 2020), in accordance with our findings. Several other studies conducted on the Mediterranean mussel *M. galloprovincialis*, indicated an antimicrobial response to micro- and nanoplastics in hemocytes and hepatopancreas (Auguste et al., 2020; Détrée and Gallardo-Escárate, 2018, 2017; Sendra et al., 2020). After repeated exposure to NPs (Exposition 1: 10 µg/L for 24h; Depuration: 72h; Exposition 2: 10 µg/L for 24h), Mytilin B, Myticin C and lysozyme were all upregulated in mussel hemocytes, while no alteration of Toll-like receptor i isoform (TLR-i) was described (Auguste et al., 2020). Conversely, PS NPs

combined with a bacterial infection with *Vibrio splendidus* caused a significant reduction in the expression of Myticin C, which was not observed when treating either with NPs or bacteria alone, while no modification of Mytilin D was detected (Sendra et al., 2020). Finally, a transcriptomic analysis of *M. galloprovincialis* mantle and hepatopancreas, after a single and repeated (Exposition 1: 30 µg/L for 18d; Depuration: 28d; Exposition 2: 30 µg/L for 18d) exposure to high density polyethylene microplastics (1-50 µm), revealed a clear modulation of immune receptors, including CTLs, and antimicrobial peptides (Mytilin-4, Mytilin B) (Détrée and Gallardo-Escárate, 2018). Our results, in accordance with literature, suggest that NPs may be perceived as non-self by crayfish immune system in the hepatopancreas, and through different pattern recognition receptor signaling pathways, they can trigger inflammatory response.

2.4.2.2.2 Detoxification-related genes

In this study, four genes involved in xenobiotic detoxification pathways were modulated in the hepatopancreas of male and female crayfish exposed to PS NPs compared to the control. Among them, *cytochrome P450 49a1* was significantly upregulated in females, while it resulted downregulated in males. Additionally, *glutathione S-transferase*, *carboxylesterase 4A-like,* and *thiopurine S-methyltransferase-like* were over-expressed in males (Table A17). Cytochrome P450 monooxygenases (P450), glutathione S-transferase (GST), and carboxylesterases (CES) are widely used biomarkers of phase I and II detoxification of endogenous and exogenous lipophilic compounds in environmental toxicology studies (Barata et al., 2004; Fernandes et al., 2002; Han et al., 2017; Porte and Escartín, 1998; Vioque-Fernández et al., 2007b). Cytochrome P450 monooxygenase (P450) is a widely distributed superfamily of heme-thiolate enzymes, which play key roles in detoxifying endogenous and exogenous lipophilic compounds (Snyder, 2000; Wu et al., 2019). CYP49a1 belongs to the mitochondrial P450 clan (Ai et al., 2011; Baldwin et al., 2009; Dai et al., 2016; Yan et al., 2012), however, its specific function has not yet been understood. It has been reported to participate in pesticide metabolism in the silkworm (Li et al., 2015) and to cadmium stress response in the wolf spider (Juan Wang et al., 2019), while in *Drosophila melanogaster* it was associated with fatty acid metabolism and cuticular hydrocarbons composition (Dembeck et al., 2015). Glutathione S-transferase (GST) is responsible for the conjugation of reduced glutathione to a wide number of exogenous and endogenous hydrophobic electrophiles to create more water-soluble compounds (Strange et al., 2001). A recent RNA-Seq analysis revealed a significant alteration of cytochrome P450 and glutathione metabolism KEGG pathways in *D. pulex* exposed to PS NPs (70 nm; 1 mg/L for

96h, Liu et al., 2021). Furthermore, P450 enzymes have been reported to respond to NP insult both *in vitro* and *in vivo* (Fröhlich et al., 2010; Wu et al., 2019). A study by Fröhlich and colleagues reported that carboxyl PS NPs (20-60 nm) were able to reach high intracellular concentrations inhibiting the catalytic activity of P450 isoenzymes and increasing the effect of known P450s inhibitors *in vitro* (Fröhlich et al., 2010). A comprehensive *in vivo* study demonstrated that the expression levels of P450s resulted in a two-phase modulation after chronic exposure of *D. pulex* to 75 nm PS NPs: P450s were induced by low concentrations (0.1-0.5 mg/L) and inhibited at high concentrations (1-2 mg/L) of NPs (Wu et al., 2019). An antioxidant response mediated by GST and other antioxidant enzymes triggered by MPs and NPs is widely reported in literature in several crustacean species (Chae et al., 2019; Jeong et al., 2017, 2016; Z. Liu et al., 2020b). Carboxylesterase 4 (CES4) belongs to the type-B carboxylesterase family, which have a key role in xenobiotics biotransformation and have been considered a valid biomarker of pesticide exposure (Barata et al., 2004; Vioque-Fernández et al., 2007b). In crustaceans, CES hydrolyzes juvenile hormone methyl farnesoate, which regulates development and molting (Homola and Chang, 1997; Tao et al., 2017). The only record of CES involvement in nanoplastics response was recently provided by Varó and collegues on *Artemia franciscana* (Varó et al., 2019). Exposure of brine shrimp larvae to amino-modified PS NPs (50 nm; 0.1–10 mg/L) for 48h or 14d resulted in oxidative stress induction and carboxylesterase and cholinesterase inhibition. Considering that larvae showed multiple molting and abnormal development, authors suggested that PS NPs may induced endocrine disruption mediated by CES inhibition and the consequent deregulation of methyl farnesoate levels (Varó et al., 2019). In this study, effects of PS NPs on molting were not assessed, due to the limited time of exposure. Moreover, differently from Varó and collegues CES resulted upregulated, possibly because of the low concentration of NPs used. Thiopurine S-methyltransferase (TPMT) is another phase II biotransformation enzyme. Even if its endogenous substrates as well as its biological role remain unknown, TPMT is widely studied for its specialized role in the S-methylation of thiopurine compounds (Jancova et al., 2010).

In this study, NP exposure induced the over-expression of several genes involved in detoxification, with a more marked response in male crayfish as compared to females. Our results further support the hypothesis that the P450 system may play a role in detoxification from NPs, even though the molecular pathway underlying cytochrome's response remains unclear. The distinct expression of cytochrome P450 49a1 may indicate a different response of the two sexes to PS NP exposure. Even though the P450s mode of action in NP response has

not been yet clarified, GST triggering is likely to be linked to the detoxification of reactive and oxygen radicals. Regarding CES4 and TPMT, the existing knowledge was not sufficient to hypothesize their direct involvement in PS NP detoxification.

2.4.2.2.3 Oxidative stress-related genes

Oxidative stress is one of the most common hurdles encountered by cells and organisms (Lushchak, 2011). The removal of non-functional oxidized cytosolic proteins is an essential part of the antioxidant defenses of cells (Grune, 2000). The ubiquitin-proteasome system (UPS) and autophagy are the two major degradation pathways maintaining cellular protein homeostasis (Kwon and Ciechanover, 2017). In the hepatopancreas of female crayfish, the UPS was altered by PS NP exposure. Indeed, six transcripts annotated as *E3 ubiquitin-protein ligase, 26S proteasome non-ATPase regulatory subunit 10*, *ubiquitin carboxyl-terminal hydrolase,* and *aminopeptidase N* resulted upregulated (Table A17). Besides, the upregulation of the *activating transcription factor 4* (ATF4) (Table A17), illustrated in section 2.4.2.2.2, may be linked to the promotion of transcription of genes involved in autophagy (B'Chir et al., 2013), and the resistance to oxidative stress in the unfolded protein response (UPR) directed by PERK (Fusakio et al., 2016; Harding et al., 2003). The alteration of the intracellular protein degradation system has been reported in crustaceans exposed to several stressors (Götze et al., 2017; Hansen et al., 2008; Jiao et al., 2019; Xu et al., 2017; Zhao et al., 2017). Nevertheless, to the best of our knowledge, this is the first investigation reporting such a clear response of the UPS to NPs in crustacea. Actually, only a recent proteomic analysis has described a similar response to MPs in the gills of zebra mussel (Magni et al., 2019). It has been outlined that intracellular proteolysis shows a biphasic response to oxidative stress: moderate stress promotes upregulation of the ubiquitination system and proteasome activity, while UPS is inactivated by sustained oxidative stress (Shang and Taylor, 2011). Thus, our results suggest that UPS was regulated under polystyrene NP exposure as an antioxidant defense in order to maintain cellular integrity. Furthermore, molecular chaperones transcription was altered in crayfish: *sacsin-like* was upregulated in females, while *heat shock protein HSP 90-alpha* was downregulated in males (Table A17). HSP90 and sacsin display several regions of sequence similarities and thus share molecular chaperone ability function and the capacity to interact with the proteasome (Anderson et al., 2011; Imai et al., 2003). Specifically, HSP90 has been proposed to play a principal role in the assembly and maintenance of the 26S proteasome (Imai et al., 2003), while sacsin is involved in protein quality control in the UPS and chaperone-mediated autophagy (Morani et al., 2019). The higher relative expression of sacsin in NP exposed female crayfish

is in line with the upregulation of the other proteasome components described above. Another explanation of sacsin overexpression may lie in its recently suggested role in mitochondrial dynamics and bioenergetics, promoting mitophagy following mitochondrial damage (Morani et al., 2019). Indeed, RNA-seq revealed two other DEGs involved in mitochondrial dynamics, namely *peptidyl-prolyl cis-trans isomerase F* (PPIF) and *MICOS complex subunit mic25-a* (Mic25/CHCHD6), which were respectively up- and downregulated in exposed females (Table A17). PPIF is a major modulator of the mitochondrial permeability transition pore (MPTP) (Gutiérrez-Aguilar and Baines, 2015) and it is reported to mediate Ca^{2+} overload- and oxidative damage-induced cell death (Baines et al., 2005) through the transient or permanent depolarization and rearrangement of the cristae (Azzolin et al., 2010). Mic25/CHCHD6 is a subunit of the mitochondrial contact site and cristae organizing system (MICOS), which is deputed to create crista junctions, in order to maintain cristae morphology, and to form contact sites with the mitochondrial outer membrane (An et al., 2012, Ding et al., 2015; Muñoz-Gómez et al., 2015). Overall, several authors reported that MPs and NPs are able to alter cellular membrane integrity by inducing lipid peroxidation in a concentration-dependent manner (Jeong et al., 2018; Y. Li et al., 2020a; Lin et al., 2019; P. Yu et al., 2018). In *Brachionus koreanus*, Jeong and colleagues unearthed NP-induced damage to mitochondrial membrane integrity, which is in line with our results (Jeong et al., 2016). Lastly, one transcript annotated as *arylsulfatase B-like* (ARSB-like) resulted also downregulated in females (Table A17). In mammals, ARSB deficiency has been associated with pathological processes (Bhattacharyya et al., 2016). In particular, it has been reported that ARSB downregulation inhibits mitochondrial membrane potential and oxygen consumption (Bhattacharyya et al., 2016) as well as leads to increased reactive oxygen species (ROS) production and activation of the MAPK signaling pathway (Q. Wang et al., 2019). Although its specific role in crayfish is unknown, it seems reasonable to speculate the ARSB contribution to oxidative stress. Mounting evidence support the idea that oxidative stress is one of the molecular mechanisms underlying the toxicity of NPs (Hu et al., 2020). PS NPs caused the over-production of ROS and activates the downstream mitogen-activated protein kinases MAPK signaling pathway in *D. pulex* (75 nm PS NPs; 0.1-2 mg/L for 48h, Z. Liu et al., 2020a), *B. koreanus* and *Paracyclopina nana* (50 nm PS NPs; 0.1-20 mg/L for 24h, Jeong et al., 2018, 2017, 2016). The gene expression of antioxidant enzymes, including GST which was found to be upregulated in male crayfish in this study, displayed an initial rise and a subsequent decline with increasing NPs dose in *D. pulex* (Z. Liu et al., 2020b) and *M. nipponense* (75 nm; 5-40 mg/L for 28d, Li et al., 2020a), suggesting that high nanoplastic concentrations can overwhelm antioxidant systems and induce loss of

compensatory mechanisms, but lower concentration induces antioxidant response. Despite our investigation used a concentration that lies the lower range of the ones used in cited NP toxicity studies, a mild antioxidant response was visible in crayfish. This seems to be interconnected with ER stress, protein degradation, and possibly mitochondrial dysfunction, which are known to be frequently related (Chaudhari et al., 2014; Liang et al., 2016).

2.4.2.2.4 Lipid metabolism and oogenesis-related genes

Environmental stress can affect the optimal allocation of energy: under moderate stress, basal maintenance takes priority over other processes, including growth, reproduction, or storage and it can negatively affect the organism's fitness (Sokolova, 2013). Crustacean hepatopancreas is the principal organ for lipid synthesis (González-Baró and Pollero, 1993) and storage (Cheng et al., 1998). In the current study, a dysfunction of the lipid metabolism pathway emerged in females (Table A17). Three genes coding for proteins involved in glycerolipids biosynthesis were downregulated: *long-chain-fatty-acid—CoA ligase* (ACSBG2), *glycerol-3-phosphate acyltransferases 3* (GPAT3), and *phosphoethanolamine N-methyltransferase-like* (Athamena et al., 2011; Mashek et al., 2007; Pellon-Maison et al., 2009; J. Yu et al., 2018). ACSBG2 is a member of acyl-CoA synthetase bubblegum protein family which is deputed to activate long-chain fatty acids (Mashek et al., 2007), generating acyl-CoA, a key intermediate in the biosynthesis of cellular lipids as well as in the degradation of fatty acids via the β-oxidation (Zheng et al., 2005). GTPA3 represent one of the two ER isoforms of the GPAT family which catalyze the acylation of glycerol-3-phosphate and acyl-CoA in the first step of glycerolipids synthesis (Pellon-Maison et al., 2009; J. Yu et al., 2018). Finally, phosphoethanolamine N-methyltransferase participates in phosphatidylcholine biosynthesis *via* phosphatidylethanolamine methylation (Athamena et al., 2011). Conversely, *gamma-butyrobetaine dioxygenase-like* (BBOX1), which play a role in the carnitine biosynthetic pathway (Lindstedt and Lindstedt, 1970; Vaz et al., 1998), was upregulated. Carnitine allows fatty acids transfer into the mitochondrial matrix where β-oxidation occurs (Bremer, 1997, 1983). Changes in carnitine concentration affect the rate of mitochondrial β-oxidation and therefore energy metabolism (Clark et al., 2017). The upregulation of BBOX1, in association with the downregulation of ACSBG2, GTPA3, and phosphoethanolamine N-methyltransferase likely reflects an increased demand for energy in the PS NP exposed crayfish as compared to control. Besides, a reduced biosynthesis of phosphatidylcholine, as a consequence of phosphoethanolamine N-methyltransferase downregulation, can affect membrane fluidity.

Consistently, four transcripts all annotated as *vitellogenin* (Vtg) were downregulated in the hepatopancreas of female crayfish (Table A17), while male crayfish did not show a marked response in this regard. Vtg is the precursor of vitellin, which is one of the major protein components in yolk, and it is closely involved in the maturation of oocytes (Jimenez-Gutierrez et al., 2019). Vtg biosynthesis is the first step of vitellogenesis and occurs both in the ovary and in the hepatopancreas of *P. clarkii* (Cai et al., 2016; Shen et al., 2014). Given that vitellus is the main energy reserve for the developing embryos, alteration in the vitellogenesis balance may result in significant reproductive impairment (Arambourou et al., 2020). Evidence of reproductive disfunction in rotifers, bivalves, crustaceans, and fish exposed to MPs and NPs have been focusing on a reduced fecundity (Cole et al., 2015; Heindler et al., 2017; Jeong et al., 2017; Lee et al., 2013; Sussarellu et al., 2016) and fertilization success (Tallec et al., 2018), fewer total offspring and offspring performance (Au et al., 2015; Cong et al., 2019; Ziajahromi et al., 2017) including increased embryonic malformations (Besseling et al., 2014; Cui et al., 2017), and a delayed reproduction time (Jaikumar et al., 2019; Jeong et al., 2016; Liu et al., 2019a). Micro- and nanoplastics have been suggested to cause endocrine disruption directly or indirectly through leaching of plastic additives and/or associated chemicals (Amereh et al., 2019; Chen et al., 2019; Mak et al., 2019; Rochman et al., 2017, 2014; Jun Wang et al., 2019). A study by Wang and colleagues reported downregulation of Vtg expression in the liver of female medaka after PS MP exposure, while an upregulation was noticed in males (Jun Wang et al., 2019). Similarly, Rochman et al. found downregulation of Vtg expression in the liver of female medaka exposed to virgin or weathered MPs, but no effect was reported in males (Rochman et al., 2014). Another study by Rochman et al. (Rochman et al., 2017), revealed a lower vitellogenin protein content in the liver of *Acipenser transmontanus* females fed with clams previously exposed to different MP polymers virgin or spiked with polychlorinated biphenyls for 28 days. Further investigations by Sarasamma et al. and Mak et al. addressed a significantly enhanced Vtg expression in zebrafish exposed to PS NPs and PE MPs, respectively (Mak et al., 2019; Sarasamma et al., 2020). Unfortunately, only Mak and collegues reported the sex of zebrafish (males) (Mak et al., 2019), while no information was provided by Sarasamma et al. (Sarasamma et al., 2020). Furthermore, an upregulation of Vtg expression was described in *Daphnia magna* after micro- and nanopolystyrene exposure (Coady et al., 2020; Z. Liu et al., 2020a). Even though a histopathologic analysis of crayfish ovaries was not conducted in this study, a significantly lower expression of vitellogenin transcripts in both ovary and hepatopancreas was previously associated with a clear inhibition of ovarian growth in *P.*

clarkii exposed to the insecticide atrazine (Silveyra et al., 2018), confirming the primary role of vitellogenin in oogenesis for this species.

A very good illustration of a significant shift in energy allocation induced by microplastic exposure was provided by Sussarellu and colleagues in Pacific oysters (Sussarellu et al., 2016). After 2-month exposure to MPs during gametogenesis (2-6 μm; 0.023 mg/L), oyster energy flows were relocated to organism maintenance and structural growth at the expense of reproduction, leading to impacts on reproductive health indices (i.e., quantity and quality of gametes produced, Sussarellu et al., 2016). Similarly, a proteomic analysis on the zebra mussel showed that MPs interfered with glycolysis and the Krebs cycle (Magni et al., 2019). In *D. magna* neonates, the glycometabolic changes enriched by PS NP exposure were suggested to increase energy production as a way to counteract NP toxicity (Liu et al., 2021a). Likewise, we suppose that the altered lipid metabolism in crayfish has to do with an increased energy demand for the innate immune response, and also to maintain cellular homeostasis. Altogether, our findings are in line with the data available in literature and may suggest that *P. clarkii*'s reproduction efficiency could be threatened by the exposure to nanoplastics. Undoubtedly, further phenotypic data collection is required to support our inference.

2.4.2.2.5 Hemocyanin

Hemocyanin (Hc) expression was upregulated in the hepatopancreas of female and male crayfish (Table A17). Hc is the main respiratory pigment of arthropods, primary synthetized in hepatopancreas and then released in hemolymph (Gellissen et al., 1991; Qin et al., 2018). Although having a primary role in oxygen transport, *P. clarkii* Hc exhibited antibacterial capacity by promoting phagocytosis and exerting phenoloxidase activity (Qin et al., 2018). In the current study, the overexpression of Hc may indicate either that challenged crayfish had a greater need for tissue oxygenation, or that Hc took part in the immune response and homeostasis maintenance following NP exposure. Consistently with our results, crabs exposed to MPs showed an enhanced Hc expression in the hepatopancreas (Liu et al., 2019a), and an altered Hc hemolymph content, albeit the magnitude and the direction of change (i.e., an increase or a decrease) varied with the exposure duration or dose level, as well as with the different particle surface coatings (COOH or NH_2) (Liu et al., 2019a; Watts et al., 2016). Along with Hc, pseudohemocyanins (PHc) belong to the arthropod hemocyanin superfamily, which further comprises phenoloxidases and the insect hexamerins (Burmester, 2015, 2002). PHcs have lost the ability to bind copper and have been proposed to be involved in molting and reproduction as storage proteins (Burmester, 1999). Here, PHc underwent a different expression

regulation based on sex, and particularly it was found to be upregulated and downregulated in females and males, respectively. The limited existing knowledge on PHc function in crustaceans, together with the diverse direction of the alteration between males and females in the current study, prevent us from inferring the possible role of PHcs in response to NP in crayfish.

2.4.2.2.6 Transcription and translation-related genes

Just like in hemocytes, PS NPs caused an alteration in gene transcription and translation in the hepatopancreas of both males and females. Two RNA helicases, *NFX1-type zinc finger-containing protein 1-like*, *la-related protein 6-like* (LARP6), and an RNA polymerase (RPABC5) were all upregulated in the hepatopancreas of females, while *serine/arginine repetitive matrix protein 1-like* was downregulated (Table A17). In males, the *transcription activator BRG1-like*, also part of the ATP-dependent helicases superfamily, was downregulated, while the *RNA-binding protein squid-like* was upregulated (Table A17). Ribosomal proteins remain consistently upregulated in all groups of samples analyzed (Table A17). As stated above, an enrichment in ribosomal proteins, both from a transcriptomic and proteomic perspective, was pointed out in several other investigations of microplastic exposure in zebrafish (LeMoine et al., 2018), the zebra mussel (Magni et al., 2019), and marine copepod *T. japonicus* (Zhang et al., 2019).

2.5. Conclusions

The present study represents the first attempt to unravel the effects of polystyrene nanoparticles at both transcriptomic and physiological levels in a freshwater decapod species. In an integrated approach, RNA sequencing data were complemented by physiological responses, revealing that after 72h exposure to relatively low concentrations of PS NPs, the studied species was able to face the induced stress, not exceeding generic stress thresholds. Our results evidence the power of RNA-Seq analysis in ecotoxicology to disclose minor physiological, immunological, and molecular alterations induced by environmental contaminants such as nanoplastics. In the red swamp crayfish, we reported that PS NPs can trigger transcriptomic pathways linked to immune response, induce oxidative stress and interfere with gene transcription and translation, protein degradation, lipid metabolism, oxygen demand, and potentially reproduction. Particularly, a quite clear transcriptomic response to NPs emerged as a strong downregulation of vitellogenin expression in female crayfish, which can lay the basis for a deeper exploration of the potential impacts of polystyrene nanosized particles at a population level. Nevertheless, these

preliminary results need to be supported by additional data obtained from the analysis of a larger number of individuals and longer exposure periods. Further studies examining the phenotypic and ecological effects of nanoplastics on decapod crustaceans are of great interest, as these species play a central role in aquatic food webs and represent potential vectors of contaminants to higher trophic levels.

Chapter 3

Evaluation of nanoplastic toxicity on Mediterranean mussel (*Mytilus galloprovincialis*) larvae: an RNA-Sequencing approach

3.1. Introduction

Bivalves are widely distributed and play a critical ecological role from freshwater to marine ecosystems. They have long been recognized as valuable bioindicators of pollution and more recently as important model species for monitoring pollution from nanomaterials (Baun et al., 2008; Canesi et al., 2012; Rocha et al., 2015), as well as micro- and nanoplastics (Bråte et al., 2018b; Sendra et al., 2021). Key features that make them suitable for ecotoxicological studies of nanoparticles toxicity are their large filtration capacity (Rosa et al., 2018; Setälä et al., 2016) and their strong and complex innate immune system (humoral and cellular defenses), which is similar to that of vertebrates (Canesi and Procházková, 2013). As filter feeders, both farmed and wild bivalves have been reported to accumulate MPs in nature, raising concern about potential transfer to humans (Browne et al., 2008; Lusher et al., 2017; Rochman et al., 2015; Sendra et al., 2021; Van Cauwenberghe et al., 2015; Zhao et al., 2018). Plastic particles uptake can occur through the gills or MPs can be inhaled via the siphon and transported to the mouth. Then, MPs can be further translocated and transported to other organs and tissues, even via the hemolymph (Sendra et al., 2021). Particle removal has been demonstrated to be size-dependent, with longer residence times for smaller particles (Ward et al., 2019). Similarly, MP and NP accumulation depends on their dimensions. Larger particles (> 1 μm) are mainly internalized in the lumen of the stomach (Gonçalves et al., 2019; González-Fernández et al., 2018; Pedersen et al., 2020a; Sussarellu et al., 2016), while NPs smaller than 1 μm have been recorded in the gills, visceral mass, muscle, hepatopancreas, foot and mantle, in addition to the digestive tract (Al-Sid-Cheikh et al., 2018; Gaspar et al., 2018; Z. Li et al., 2020; Sendra et al., 2020). Exposure to MPs and NPs has been found to induce shifts at physiological, histopathological, molecular levels and even to impact bivalve life cycle (Sendra et al., 2021). MPs can cause a reduction in energy reserves in the form of lower lipid content in sediment-dwelling bivalves (Auclair et al., 2020; Bour et al., 2018) and a shift in energy allocation from reproduction to structural growth in oysters, affecting fecundity and offspring performance during larval stages (Sussarellu et al.,

2016). Altered filtration rates (Green et al., 2017; Rist et al., 2016; Woods et al., 2018) and reduced byssus production (Green et al., 2019; Rist et al., 2016; Webb et al., 2020) have been described due to plastic ingestion. Structural changes in the digestive gland and gills, intestine and stomach due to MP and NP exposure have been suggested (Bråte et al., 2018a; Gonçalves et al., 2019; González-Soto et al., 2019; Z. Li et al., 2020; Paul-Pont et al., 2016). Bivalves represent a potential transfer of NPs through food chains (Chae et al., 2019; Farrell and Nelson, 2013) and, owing to their role as ecosystem engineers, the induced effects are likely to permeate beyond the individual organism (Green et al., 2017). Field mesocosm experiments have recorded changes in structure, diversity, abundance, and biomass of bivalve associated benthic invertebrate assemblages under MP exposure (Green, 2016; Green et al., 2017). Antioxidant activity, lipid peroxidation, and neurotoxicity are regularly studied through common biomarker approaches (Brandts et al., 2018; Cole et al., 2020; Z. Li et al., 2020; Magni et al., 2018; Ribeiro et al., 2017). In addition, hemocytes are widely used as models for in vitro studies. Cell viability, ROS production, phagocytosis activity, apoptosis, lysosome membrane stability and granulocyte/hyalinocyte ratio are the most commonly measured responses (Canesi et al., 2016; Paul-Pont et al., 2016; Sendra et al., 2020; Sussarellu et al., 2016). In the mussel *M. galloprovincialis*, amino-modified polystyrene particles were rapidly taken up by hemocytes, and provoked altered lysosomal function and phagocytic activity, oxyradical production, and even induction of pro-apoptotic processes (Canesi et al., 2015). Interestingly, it has been suggested that *M. galloprovincialis* hemocytes may develop immunological memory to exhibit compensatory mechanisms and maintain immune homeostasis after repeated exposure to MPs or NPs (Auguste et al., 2020; Détrée and Gallardo-Escárate, 2018). Although most of the literature focuses on the effects of MPs and NPs on adult organisms, assessing toxicity in the early life stages should be a more common practice in ecotoxicology, as sensitivity to contaminants can vary by life cycle and early life stages are critical for species and ecosystem development (Canesi and Corsi, 2015; Sendra et al., 2021). Indeed, gametogenesis and fertilization rates (González-Fernández et al., 2018; Sussarellu et al., 2016; Tallec et al., 2018), as well as embryogenesis factors such as hatching rates, embryo-larval development and shell formation (Balbi et al., 2017; Gardon et al., 2020; Luan et al., 2019; Rist et al., 2019; Sussarellu et al., 2016) are already known to be impaired by MP and NP exposure. As indicated earlier, understanding the specific effects on early life stages would be valuable in pursuing an implementation of an adverse outcome pathway to characterize toxicity pathways of NPs in aquatic organisms (Galloway and Lewis, 2016; Sendra et al., 2021). In this regard, transcriptomics can play a major role in the formulation of AOPs (Vinken, 2019).

This chapter illustrates a transcriptomic investigation on trocophora larvae of the mussel *M. galloprovincialis* under NPs exposure, which integrates and complements a previous study by Balbi and colleagues (Balbi et al., 2017). The previous work was the first to investigate the potential effects of exposure to aminomodified polystyrene NPs (PS -NH2) on early embryonic development in the mussel *M. galloprovincialis* in a 48 h embryotoxicity assay using a morphological and gene expression approach. The aim of this study was to deeper investigate nanoplastics early alterations at the molecular level in the broader perspective by using the transcriptomic approach. Transcriptomic data may help to better elucidate the molecular pathways underlying the toxicity of NPs, but it may also identify a set of biomarkers for more specific toxicity screening (Vinken, 2019).

3.2. Materials and methods

3.2.1. Embryotoxicity test

The exposure test was conducted at the University of Genova. All detailed information can be found in Balbi et al. (2017). Briefly, unlabeled amino-modified polystyrene nanoparticles (PS-NH_2) 50 nm in size were purchased from Bangs Laboratories and appropriately characterized. Sexually mature mussels (*M. galloprovincialis*) were retrieved from an aquaculture farm in the Ligurian Sea (La Spezia, Italy) and acclimatized in laboratory conditions for gamete collection in static tanks containing aerated artificial seawater (ASW, 1 L/animal) (pH 7.9-8.1, 36 ppt salinity, 16 ± 1 °C) (ASTM, 2004) for a maximum of two days. Eggs were fertilized (egg:sperm ratio 1:10) in polystyrene 6-well plates and fertilization success was assessed by microscopical inspection. Fertilized eggs 30 min post-fertilization (pf) were exposed to a concentration of 0.150 mg/L PS-NH_2, by adding in each well a proper amount of a 20 g/L concentrated stock solution previously prepared in MilliQ water. Concentration was chosen as it was close to the EC_{50} value at 48 hours pf (hpf) obtained in a parallel experiment (EC_{50} = 0.142 mg/L) within the same study (Balbi et al., 2017). Control wells contained only ASW. Trocophora and D-veliger larvae were collected by a nylon mesh (20 µm pore-filter) at 24 and 48 hpf, respectively. For each condition, larval suspensions from three wells were pooled in order to achieve approximately 7000 embryos per replicate and centrifuged at 800 × g for 10 min at 4 °C. Larval pellets were lysed in 1 mL of the TRI Reagent (Sigma Aldrich, Milan, Italy) and total RNA was extracted following manufacturer's instructions. Four replicates of the experiment were performed.

3.2.2. Library generation and Illumina *de novo* sequencing

The extracted RNA was quantitatively and qualitatively evaluated at the University of Trieste. For this purpose, a Qubit® 2.0 fluorometer (Life Technologies, Carlsbad, CA, USA) with the Qubit® RNA HS Assay Kit (Catalog No. Q32852; Invitrogen; Thermo Fisher Scientific, Inc.) and an Agilent RNA 6000 Nano Kit (Catalog No. 5067-1511; Agilent Technologies, Palo Alto, CA, USA) for the 2100 Bioanalyzer System were used. This initial analysis revealed that RNA extracted from veliger larvae was degraded and thus lacked sufficient quality standards for library preparation. Therefore, only RNA samples from trochophora larvae (N = 8) were used for *de novo* transcriptome assembly and subsequent DEG analysis. Between 0.5 and 1 µg of total RNA was used for the preparation of Illumina-compatible cDNA libraries. Libraries generation was performed using the SENSE mRNA- Seq Kit V2 (Catalog No. 001.96; Lexogen GmbH, Vienna, Austria), according to the manufacturer's instructions.

Despite the use of ≥500 ng RNA, the low-input protocol modifications recommended for total RNA inputs of 50 ng or less were followed. In our experience, these modifications actually resulted in higher quality libraries. Briefly, the first step consists of a highly specific, magnetic bead-based poly(A) selection step that allows removal of non-polyadenylated RNAs. Library generation begins with the random hybridization of starter/stopper heterodimers containing Illumina-compatible linker sequences to the poly(A) RNA still bound to the magnetic beads. During the reverse transcription and ligation step, the starter is extended to the next hybridized heterodimer, where the newly synthesized cDNA insert is ligated to the stopper. The size of the insert is determined by the distance between the starter and stopper binding sites, so further RNA fragmentation is not required. Size selection is achieved by modulating the conditions for the reverse transcription/ligation reaction, which in turn results from two different buffer inputs. We followed the adapted protocol for sequencing lengths up to PE100. A second strand synthesis is performed to detach the library from magnetic beads, and the library is purified. Finally, the cDNA library was amplified to introduce the sequences needed for cluster generation and i7 indices for multiplexing. The final library was purified from PCR components. The quality of purified libraries was assessed by size distribution and absence of primer species using an Agilent High Sensitivity DNA Kit (Catalog No. 5067-4626 and 5067-4627; Agilent Technologies, Palo Alto, CA, USA) for the 2100 Bioanalyzer System. To ensure consistent pooling of samples, the indexed cDNA libraries were quantified, normalized to 10 nM, and pooled in equal volumes. The concentrations of the libraries ranged from 3.40 to 10.8 ng/µL. High-throughput sequencing was performed as paired-end 150 base pairs (bp)

sequencing using a NovaSeq™ 6000 platform (Illumina, San Diego, CA, USA) at CBM S.c.r.l. (Area Science Park, Trieste, Italy) using standard protocols.

3.2.3. Bioinformatic analysis

3.2.3.1 Preparing sequencing reads

Read demultiplexing was carried out at the CBM Institute. Initial quality control of the raw sequencing reads in FASTQ format was accomplished using fastQC (v. 0.11.9, Andrews, 2010) plus the MultiQC tool (v. 0.9, Ewels et al., 2016). The trimming procedure was performed using fastp v. 0.20.0 (Chen et al., 2018) and included the removal of residual Illumina adapters, ambiguous nucleotides (a maximum of 2 ambiguous nucleotides were allowed), poly(X) sequence stretches and short reads (a minimum length of 75 nucleotides was set). In addition, the raw reads were quality-trimmed at the 3' end according to the default fastp options (> 40% of the bases in each read have PHRED > 15). Additional 5 and 11 nucleotides were discarded at 3' and 5' end, respectively, to remove a compositional nucleotide bias observed in the preliminary quality evaluation. A further filtering procedure was required to remove any remaining *non*-mRNA contamination, which was evident by a high degree of duplication. A total of 72 sequences consisting of *M. galloprovincialis* complete mitochondrial genome and ribosomal RNA sequences, were retrieved from the National Center for Biotechnology Information (NCBI) (http://www.ncbi.nlm.nih.gov/taxonomy, accessed 29 March 2020) and clustered by similarity (identity threshold was set to 0.99) using CD-HIT-EST program from the CD-HIT software bundle (Fu et al., 2012; Li and Godzik, 2006), resulting in 28 clusters. Trimmed reads were mapped against the aforementioned clustered sequences using the Salmon pseudo-mapping software tool (v. 0.14.1, Patro et al., 2017) and only the unmapped reads were saved for subsequent analysis. The average mapping rate was 17.8%. The quality of the filtered reads was further assessed using fastQC (v. 0.11.9, Andrews, 2010) plus MultiQC (v. 0.9, Ewels et al., 2016).

3.2.3.2 *De novo* assembly and functional annotation of *M. galloprovincialis* trocophora transcriptome

Before assembly, the reads files were concatenated by keeping forward and reverse reads separate to obtain two different reads files. To reduce the computational resources required for transcriptome assembly, the reads files were normalized using bbnorm from the bbtools suite (https://jgi.doe.gov/data-and-tools/bbtools/), reducing the maximum number of copies for each read to 100. *De novo* assembly of processed reads was performed with Oyster River Protocol

(ORP) (v. 2.3.1, MacManes, 2018). ORP combines several de Bruijn graph-based assemblers that work by chopping up reads into shorter units of uniform size, called *k*-mers (substrings of length k), and then build a de Bruijn graph that allows reconstruction of the transcript sequences (Pevzner et al., 2001). For this type of assemblers, *k* is the most significant parameter (Chikhi and Medvedev, 2014). In general, larger *k*-mers produce more reliable and accurate transcripts by reducing ambiguities in the graph between similar regions (high specificity) and preventing contigs from breaking due to coverage gaps or ambiguities (multiple occurrences of a single *k*-mer). However, large *k*-mers are more sensitive to sequencing errors, heterozygosity, and coverage, and assembly of rare transcripts may be compromised. ORP assembles the transcriptome using a multi *k*-mer multi-assembler approach that ultimately combines all unique assemblies into a final assembly. This method takes advantage of combining different assemblers, or assembler *k*-mer lengths, and seeks to optimize the strengths and weaknesses of each (MacManes, 2018). The assemblers used by ORP are Trinity (Grabherr et al., 2011) with a default *k*-mer length of 25, SPAdes in two different runs with *k*-mer sizes of 55 and 75 (Bankevich et al., 2012), and Trans-ABySS with a default *k*-mer size of 32 (Robertson et al., 2010). The four assemblies were automatically merged by the OrthoFuse scrip included in ORP, which forms groups of homologous transcripts and stores the highest scoring contig for each orthogroup to represent the entire group in downstream analysis (MacManes, 2018).

The completeness of the assembled transcriptome was assessed using BUSCO v. 3 (Benchmarking Universal Single-Copy Orthologs; Seppey et al., 2019) by comparison with the Metazoa database from orthoDB (v. 9, Zdobnov et al., 2017). BUSCO is based on the concept of single-copy orthologs that should be highly conserved among closely related species. It searches sequences from a genome, transcriptome or proteome against a database of orthologous genes (called BUSCOs) and provides quantitative measures of assembly completeness by assessing the relative content of complete (in single or multiple copies), fragmented and missing BUSCOs from the selected database of contigs.

The resulting non-redundant transcriptome of *M. galloprovincialis* trocophora larva was annotated using a custom pipeline (annot.aM) (https://gitlab.com/54mu/annotaM) developed by Dr. Samuele Greco at the Laboratory of Applied and Comparative Genomics at the University of Trieste. In detail, assembled transcriptome contigs were aligned to the UniProtKB/Swiss-Prot (Bateman, 2019) and OrthoDB (Zdobnov et al., 2017) databases for similarities using DIAMOND alignment tool (Buchfink et al., 2014). Likely coding regions within transcripts were predicted using TransDecoder (transdecoder.github.io) and the resulting

amino acid sequences were searched for similarities against the database mentioned above. Functional conserved domains were identified within the PFAM domain database (El-Gebali et al., 2019) using HMMER (Finn et al., 2011), while signal peptides were predicted using SignalP (Nielsen et al., 2019). UniProtKB/Swiss-Prot database alignments were used to assign Gene Ontology (GO) functional annotation.

3.2.3.3 Refinement of *M. galloprovincialis* trocophora transcriptome

Qualitative analysis of the original assembled transcriptome showed a persistent non-mRNA contamination revealed by overexpressed sequences. A more comprehensive list of mitochondrial and ribosomal sequences was created, by retrieving *M. galloprovincialis* 16S sequences (1124 sequences; NCBI query (("Mytilus galloprovincialis"[Organism] OR Mytilus galloprovincialis[All Fields]) AND 16S[All Fields]) AND animals[filter]) and *M. edulis* 16S sequences (717 sequences; NCBI query (("Mytilus edulis"[Organism] OR Mytilus edulis[All Fields]) AND 16S[All Fields]) AND animals[filter]) from NCBI (http://www.ncbi.nlm.nih.gov/taxonomy, accessed 30 March 2020), resulting in a total of 1841 sequences. The latter were clustered by similarity (identity threshold was set to 0.99) using CD_HIT_EST (Fu et al., 2012; Li and Godzik, 2006), resulting in 117 clusters, which were added to the 72 sequences used for trocophora larvae decontamination, finally yielding a list of 189 sequences. The assembled transcriptome was aligned against the 189 sequences using BLASTn (v. 2.10.1+) (Altschul et al., 1990; Barajas et al., 2019; Zhang et al., 2000) (E-value threshold 1e-50) and the mapping contigs (3055 sequences) were discarded from the transcriptome (Figure 4). To make the transcriptome more informative, consecutive filtering by contig length and expression was performed (Figure 4). The length filtering threshold was set at 250 bp to remove artificial constructs created during assembly, as most protein-coding transcripts (mRNA) are longer (e.g., the smallest mRNA in the human genome is 186 bp, Piovesan et al., 2016). Filtering by expression was performed by mapping reads to the transcriptome and then removing less expressed contigs based on different percentile thresholds (99^{th} to 90^{th} percentiles on the basis of transcripts per million, TPM, normalization). Finally, all resulting implemented transcriptomes were rechecked for completeness using BUSCO analysis (see paragraph 3.2.3.2.) and the relative percentage of annotated sequences was evaluated.

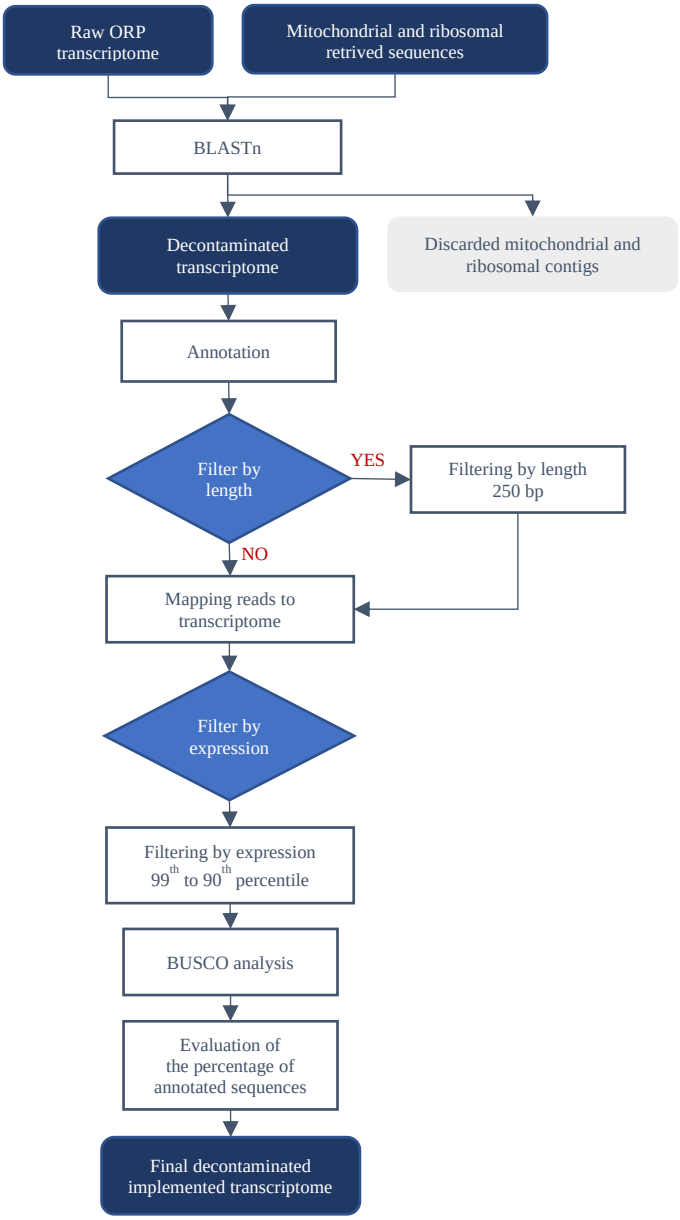

Figure 4: Workflow of M. galloprovincialis *transcriptome refinement.*

3.2.3.4 Differential gene expression analysis

Clean reads from each library were aligned to the decontaminated refined transcriptome of *M. galloprovincialis* trocophora larvae using the Salmon pseudo-mapping software tool (v. 0.14.1, Patro et al., 2017) with default mapping parameters. Mapping outcomes, as read counts per gene per sequencing library, were analyzed using the Bioconductor (v. 3.11) packages EdgeR (v. 3.30.3, McCarthy et al., 2012; Robinson et al., 2010) and DESeq2 (v. 1.28.1, Love et al., 2014) developed for R version 4.0.2 software (R Core Team, 2020). Differentially expressed genes were identified by setting the adjusted *p*-value (false discovery rate - FDR) and absolute fold change thresholds to 0.05 and 2, respectively.

3.3. Results

3.3.1. RNA sequencing results

A total of 224.8 million (M) read pairs were obtained from Illumina-based RNA-seq, with a mean of 28.1 (Range 9.9 – 83.5) M read pairs per sample and an average length of 146 ± 5 bp (Mean ± S.D.) (Table 3).

Table 3: General information on RNA-Seq output and read trimming and filtering results from MultiQC analysis. The percentage of retained reads are provided as compared to raw reads. Abbreviations are as follows: M – million; bp – base pairs.

Terms	Raw reads	After trimming	After filtering
Total number of read pairs (M)	224.8	214.7	176.5
Mean number of read pairs per sample (M)	28.1 (9.9 – 83.5)	26.8 (9.5 – 80.3)	22.1 (7.4 – 67.2)
Mean read length (bp)	146	126	125
% retained sequences	/	95.3 (83.9 – 97.6)	77.8 (71.6 – 80.5)
% GC content	41.7	40.9	39.3
Q20	95.2	96.4	/
Q30	89.3	90.6	/

After reads trimming and filtering to remove low-quality sequences, Illumina adapters, indeterminate bases, and residual non-mRNA contamination, 14,764,960 to 134,412,758 clean read pairs were retained per sample (Table B1), representing 71.6 – 80.5% of the raw read pairs (Table 3).

3.3.2. *De novo* transcriptome assembly, annotation, and refinement

A total of 352,908,360 clean reads (176,454,180 read pairs) were used to assemble the *de novo* nonredundant transcriptome, which originally included 295,289 contigs, with a N50 value of 605 bp (Table B2). This assembly represents the first transcriptome of *M. galloprovincialis* trocophora larval stage. A total of 91,040 (30.8%) unique sequences were functionally annotated at least in one of the selected databases (UniProtKB/Swiss-Prot, OrthoDB and PFAM) (Table 4).

Table 4: Summary of Illumina NovaSeq™ 6000 assembly and analysis of M. galloprovincialis *trocophora larvae transcriptome.*

Terms	Original transcriptome	Final transcriptome
Total number of contigs	295,289	117,887
%GC	34.83	34.72
Mean length (bp)	486.16	821.26
Median length (bp)	291	558
BUSCO parameters		
Complete (C)	90.1%	91.6%
Fragmented (F)	9.9%	6.3%
Missing (M)	0%	2.1%
Gene annotation		
Total annotated unique contigs	91,040	44,230
Annotated in UniProtKB	64,640	28,767
Annotated in GO	63,782	28,154
Annotated in PFAM	40,631	32,563
Annotated in OrthoDB	86,422	40,863

An additional refinement procedure was performed to maximize the informativeness of the transcriptome and resulted in 22 putative final implemented transcriptomes. Detailed information on the BUSCO completeness assessment and the relative number of annotated sequences can be viewed at Table B2. Based on the quality assessment results, the selected final refined transcriptome was obtained by filtering the original transcriptome by length (> 250 bp) and by expression (95^{th} percentile of most expressed genes) and comprised 117,887 contigs with a mean length of 821 bp and a median length of 558 bp (Table 4). BUSCO parameters indicated improved quality of the final assembly (Table 4). A total of 44,230 (37.5%) unique contigs were functionally annotated, with 28,768 (24.4% of total contigs) yielding significant BLASTx matches in UniProtKB and 32,563 (27.6% of total contigs) associated to one or more PFAM conserved domains (Table 4). The observed mapping rate averaged 68.5% (Table B1).

3.3.3. Analysis of differentially expressed genes (DEGs)

A preliminary Multidimensional Scaling (MDS) analysis was performed to visualize the level of similarity between samples based on gene expression profiles (Figure 5).

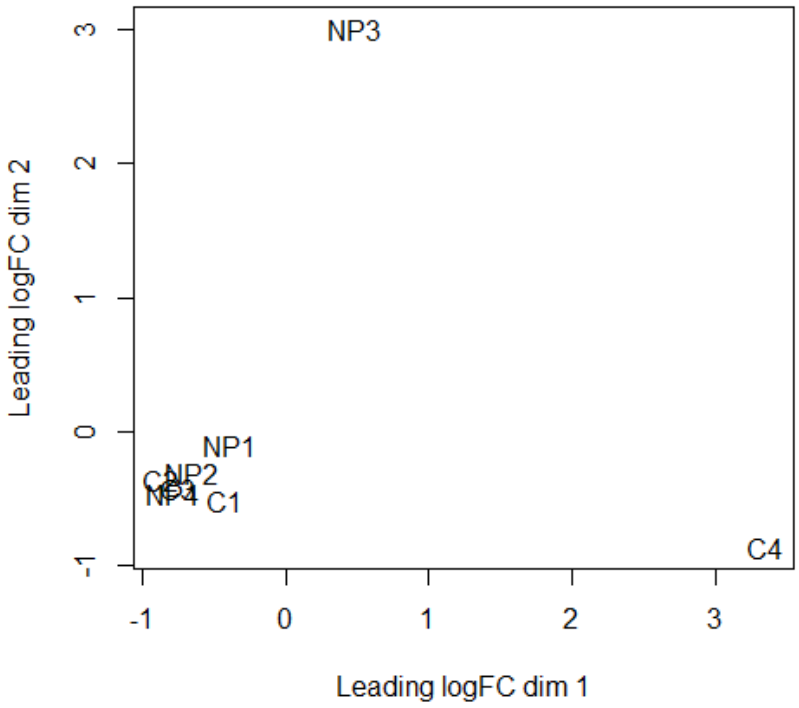

Figure 5: Multidimensional scaling (MDS) plot of M. galloprovincialis *samples with total counts used as expression value parameter. Distances correspond to leading log-fold-changes, i.e., the average (root-mean-square) of the largest absolute log-fold-changes, between each pair of samples. Abbreviations are as follows: NP, nanoplastic exposed group; C, control group.*

The MDS revealed no clear clustering or separation of samples due to experimental treatment along any dimension. (Figure 5). Only two samples, i.e., PS NPs exposed sample NP3 and control sample C4, showed a distinctly different expression pattern compared to all other samples. Differential expression analysis was performed between PS NP exposed larvae and control counterpart using two different packages: EdgeR and DESeq2. As expected from the MDS plot, the overall changes induced by PS NP exposure were negligible. Indeed, only 7 and 5 DEGs were identified by EdgeR and DESeq2 analysis, respectively (Table 5 and 6). Most of DEGs were upregulated (Figure 6). The two analyses shared 3 DEGs (i.e., TRINITY_DN3296_c0_g2_i1, TRINITY_DN527_c2_g1_i6 and NODE_77963_length_594_cov_56.077922_g53693_i0,) that were not functionally annotated.

Table 5: Differentially expressed genes found in M. galloprovincialis *trocophora larvae (N = 8) by EdgeR analysis, after exposure to 50 nm amino-modified polystyrene nanoparticles. Transcript name and length (in base pairs) are reported, together with the average values of expression given as Log_2 Counts PerMillion (CPM). Differential gene expression analysis results are provided as Log2 fold change and FDR p-value. When possible, a complete annotation is presented.*

Accession ID at NCBI	Length (bp)	Log2 CPM	Log2 fc	FDR p-value	Description	Species
TRINITY_DN3296_c0_g2_i1	1228	0.58	4.73	3.95E-08	Predicted protein	
TRINITY_DN527_c2_g1_i6	769	0.13	5.55	3.95E-08		
NODE_77963_length_594_cov_56.077922_g53693_i0	594	2.25	1.99	1.01E-03		
P51906	725	0.47	2.40	2.28E-03	Excitatory amino acid transporter 3	*Mus musculus*
Q17N71	679	-0.05	4.27	9.29E-03	Clustered mitochondria protein homolog	*Aedes aegypti*
P54145	2119	0.14	2.54	2.40E-02	Putative ammonium transporter 1	*Caenorhabditis elegans*
NODE_60894_length_691_cov_21.646104_g29349_i2	691	0.47	1.94	4.30E-02		

Table 6: Differentially expressed genes found in M. galloprovincialis *trocophora larvae (N = 8) by DESeq2 analysis, after exposure to 50 nm amino-modified polystyrene nanoparticles. Transcript name and length (in base pairs) are reported, together with the average values of expression given as Base mean: the average of the normalized count values, dividing by size factors, taken over all samples. Differential gene expression analysis results are provided as Log2 fold change and FDR p-value. When possible, a complete annotation is presented.*

Accession ID at NCBI	Length (bp)	Base mean	Log2 fc	FDR p-value	Description
NODE_77963_length_594_cov_56.077922_g53693_i0	594	65.06	1.99	4.26E-04	
TRINITY_DN3296_c0_g2_i1	1228	16.81	4.81	4.26E-04	Predicted protein
NODE_26887_length_1160_cov_17.644240_g13422_i0	1160	6.90	-6.58	5.05E-04	
TRINITY_DN527_c2_g1_i6	769	13.42	5.36	4.66E-03	
TRINITY_DN50_c0_g1_i10	1327	1169.81	1.12	1.71E-02	Hypothetical Chloroplast RF68

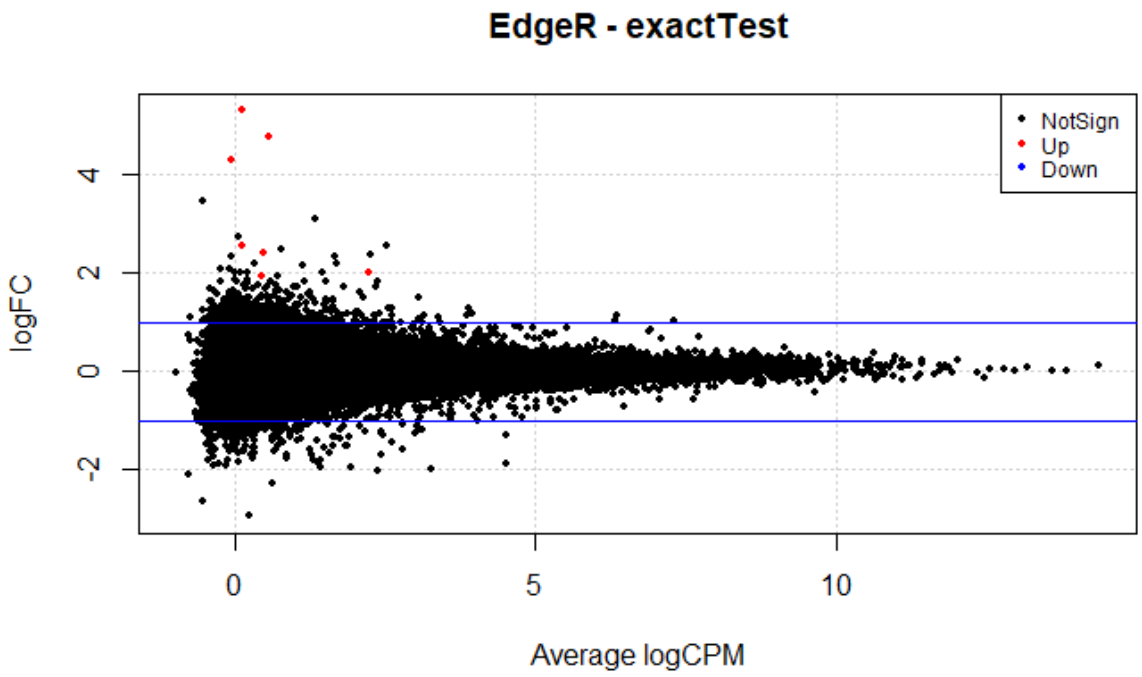

Figure 6: A mean-difference plot (MD-plot) of expressed genes generated using EdgeR package. The scatter plot represents log2 fold changes (on the y-axis) versus the log2 mean of normalized counts (log2 count per million) (on the x-axis) of each expressed gene. DEGs are in red.

3.4. Discussion

Bivalves, and *Mytilus* spp. in particular, have recently been proposed as human health models and bioindicators for microplastic studies (Fernández Robledo et al., 2019). The transcriptomic analysis performed in the current study implemented and complemented a previous work by Balbi and colleagues (Balbi et al., 2017). The main objective of the original work was to identify potential adverse effects of 50 nm amino-modified NPs, performing an exposure study during the early life stages of *M. galloprovincialis*, which are potentially the most sensitive stages of the organism to environmental perturbations (Balbi et al., 2016). The authors investigated the developmental effects from fertilized eggs to trocophora (24 hpf) to D-veliger (48 hpf) larval stages. The 48 h embryotoxicity assay examined a wide range of NPs exposure concentrations, from 0.001 to 20 mg/L and showed a PS NPs induced dose-dependent decrease in normal larval development. Specifically, the authors reported a biphasic effect PS-NH_2 on embryonic development at 48 hpf, with lower concentrations (from 0.001 to 1 mg/L) mainly inducing shell malformations and affecting shell mineralization, while higher concentrations caused a delay, even arrest, in larval development. An EC50 value of 0.142 mg/L was calculated and this concentration was chosen to identify possible pathways of PS NPs toxicity in early developmental stages of *M. galloprovincialis*, through a gene expression (Balbi et al., 2017)

and a transcriptomic (this study) approach. In the study by Balbi and co-workers, the transcription of 12 selected genes related to neuroendocrine signaling (serotonin receptor, 5-HTR), antioxidant defense (catalase, CAT; superoxide dismutase, SOD), biotransformation (glutathione transferase, GST; ABC transporter p-glycoprotein, ABCB), biomineralization (extrapallial protein, EP; carbonic anhydrase, CA), autophagy, growth and metabolism (serine/threonine-protein kinase, mTor), apoptosis (p53), immune response (Toll-like receptor, TLR-i), shell formation (chitin synthetase, CS), and immune response/intracellular digestion (lysozyme, LYSO) was evaluated. The overall induced response was not as pronounced. PS-NH_2 exposure induced downregulation of genes involved in early shell formation, i.e., CS, CA and EP, at 48 hpf, which was consistent with the morphological findings. In addition, significantly lower expression for ABCB and LYSO was observed at 48 hpf, indicating a possible impairment of immunocompetence, digestive function and phase 0 biotransformation of xenobiotics in D-veligers. No effects were observed in transcription of all other genes at 24 and 48 hpf.

In light of these results, our subsequent analysis aimed to evaluate possible changes induced by exposure to nanoplastics in a broader perspective by looking at the whole transcriptome of *M. galloprovincialis* trocophora larvae. Transcriptomic analyses have indeed recently gained much attention in ecotoxicological studies, as they allow us to better understand the mechanisms of action associated with exposure to contaminants (Prat and Degli-Esposti, 2019). In contrast to conventional gene expression analysis, which can only detect known sequences, RNA sequencing is a hypothesis-free approach capable of detecting both known and novel transcripts without requiring prior knowledge of sequence information. Furthermore, transcriptomic analysis allows the integration of expression levels of possible multiple isoforms of genes. Our analysis led to the assembly of the first *de novo* transcriptome of *M. galloprovincialis* at trocophora larval stage. The transcriptome shows high quality levels and a good proportion of accurately functionally annotated sequences, thus representing a valuable scientific resource for future studies on the early larval stages of this bivalve species.

Differential gene expression analysis did not yield noticeable results. Indeed, only a few DEGs were identified from the statistical comparison of expression levels between control and exposed trocophora larvae. This result seems to be in contrast with the developmental delay and impaired shell mineralization shown by microscopy analysis (Balbi et al., 2017). The explanation may be that, as suggested by Balbi and co-workers, embryotoxicity is not primarily dependent on the exposure time, but rather related to the transition from the trocophora stage

to the first shelled embryo D-veliger. Interestingly, PERMANOVA and permutation t-test analyses on gene expression data performed by Balbi et al. (2017) showed that the effects of PS-NH_2 were statistically significant only at the D-veliger stage and not at the trocophora stage, which is consistent with our results. In a similar work, 24 hpf and 48 hpf larvae of *M. galloprovincialis* were exposed to MPs (3 µm) at a concentration of 50 – 10,000 particles/mL and the differential expression of several genes involved in neuroendocrine signaling, shell biogenesis, lysosomal and immune responses was evaluated (Capolupo et al., 2018). In line with the results obtained by Balbi et al. (2017), expression profiles were found to be strongly dependent on embryonic development, and MP treatment accounted for only about 8% of the total variation. The largest changes in transcript expressions were found at 48 hpf, although antioxidant and neuroendocrine signaling responses peaked at earlier developmental stages. Ultimately, it must be taken into account that each RNA sample used in the current analysis was obtained by pooling more than 7000 individual larvae, which may have diluted the effects induced by PS NPs. A transcriptomic approach for early life stages has already been used to evaluate the toxicity of NPs in *D. pulex* neonates (< 24 h) (Liu et al., 2021a). *D. pulex* were exposed to 1 mg/L of ~70 nm PS NPs for 96 h, resulting in a total of 208 DEGs mainly involved in oxidative stress, immune defense, and glycometabolism. Differences with our results could be due to the slightly higher plastic concentration used and the longer exposure time. In addition, the analyses were performed on single neonates and this may have limited the dilution effect (Liu et al., 2021a).

Our results showed that the PS NPs effects were not pronounced in *M. galloprovincialis* at the trocophora stage under exposure to a concentration close to the EC50. Future work should be targeted to single-cell whole-transcriptome analysis (Wu et al., 2014) to investigate gene expression profiles at an even higher resolution. In addition, forthcoming studies should focus on the D-veliger larval stage, as the transition from the trocophora stage to the first D-shelled larva has been shown to be a more sensitive step to abiotic stressors.

3.5. Conclusions

Transcriptomic analyses are powerful tools in the field of ecotoxicology to investigate the physiological, immunological, and molecular alterations that are induced by environmental contaminants such as nanoplastics to aquatic organisms and thus for the development of an Adverse Outcome Pathway. In the current study, a complete transcriptome of *M. galloprovincialis* trocophora larval stage has been assembled for the first time and can represent

a valid scientific resource for future studies. The exposure to amino-modified PS NPs at a concentration close to the EC50 value of 0.142 mg/L did not cause noticeable shifts in the overall gene expression profile of exposed larvae. This result may be explained by a dilution effect of the responses due to the pooling of more than 7000 individual larvae in each sample. Otherwise, the early life stage of trocophora may not represent the most sensitive phase of mussel larval development. Further studies investigating transcriptomic response, together with phenotypic effects, of nanoplastics on aquatic organisms' early life stages are needed to better circumstantiate these results, given their susceptibility to stress and their key role in the marine and freshwater ecosystems.

Chapter 4

Concluding remarks and future outlooks

Nanoplastics (NPs) represent an emerging field of research in ecotoxicology. A brief overview of NPs issue is given in Chapter 1.

NPs are defined as the smallest fraction of plastic litter and may result in the aquatic environment as degradation products of larger plastic material. Therefore, they are highly heterogeneous particles in both composition and physical properties, which makes their identification and quantification in real environments a major challenge. The high exposure potential, together with the physical and chemical heterogeneity of NPs, the likely significant diffusive release of plastic additives and adsorbed substances, combined with their small size and enhanced accessibility to biological tissues, raise concerns about the potential health and environmental impacts of NPs. In the context of implementation of an environmental risk assessment, the evaluation should not disregard both the intrinsic hazard of the substance under consideration and the expected load and frequency of exposure by individuals or the environment.

In the absence of reliable environmental exposure estimates to date, ecotoxicological research has focused on defining a hazard assessment of NPs.

The research effort developed in this thesis was aimed at investigating the mechanism of toxicity of NPs, taking advantage of high-throughput sequencing technologies.

In an initial experiment, described in Chapter 2, individuals of the freshwater benthic crayfish *P. clarkii* were exposed to relatively low concentrations of NPs in a 72 h dietary exposure experiment. The red swamp crayfish is a widely distributed invasive species capable of tolerating highly disturbed environments (Gherardi, 2006) and was selected here as a representative non-model decapod of the freshwater ecosystem. Due to its high environmental tolerance, this species has long been used as a bioindicator of environmental pollution (Gherardi et al., 2002; Tricarico et al., 2008; Vioque-Fernández et al., 2007a) and has recently been documented to ingest plastic from soil (Lv et al., 2019; D. Zhang et al., 2020). The importance of recognizing the ecotoxicological impacts of plastic pollution in non-model species has recently been widely urged (Browne et al., 2015). In particular, ecotoxicogenomics studies are

mainly focused on model species, while ecologically relevant species, such as freshwater decapods, have received less attention. An integrated approach was conceived to assess the biological effects of polystyrene NPs, by analyzing both transcriptomic and physiological responses. At the physiological level, crayfish were able to compensate for the induced stress by not exceeding the generic stress thresholds. RNA-Seq analysis revealed an altered gene expression profile in hemocytes and hepatopancreas tissues of *P. clarkii* exposed to NPs. We reported that PS NPs can induce oxidative stress, trigger an immune response, and affect gene transcription and translation, protein degradation, lipid metabolism, oxygen demand, and possibly reproduction. Activation of oxidative stress pathways and inflammatory responses has been widely recognized as primary molecular mechanisms of NPs-induced toxicity, in agreement with our findings (Hu and Palić, 2020). In particular, we note an alteration of several genes related to the ubiquitin-proteasome system (UPS), one of the major degradation pathways for maintaining cellular protein homeostasis, which has not been described before. Moreover, a rather clear transcriptomic response to NPs emerged as a strong downregulation of vitellogenin expression in the hepatopancreas of female crayfish, which may indicate a shift in energy allocation induced by plastic exposure from reproduction to organism maintenance, as previously advocated for Pacific oysters (Sussarellu et al., 2016). This finding may provide the basis for a deeper exploration of the potential population-level effects of nanosized polystyrene particles. Overall, this study suggests that a low concentration of PS NPs may induce mild stress in crayfish, and sheds light on molecular pathways possibly involved in nanoplastic toxicity. The results obtained demonstrate the power of transcriptomic analysis in ecotoxicology to reveal minor physiological, immunological and molecular changes induced by environmental contaminants such as nanoplastics.

Chapter 3 examined the underlying mechanism of NPs toxicity in a sensitive early developmental stage of a key marine invertebrate species, the bivalve *M. galloprovincialis*. Bivalves are widely distributed and play a crucial ecological role from freshwater to marine ecosystems. Due to their large filtration capacity and strong and complex innate immune system, they have been recognized as valuable bioindicators for MPs and NPs (Bråte et al., 2018b; Canesi and Procházková, 2013). This work integrated and complemented a previous study by Balbi and colleagues (Balbi et al., 2017) and consisted in a transcriptomic investigation of the effects of exposure to amino-modified NPs in trocophora larvae of the mollusc *M. galloprovincialis.*

Several previous ecotoxicological studies in marine invertebrates have recognized the value of exploiting the vulnerable early life stages of organisms to investigate the developmental perturbations induced by different types of nanoparticles. Our analysis led to the assembly of the first de novo transcriptome of *M. galloprovincialis* in the larval stage of trocophora. The transcriptome shows high quality and a good proportion of accurately functionally annotated sequences, thus providing a valuable scientific resource for future studies on the early larval stages of this bivalve species. Nevertheless, exposure to amino-modified PS NPs at concentrations close to the EC50 did not cause noticeable shifts in the overall gene expression profile of the exposed larvae, as shown by differential gene expression analysis. A possible explanation for this result is a dilution effect of the transcriptomic responses due to the pooling of more than 7000 individual larvae in each analyzed sample. Otherwise, the early life stage of trocophora may not represent the most sensitive phase of mussel larval development, but the transition from the trocophora stage to the first D-shelled larva might represent a more sensitive step to abiotic stressors.

Plastic pollution is a global problem. Although this issue has been the focus of global research for a decade, there is still insufficient scientific data to conduct a proper risk assessment. Although unraveling toxicological hazard of nanoplastics there is a need for hard data to understand the impact these materials could have in the real world and to suggest options for risk mitigation. Next Generation Sequencing technologies, particularly RNA sequencing, have proven to be a powerful tool to better elucidate the molecular pathways underlying nanoplastics toxicity and also identify biomarkers for more specific toxicity screening. Here we present preliminary results on the toxicity of polystyrene nanoparticles with a size of ≤ 100 nm to a non-model freshwater decapod species and to early developmental stages of the marine bivalve *M. galloprovincialis*. Further studies examining phenotypic and ecological effects of nanoplastics on freshwater decapods would be useful to support and complement our findings and in view of the crucial role of the riverine system as a potential sink of accumulation of MPs and NPs. Further studies examining transcriptomic response along with phenotypic effects of nanoplastics on early life stages of aquatic organisms are also needed to better interpret our results, given the high stress susceptibility of larval stages and thus their promising employment in ecotoxicogenomics.

References

Adam, V., Yang, T., Nowack, B., 2019. Toward an ecotoxicological risk assessment of microplastics: Comparison of available hazard and exposure data in freshwaters. Environ. Toxicol. Chem. 38, 436–447. https://doi.org/10.1002/etc.4323

Ai, J., Zhu, Y., Duan, J., Yu, Q., Zhang, G., Wan, F., Xiang, Z. huai, 2011. Genome-wide analysis of cytochrome P450 monooxygenase genes in the silkworm, *Bombyx mori*. Gene 480, 42–50. https://doi.org/10.1016/j.gene.2011.03.002

Al-Sid-Cheikh, M., Rowland, S.J., Stevenson, K., Rouleau, C., Henry, T.B., Thompson, R.C., 2018. Uptake, Whole-Body Distribution, and Depuration of Nanoplastics by the Scallop *Pecten maximus* at Environmentally Realistic Concentrations. Environ. Sci. Technol. 52, 14480–14486. https://doi.org/10.1021/acs.est.8b05266

Alcorlo, P., Geiger, W., Otero, M., 2009. Reproductive biology and life cycle of the invasive crayfish *Procambarus clarkii* (Crustacea: Decapoda) in diverse aquatic habitats of South-Western Spain: Implications for population control. Fundam. Appl. Limnol. 197–212. https://doi.org/10.1127/1863-9135/2008/0173-0197

Alimi, O.S., Farner Budarz, J., Hernandez, L.M., Tufenkji, N., 2018. Microplastics and Nanoplastics in Aquatic Environments: Aggregation, Deposition, and Enhanced Contaminant Transport. Environ. Sci. Technol. https://doi.org/10.1021/acs.est.7b05559

Altschul, S.F., Gish, W., Miller, W., Myers, E.W., Lipman, D.J., 1990. Basic local alignment search tool. J. Mol. Biol. 215, 403–410. https://doi.org/10.1016/S0022-2836(05)80360-2

Amaral-Zettler, L.A., Zettler, E.R., Mincer, T.J., 2020. Ecology of the plastisphere. Nat. Rev. Microbiol. https://doi.org/10.1038/s41579-019-0308-0

Amereh, F., Eslami, A., Fazelipour, S., Rafiee, M., Zibaii, M.I., Babaei, M., 2019. Thyroid endocrine status and biochemical stress responses in adult male Wistar rats chronically exposed to pristine polystyrene nanoplastics. Toxicol. Res. (Camb). 8, 953–963. https://doi.org/10.1039/c9tx00147f

Anderson, J.F., Siller, E., Barral, J.M., 2011. The neurodegenerative-disease-related protein sacsin is a molecular chaperone. J. Mol. Biol. 411, 870–880. https://doi.org/10.1016/j.jmb.2011.06.016

Anderson, P., Kedersha, N., 2009. RNA granules: Post-transcriptional and epigenetic modulators of gene expression. Nat. Rev. Mol. Cell Biol. https://doi.org/10.1038/nrm2694

Andrady A. L., 2015. Persistence of Plastic Litter in the Oceans, Marine Anthropogenic Litter. https://doi.org/10.1007/978-3-319-16510-3

Andrews, S., 2010. FastQC: A Quality Control Tool for High Throughput Sequence Data. [WWW Document]. URL http://www.bioinformatics.babraham.ac.uk/projects/fastqc/

Ankley, G.T., Bennett, R.S., Erickson, R.J., Hoff, D.J., Hornung, M.W., Johnson, R.D., Mount, D.R., Nichols, J.W., Russom, C.L., Schmieder, P.K., Serrrano, J.A., Tietge, J.E., Villeneuve, D.L., 2010. Adverse outcome pathways: A conceptual framework to support ecotoxicology research and risk assessment. Environ. Toxicol. Chem. https://doi.org/10.1002/etc.34

Apitanyasai, K., Amparyup, P., Charoensapsri, W., Senapin, S., Tassanakajon, A., 2015. Role

of Penaeus monodon hemocyte homeostasis associated protein (PmHHAP) in regulation of caspase-mediated apoptosis. Dev. Comp. Immunol. 53, 234–243. https://doi.org/10.1016/j.dci.2015.06.004

Apitanyasai, K., Noonin, C., Tassanakajon, A., Söderhäll, I., Söderhäll, K., 2016. Characterization of a hemocyte homeostasis-associated-like protein (HHAP) in the freshwater crayfish *Pacifastacus leniusculus*. Fish Shellfish Immunol. 58, 429–435. https://doi.org/10.1016/j.fsi.2016.09.038

Arambourou, H., Llorente, L., Moreno-Ocio, I., Herrero, Ó., Barata, C., Fuertes, I., Delorme, N., Méndez-Fernández, L., Planelló, R., 2020. Exposure to heavy metal-contaminated sediments disrupts gene expression, lipid profile, and life history traits in the midge *Chironomus riparius*. Water Res. 168, 115165. https://doi.org/10.1016/j.watres.2019.115165

Arthur, C., Baker, J., Bamford, H., 2009. Proceedings of the International Research Workshop on the Occurrence, Effects, and Fate of Microplastic Marine Debris, NOAA Technical Memorandum NOS-OR&R-30.

ASTM, 2004. Standard Guide for Conducting Static Acute Toxicity Tests Starting with Embryos of Four Species of Saltwater Bivalve Molluscs. https://doi.org/http://dx.doi.org/10.1520/E0724-98

Athamena, A., Brichon, G., Trajkovic-Bodennec, S., Péqueux, A., Chapelle, S., Bodennec, J., Zwingelstein, G., 2011. Salinity regulates N-methylation of phosphatidylethanolamine in euryhaline crustaceans hepatopancreas and exchange of newly-formed phosphatidylcholine with hemolymph. J. Comp. Physiol. B Biochem. Syst. Environ. Physiol. 181, 731–740. https://doi.org/10.1007/s00360-011-0562-6

Atwood, E.C., Falcieri, F.M., Piehl, S., Bochow, M., Matthies, M., Franke, J., Carniel, S., Sclavo, M., Laforsch, C., Siegert, F., 2019. Coastal accumulation of microplastic particles emitted from the Po River, Northern Italy: Comparing remote sensing and hydrodynamic modelling with in situ sample collections. Mar. Pollut. Bull. 138, 561–574. https://doi.org/10.1016/J.MARPOLBUL.2018.11.045

Au, S.Y., Bruce, T.F., Bridges, W.C., Klaine, S.J., 2015. Responses of *Hyalella azteca* to acute and chronic microplastic exposures. Environ. Toxicol. Chem. 34, 2564–2572. https://doi.org/10.1002/etc.3093

Auclair, J., Quinn, B., Peyrot, C., Wilkinson, K.J., Gagné, F., 2020. Detection, biophysical effects, and toxicity of polystyrene nanoparticles to the cnidarian *Hydra attenuata*. Environ. Sci. Pollut. Res. 27, 11772–11781. https://doi.org/10.1007/s11356-020-07728-1

Auguste, M., Balbi, T., Ciacci, C., Canonico, B., Papa, S., Borello, A., Vezzulli, L., Canesi, L., 2020. Shift in Immune Parameters After Repeated Exposure to Nanoplastics in the Marine Bivalve *Mytilus*. Front. Immunol. 11, 426. https://doi.org/10.3389/fimmu.2020.00426

Azzolin, L., von Stockum, S., Basso, E., Petronilli, V., Forte, M.A., Bernardi, P., 2010. The mitochondrial permeability transition from yeast to mammals. FEBS Lett. https://doi.org/10.1016/j.febslet.2010.04.023

B'Chir, W., Maurin, A.C., Carraro, V., Averous, J., Jousse, C., Muranishi, Y., Parry, L., Stepien, G., Fafournoux, P., Bruhat, A., 2013. The eIF2α/ATF4 pathway is essential for stress-induced autophagy gene expression. Nucleic Acids Res. 41, 7683–7699. https://doi.org/10.1093/nar/gkt563

Baines, C.P., Kaiser, R.A., Purcell, N.H., Blair, N.S., Osinska, H., Hambleton, M.A., Brunskill, E.W., Sayen, M.R., Gottlieb, R.A., Dorn, G.W., Bobbins, J., Molkentin, J.D., 2005. Loss of cyclophilin D reveals a critical role for mitochondrial permeability transition in cell death. Nature. https://doi.org/10.1038/nature03434

Baini, M., Fossi, M.C., Galli, M., Caliani, I., Campani, T., Finoia, M.G., Panti, C., 2018. Abundance and characterization of microplastics in the coastal waters of Tuscany (Italy): The application of the MSFD monitoring protocol in the Mediterranean Sea. Mar. Pollut. Bull. 133, 543–552. https://doi.org/10.1016/j.marpolbul.2018.06.016

Balbi, T., Camisassi, G., Montagna, M., Fabbri, R., Franzellitti, S., Carbone, C., Dawson, K., Canesi, L., 2017. Impact of cationic polystyrene nanoparticles (PS-NH2) on early embryo development of *Mytilus galloprovincialis*: Effects on shell formation. Chemosphere 186, 1–9. https://doi.org/10.1016/j.chemosphere.2017.07.120

Balbi, T., Franzellitti, S., Fabbri, R., Montagna, M., Fabbri, E., Canesi, L., 2016. Impact of bisphenol A (BPA) on early embryo development in the marine mussel *Mytilus galloprovincialis*: Effects on gene transcription. Environ. Pollut. 218, 996–1004. https://doi.org/10.1016/j.envpol.2016.08.050

Baldwin, W.S., Marko, P.B., Nelson, D.R., 2009. The cytochrome P450 (CYP) gene superfamily in *Daphnia pulex*. BMC Genomics 10, 169. https://doi.org/10.1186/1471-2164-10-169

Bankevich, A., Nurk, S., Antipov, D., Gurevich, A.A., Dvorkin, M., Kulikov, A.S., Lesin, V.M., Nikolenko, S.I., Pham, S., Prjibelski, A.D., Pyshkin, A. V., Sirotkin, A. V., Vyahhi, N., Tesler, G., Alekseyev, M.A., Pevzner, P.A., 2012. SPAdes: A new genome assembly algorithm and its applications to single-cell sequencing. J. Comput. Biol. 19, 455–477. https://doi.org/10.1089/cmb.2012.0021

Barajas, H.R., Romero, M.F., Martínez-Sánchez, S., Alcaraz, L.D., 2019. Global genomic similarity and core genome sequence diversity of the *Streptococcus* genus as a toolkit to identify closely related bacterial species in complex environments. PeerJ 2019. https://doi.org/10.7717/peerj.6233

Barata, C., Solayan, A., Porte, C., 2004. Role of B-esterases in assessing toxicity of organophosphorus (chlorpyrifos, malathion) and carbamate (carbofuran) pesticides to *Daphnia magna*. Aquat. Toxicol. 66, 125–139. https://doi.org/10.1016/j.aquatox.2003.07.004

Barton, K., 2020. MuMIn: Multi-Model Inference. R package version 1.43.17.

Bateman, A., 2019. UniProt: A worldwide hub of protein knowledge. Nucleic Acids Res. 47, D506–D515. https://doi.org/10.1093/nar/gky1049

Baun, A., Hartmann, N.B., Grieger, K., Kusk, K.O., 2008. Ecotoxicity of engineered nanoparticles to aquatic invertebrates: A brief review and recommendations for future toxicity testing. Ecotoxicology. https://doi.org/10.1007/s10646-008-0208-y

Bergami, E., Krupinski Emerenciano, A., González-Aravena, M., Cárdenas, C.A., Hernández, P., Silva, J.R.M.C., Corsi, I., 2019. Polystyrene nanoparticles affect the innate immune system of the Antarctic sea urchin *Sterechinus neumayeri*. Polar Biol. 42, 743–757. https://doi.org/10.1007/s00300-019-02468-6

Bergami, E., Manno, C., Cappello, S., Vannuccini, M.L., Corsi, I., 2020. Nanoplastics affect

moulting and faecal pellet sinking in Antarctic krill (*Euphausia superba*) juveniles. Environ. Int. 143, 105999. https://doi.org/10.1016/j.envint.2020.105999

Bergmann, M., Mützel, S., Primpke, S., Tekman, M.B., Trachsel, J., Gerdts, G., 2019. White and wonderful? Microplastics prevail in snow from the Alps to the Arctic. Sci. Adv. 5, eaax1157. https://doi.org/10.1126/sciadv.aax1157

Bergmann, M., Wirzberger, V., Krumpen, T., Lorenz, C., Primpke, S., Tekman, M.B., Gerdts, G., 2017. High Quantities of Microplastic in Arctic Deep-Sea Sediments from the HAUSGARTEN Observatory. Environ. Sci. Technol. 51, 11000–11010. https://doi.org/10.1021/acs.est.7b03331

Besseling, E., Redondo-Hasselerharm, P., Foekema, E.M., Koelmans, A.A., 2019. Quantifying ecological risks of aquatic micro- and nanoplastic. Crit. Rev. Environ. Sci. Technol. 49, 32–80. https://doi.org/10.1080/10643389.2018.1531688

Besseling, E., Wang, B., Lürling, M., Koelmans, A.A., 2014. Nanoplastic affects growth of *S. obliquus* and reproduction of *D. magna*. Environ. Sci. Technol. 48, 12336–12343. https://doi.org/10.1021/es503001d

Bhattacharyya, S., Feferman, L., Tobacman, J.K., 2016. Restriction of Aerobic Metabolism by Acquired or Innate Arylsulfatase B Deficiency: A New Approach to the Warburg Effect. Sci. Rep. 6, 1–15. https://doi.org/10.1038/srep32885

Bi, J., Ning, M., Xie, X., Fan, W., Huang, Y., Gu, W., Wang, W., Wang, L., Meng, Q., 2020. A typical C-type lectin, perlucin-like protein, is involved in the innate immune defense of whiteleg shrimp *Litopenaeus vannamei*. Fish Shellfish Immunol. 103, 293–301. https://doi.org/10.1016/j.fsi.2020.05.046

Bläsing, M., Amelung, W., 2018. Plastics in soil: Analytical methods and possible sources. Sci. Total Environ. https://doi.org/10.1016/j.scitotenv.2017.08.086

Bonvillain, C.P., Rutherford, D.A., Kelso, W.E., Green, C.C., 2012. Physiological biomarkers of hypoxic stress in red swamp crayfish *Procambarus clarkii* from field and laboratory experiments. Comp. Biochem. Physiol. - A Mol. Integr. Physiol. 163, 15–21. https://doi.org/10.1016/j.cbpa.2012.04.015

Boucher, J., Friot, D., 2017. Primary microplastics in the oceans: A global evaluation of sources, IUCN. IUCN, Gland, Switzerland. https://doi.org/10.2305/iucn.ch.2017.01.en

Bour, A., Haarr, A., Keiter, S., Hylland, K., 2018. Environmentally relevant microplastic exposure affects sediment-dwelling bivalves. Environ. Pollut. 236, 652–660. https://doi.org/10.1016/j.envpol.2018.02.006

Boyle, K., Örmeci, B., 2020. Microplastics and nanoplastics in the freshwater and terrestrial environment: A review. Water (Switzerland). https://doi.org/10.3390/w12092633

Brandts, I., Teles, M., Gonçalves, A.P., Barreto, A., Franco-Martinez, L., Tvarijonaviciute, A., Martins, M.A., Soares, A.M.V.M., Tort, L., Oliveira, M., 2018. Effects of nanoplastics on *Mytilus galloprovincialis* after individual and combined exposure with carbamazepine. Sci. Total Environ. 643, 775–784. https://doi.org/10.1016/j.scitotenv.2018.06.257

Bråte, I.L.N., Blázquez, M., Brooks, S.J., Thomas, K. V., 2018a. Weathering impacts the uptake of polyethylene microparticles from toothpaste in Mediterranean mussels (*M. galloprovincialis*). Sci. Total Environ. 626, 1310–1318. https://doi.org/10.1016/j.scitotenv.2018.01.141

Bråte, I.L.N., Hurley, R., Iversen, K., Beyer, J., Thomas, K. V., Steindal, C.C., Green, N.W., Olsen, M., Lusher, A., 2018b. *Mytilus* spp. as sentinels for monitoring microplastic pollution in Norwegian coastal waters: A qualitative and quantitative study. Environ. Pollut. 243, 383–393. https://doi.org/10.1016/j.envpol.2018.08.077

Bremer, J., 1997. The Role of Carnitine in Cell Metabolism, in: De Simone, C., Famularo, G. (Eds.), Carnitine Today. Springer US, pp. 1–37. https://doi.org/10.1007/978-1-4615-6005-0_1

Bremer, J., 1983. Carnitine. Metabolism and functions. Physiol. Rev. https://doi.org/10.1152/physrev.1983.63.4.1420

Brown, A., Dalpé, G., Mathieu, M., Kothary, R., 1995. Cloning and characterization of the neural isoforms of human dystonin. Genomics 29, 777–780. https://doi.org/10.1006/geno.1995.9936

Browne, M.A., Crump, P., Niven, S.J., Teuten, E., Tonkin, A., Galloway, T., Thompson, R., 2011. Accumulation of microplastic on shorelines woldwide: Sources and sinks. Environ. Sci. Technol. 45, 9175–9179. https://doi.org/10.1021/es201811s

Browne, M.A., Dissanayake, A., Galloway, T.S., Lowe, D.M., Thompson, R.C., 2008. Ingested microscopic plastic translocates to the circulatory system of the mussel, *Mytilus edulis* (L.). Environ. Sci. Technol. 42, 5026–5031. https://doi.org/10.1021/es800249a

Browne, M.A., Underwood, A.J., Chapman, M.G., Williams, R., Thompson, R.C., Van Franeker, J.A., 2015. Linking effects of anthropogenic debris to ecological impacts. Proc. R. Soc. B Biol. Sci. https://doi.org/10.1098/rspb.2014.2929

Brun, N.R., van Hage, P., Hunting, E.R., Haramis, A.P.G., Vink, S.C., Vijver, M.G., Schaaf, M.J.M., Tudorache, C., 2019. Polystyrene nanoplastics disrupt glucose metabolism and cortisol levels with a possible link to behavioural changes in larval zebrafish. Commun. Biol. 2, 1–9. https://doi.org/10.1038/s42003-019-0629-6

Buchfink, B., Xie, C., Huson, D.H., 2014. Fast and sensitive protein alignment using DIAMOND. Nat. Methods. https://doi.org/10.1038/nmeth.3176

Burmester, T., 2015. Evolution of Respiratory Proteins across the Pancrustacea. Integr. Comp. Biol. 55, 792–801. https://doi.org/10.1093/icb/icv079

Burmester, T., 2002. Origin and evolution of arthropod hemocyanins and related proteins. J. Comp. Physiol. B Biochem. Syst. Environ. Physiol. https://doi.org/10.1007/s00360-001-0247-7

Burmester, T., 1999. Identification, molecular cloning, and phylogenetic analysis of a non-respiratory pseudo-hemocyanin of *Homarus americanus*. J. Biol. Chem. 274, 13217–13222. https://doi.org/10.1074/jbc.274.19.13217

Cai, Y.-J., Guan, Z.-B., Shui, Y., Chen, K., Liao, X.-R., Yin, J., 2016. The hepatopancreas and ovary are the sites of vitellogenin synthesis in female red swamp crayfish (P*rocambarus clarkii* (Girard, 1852)) (Decapoda: Astacoidea: Cambaridae). J. Crustac. Biol. 36, 637–641. https://doi.org/10.1163/1937240X-00002459

Canesi, L., Ciacci, C., Bergami, E., Monopoli, M.P., Dawson, K.A., Papa, S., Canonico, B., Corsi, I., 2015. Evidence for immunomodulation and apoptotic processes induced by cationic polystyrene nanoparticles in the hemocytes of the marine bivalve *Mytilus*. Mar. Environ. Res. 111, 34–40. https://doi.org/10.1016/j.marenvres.2015.06.008

Canesi, L., Ciacci, C., Fabbri, R., Balbi, T., Salis, A., Damonte, G., Cortese, K., Caratto, V., Monopoli, M.P., Dawson, K., Bergami, E., Corsi, I., 2016. Interactions of cationic polystyrene nanoparticles with marine bivalve hemocytes in a physiological environment: Role of soluble hemolymph proteins. Environ. Res. 150, 73–81. https://doi.org/10.1016/j.envres.2016.05.045

Canesi, L., Ciacci, C., Fabbri, R., Marcomini, A., Pojana, G., Gallo, G., 2012. Bivalve molluscs as a unique target group for nanoparticle toxicity. Mar. Environ. Res. 76, 16–21. https://doi.org/10.1016/j.marenvres.2011.06.005

Canesi, L., Corsi, I., 2015. Effects of nanomaterials on marine invertebrates. Sci. Total Environ. 565, 933–940. https://doi.org/10.1016/j.scitotenv.2016.01.085

Canesi, L., Procházková, P., 2013. The Invertebrate Immune System as a Model for Investigating the Environmental Impact of Nanoparticles, in: Nanoparticles and the Immune System: Safety and Effects. Elsevier Inc., pp. 91–112. https://doi.org/10.1016/B978-0-12-408085-0.00007-8

Capolupo, M., Franzellitti, S., Valbonesi, P., Lanzas, C.S., Fabbri, E., 2018. Uptake and transcriptional effects of polystyrene microplastics in larval stages of the Mediterranean mussel *Mytilus galloprovincialis*. Environ. Pollut. 241, 1038–1047. https://doi.org/10.1016/j.envpol.2018.06.035

Cau, A., Avio, C.G., Dessì, C., Follesa, M.C., Moccia, D., Regoli, F., Pusceddu, A., 2019. Microplastics in the crustaceans *Nephrops norvegicus* and *Aristeus antennatus*: Flagship species for deep-sea environments? Environ. Pollut. 255. https://doi.org/10.1016/j.envpol.2019.113107

Cau, A., Avio, C.G., Dessì, C., Moccia, D., Pusceddu, A., Regoli, F., Cannas, R., Follesa, M.C., 2020. Benthic Crustacean Digestion Can Modulate the Environmental Fate of Microplastics in the Deep Sea. Environ. Sci. Technol. 54, 4886–4892. https://doi.org/10.1021/acs.est.9b07705

Cedervall, T., Hansson, L.-A., Lard, M., Frohm, B., Linse, S., 2012. Food Chain Transport of Nanoparticles Affects Behaviour and Fat Metabolism in Fish. PLoS One 7, e32254. https://doi.org/10.1371/journal.pone.0032254

Cedervall, T., Lynch, I., Lindman, S., Berggård, T., Thulin, E., Nilsson, H., Dawson, K.A., Linse, S., 2007. Understanding the nanoparticle-protein corona using methods to quntify exchange rates and affinities of proteins for nanoparticles. Proc. Natl. Acad. Sci. U. S. A. 104, 2050–2055. https://doi.org/10.1073/pnas.0608582104

Celi, M., Filiciotto, F., Parrinello, D., Buscaino, G., Damiano, M.A., Cuttitta, A., D'Angelo, S., Mazzola, S., Vazzana, M., 2013. Physiological and agonistic behavioural response of *Procambarus clarkii* to an acoustic stimulus. J. Exp. Biol. 216, 709–718. https://doi.org/10.1242/jeb.078865

Cerenius, L., Söderhäll, K., 2018. Crayfish immunity – Recent findings. Dev. Comp. Immunol. 80, 94–98. https://doi.org/10.1016/j.dci.2017.05.010

Cerenius, L., Söderhäll, K., 2004. The prophenoloxidase-activating system in invertebrates. Immunol. Rev. 198, 116–126. https://doi.org/10.1111/j.0105-2896.2004.00116.x

Chae, Y., Kim, D., Choi, M.J., Cho, Y., An, Y.J., 2019. Impact of nano-sized plastic on the nutritional value and gut microbiota of whiteleg shrimp *Litopenaeus vannamei* via dietary

exposure. Environ. Int. 130, 104848. https://doi.org/10.1016/j.envint.2019.05.042

Chae, Y., Kim, D., Kim, S.W., An, Y.-J., 2018. Trophic transfer and individual impact of nano-sized polystyrene in a four-species freshwater food chain. Sci. Rep. 8, 284. https://doi.org/10.1038/s41598-017-18849-y

Chai, L.Q., Meng, J.H., Gao, J., Xu, Y.H., Wang, X.W., 2018. Identification of a crustacean β-1,3-glucanase related protein as a pattern recognition protein in antibacterial response. Fish Shellfish Immunol. 80, 155–164. https://doi.org/10.1016/j.fsi.2018.06.004

Chamas, A., Moon, H., Zheng, J., Qiu, Y., Tabassum, T., Jang, J.H., Abu-Omar, M., Scott, S.L., Suh, S., 2020. Degradation Rates of Plastics in the Environment. ACS Sustain. Chem. Eng. 8, 3494–3511. https://doi.org/10.1021/acssuschemeng.9b06635

Charoensapsri, W., Sangsuriya, P., Lertwimol, T., Gangnonngiw, W., Phiwsaiya, K., Senapin, S., 2015. Laminin receptor protein is implicated in hemocyte homeostasis for the whiteleg shrimp *Penaeus* (*Litopenaeus*) *vannamei.* Dev. Comp. Immunol. 51, 39–47. https://doi.org/10.1016/j.dci.2015.02.012

Chaudhari, N., Talwar, P., Parimisetty, A., d'Hellencourt, C.L., Ravanan, P., 2014. A molecular web: Endoplasmic reticulum stress, inflammation, and oxidative stress. Front. Cell. Neurosci. https://doi.org/10.3389/fncel.2014.00213

Chen, D.D., Meng, X.L., Xu, J.P., Yu, J.Y., Meng, M.X., Wang, J., 2013. PcLT, a novel C-type lectin from *Procambarus clarkii*, is involved in the innate defense against Vibrio alginolyticus and WSSV. Dev. Comp. Immunol. 39, 255–264. https://doi.org/10.1016/j.dci.2012.10.003

Chen, Q., Allgeier, A., Yin, D., Hollert, H., 2019. Leaching of endocrine disrupting chemicals from marine microplastics and mesoplastics under common life stress conditions. Environ. Int. 130, 104938. https://doi.org/10.1016/j.envint.2019.104938

Chen, S., Zhou, Y., Chen, Y., Gu, J., 2018. Fastp: An ultra-fast all-in-one FASTQ preprocessor, in: Bioinformatics. Oxford University Press, pp. i884–i890. https://doi.org/10.1093/bioinformatics/bty560

Cheng, Y.X., Du, N.S., Lai, W., 1998. Lipid composition in hepatopancreas of Chinese mitten crab *Eriocheir sinensis* at different stages. Acta Zool. Sin. 44, 420–429.

Chikhi, R., Medvedev, P., 2014. Informed and automated k-mer size selection for genome assembly. Bioinformatics 30, 31–37. https://doi.org/10.1093/bioinformatics/btt310

Cincinelli, A., Scopetani, C., Chelazzi, D., Lombardini, E., Martellini, T., Katsoyiannis, A., Fossi, M.C., Corsolini, S., 2017. Microplastic in the surface waters of the Ross Sea (Antarctica): Occurrence, distribution and characterization by FTIR. Chemosphere 175, 391–400. https://doi.org/10.1016/j.chemosphere.2017.02.024

Clark, K.F., Yang, J., Acorn, A.R., Garland, J.J., Stewart-Clark, S.E., Greenwood, S.J., 2017. The impact of harvesting location on the physiological indicators of the American lobster (*Homarus americanus* H. Milne Edwards, 1837) (Decapoda: Nephropidae) during live storage. J. Crustac. Biol. 37, 303–314. https://doi.org/10.1093/jcbiol/rux033

Coady, K.K., Burgoon, L., Doskey, C., Davis, J.W., 2020. Assessment of Transcriptomic and Apical Responses of *Daphnia magna* Exposed to a Polyethylene Microplastic in a 21-d Chronic Study. Environ. Toxicol. Chem. https://doi.org/10.1002/etc.4745

Coates, C.J., Söderhäll, K., 2020. The stress–immunity axis in shellfish. J. Invertebr. Pathol. 107492. https://doi.org/10.1016/j.jip.2020.107492

Cole, M., Coppock, R., Lindeque, P.K., Altin, D., Reed, S., Pond, D.W., Sørensen, L., Galloway, T.S., Booth, A.M., 2019. Effects of Nylon Microplastic on Feeding, Lipid Accumulation, and Moulting in a Coldwater Copepod. Environ. Sci. Technol. 53, 7075–7082. https://doi.org/10.1021/acs.est.9b01853

Cole, M., Liddle, C., Consolandi, G., Drago, C., Hird, C., Lindeque, P.K., Galloway, T.S., 2020. Microplastics, microfibres and nanoplastics cause variable sub-lethal responses in mussels (*Mytilus* spp.). Mar. Pollut. Bull. 160, 111552. https://doi.org/10.1016/j.marpolbul.2020.111552

Cole, M., Lindeque, P., Fileman, E., Halsband, C., Galloway, T.S., 2015. The Impact of Polystyrene Microplastics on Feeding, Function and Fecundity in the Marine Copepod *Calanus helgolandicus*. Environ. Sci. Technol. 49, 1130–1137. https://doi.org/10.1021/es504525u

Cong, Y., Jin, F., Tian, M., Wang, J., Shi, H., Wang, Y., Mu, J., 2019. Ingestion, egestion and post-exposure effects of polystyrene microspheres on marine medaka (*Oryzias melastigma*). Chemosphere 228, 93–100. https://doi.org/10.1016/j.chemosphere.2019.04.098

Coppock, R.L., Galloway, T.S., Cole, M., Fileman, E.S., Queirós, A.M., Lindeque, P.K., 2019. Microplastics alter feeding selectivity and faecal density in the copepod, *Calanus helgolandicus*. Sci. Total Environ. 687, 780–789. https://doi.org/10.1016/j.scitotenv.2019.06.009

Cózar, A., Echevarría, F., González-Gordillo, J.I., Irigoien, X., Úbeda, B., Hernández-León, S., Palma, Á.T., Navarro, S., García-de-Lomas, J., Ruiz, A., Fernández-de-Puelles, M.L., Duarte, C.M., 2014. Plastic debris in the open ocean. Proc. Natl. Acad. Sci. U. S. A. 111, 10239–10244. https://doi.org/10.1073/pnas.1314705111

Cózar, A., Martí, E., Duarte, C.M., García-de-Lomas, J., Van Sebille, E., Ballatore, T.J., Eguíluz, V.M., Ignacio González-Gordillo, J., Pedrotti, M.L., Echevarría, F., Troublè, R., Irigoien, X., 2017. The Arctic Ocean as a dead end for floating plastics in the North Atlantic branch of the Thermohaline Circulation. Sci. Adv. 3, e1600582. https://doi.org/10.1126/sciadv.1600582

Cui, R., Kim, S.W., An, Y.-J., 2017. Polystyrene nanoplastics inhibit reproduction and induce abnormal embryonic development in the freshwater crustacean *Daphnia galeata*. Sci. Rep. 7, 12095. https://doi.org/10.1038/s41598-017-12299-2

Dai, L., Ma, M., Gao, G., Chen, H., 2016. *Dendroctonus armandi* (Curculionidae: Scolytinae) cytochrome P450s display tissue specificity and responses to host terpenoids. Comp. Biochem. Physiol. Part - B Biochem. Mol. Biol. 201, 1–11. https://doi.org/10.1016/j.cbpb.2016.06.006

Danso, D., Chow, J., Streita, W.R., 2019. Plastics: Environmental and biotechnological perspectives on microbial degradation. Appl. Environ. Microbiol. https://doi.org/10.1128/AEM.01095-19

Dawson, A.L., Kawaguchi, S., King, C.K., Townsend, K.A., King, R., Huston, W.M., Bengtson Nash, S.M., 2018. Turning microplastics into nanoplastics through digestive fragmentation by Antarctic krill. Nat. Commun. 9, 1001. https://doi.org/10.1038/s41467-

018-03465-9

DeLeo, D.M., Pérez-Moreno, J.L., Vázquez-Miranda, H., Bracken-Grissom, H.D., 2018. RNA profile diversity across arthropoda: guidelines, methodological artifacts, and expected outcomes. Biol. Methods Protoc. 3. https://doi.org/10.1093/BIOMETHODS/BPY012

Dembeck, L.M., Böröczky, K., Huang, W., Schal, C., Anholt, R.R.H., Mackay, T.F.C., 2015. Genetic architecture of natural variation in cuticular hydrocarbon composition in *Drosophila melanogaster*. Elife 4. https://doi.org/10.7554/eLife.09861.001

Détrée, C., Gallardo-Escárate, C., 2018. Single and repetitive microplastics exposures induce immune system modulation and homeostasis alteration in the edible mussel *Mytilus galloprovincialis*. Fish Shellfish Immunol. 83, 52–60. https://doi.org/10.1016/j.fsi.2018.09.018

Détrée, C., Gallardo-Escárate, C., 2017. Polyethylene microbeads induce transcriptional responses with tissue-dependent patterns in the mussel *Mytilus galloprovincialis*. J. Molluscan Stud. 83, 220–225. https://doi.org/10.1093/mollus/eyx005

Devriese, L.I., van der Meulen, M.D., Maes, T., Bekaert, K., Paul-Pont, I., Frère, L., Robbens, J., Vethaak, A.D., 2015. Microplastic contamination in brown shrimp (*Crangon crangon*, Linnaeus 1758) from coastal waters of the Southern North Sea and Channel area. Mar. Pollut. Bull. 98, 179–187. https://doi.org/10.1016/J.MARPOLBUL.2015.06.051

Ding, C., Wu, Z., Huang, L., Wang, Y., Xue, J., Chen, Si, Deng, Z., Wang, L., Song, Z., Chen, Shi, 2015. Mitofilin and CHCHD6 physically interact with Sam50 to sustain cristae structure. Sci. Rep. 5, 16064. https://doi.org/10.1038/srep16064

Duan, Y., Xiong, D., Wang, Y., Zhang, Z., Li, H., Dong, H., Zhang, J., 2020. Toxicological effects of microplastics in *Litopenaeus vannamei* as indicated by an integrated microbiome, proteomic and metabolomic approach. Sci. Total Environ. 143311. https://doi.org/10.1016/j.scitotenv.2020.143311

Eerkes-Medrano, D., Thompson, R.C., Aldridge, D.C., 2015. Microplastics in freshwater systems: A review of the emerging threats, identification of knowledge gaps and prioritisation of research needs. Water Res. 75, 63–82. https://doi.org/10.1016/J.WATRES.2015.02.012

EFSA CONTAM Panel (EFSA Panel on Contaminants in the Food Chain), 2016. Statement on the presence of microplastics and nanoplastics in food, with particular focus on seafood. EFSA J. 14, 4501. https://doi.org/doi:10.2903/j.efsa.2016.4501

Egger, M., Sulu-Gambari, F., Lebreton, L., 2020. First evidence of plastic fallout from the North Pacific Garbage Patch. Sci. Rep. 10, 1–10. https://doi.org/10.1038/s41598-020-64465-8

Ekvall, M.T., Lundqvist, M., Kelpsiene, E., Šileikis, E., Gunnarsson, S.B., Cedervall, T., 2019. Nanoplastics formed during the mechanical breakdown of daily-use polystyrene products. Nanoscale Adv. 1, 1055–1061. https://doi.org/10.1039/c8na00210j

El-Bakary, Z.A., Sayed, A.E.-D.H., 2011. Effects of short time UV-A exposures on compound eyes and haematological parameters in *Procambarus clarkii* (Girad, 1852). Ecotoxicol. Environ. Saf. 74, 960–966. https://doi.org/10.1016/J.ECOENV.2011.01.010

El-Gebali, S., Mistry, J., Bateman, A., Eddy, S.R., Luciani, A., Potter, S.C., Qureshi, M., Richardson, L.J., Salazar, G.A., Smart, A., Sonnhammer, E.L.L., Hirsh, L., Paladin, L., Piovesan, D., Tosatto, S.C.E., Finn, R.D., 2019. The Pfam protein families database in

2019. Nucleic Acids Res. 47, D427–D432. https://doi.org/10.1093/nar/gky995

Enfrin, M., Lee, J., Gibert, Y., Basheer, F., Kong, L., Dumée, L.F., 2020. Release of hazardous nanoplastic contaminants due to microplastics fragmentation under shear stress forces. J. Hazard. Mater. 384, 121393. https://doi.org/10.1016/j.jhazmat.2019.121393

Erni-Cassola, G., Zadjelovic, V., Gibson, M.I., Christie-Oleza, J.A., 2019. Distribution of plastic polymer types in the marine environment; A meta-analysis. J. Hazard. Mater. 369, 691–698. https://doi.org/10.1016/j.jhazmat.2019.02.067

European Commission, 2011. Commission recommendation of 18 October 2011 on the definition of nanomaterial (2011/696/EU). Off. J. Eur. Union 54, 38–40.

Everaert, G., Van Cauwenberghe, L., De Rijcke, M., Koelmans, A.A., Mees, J., Vandegehuchte, M., Janssen, C.R., 2018. Risk assessment of microplastics in the ocean: Modelling approach and first conclusions. Environ. Pollut. 242, 1930–1938. https://doi.org/10.1016/j.envpol.2018.07.069

Ewels, P., Magnusson, M., Lundin, S., Käller, M., 2016. MultiQC: summarize analysis results for multiple tools and samples in a single report. Bioinformatics 32, 3047–3048. https://doi.org/10.1093/bioinformatics/btw354

Fadare, O.O., Wan, B., Liu, K., Yang, Y., Zhao, L., Guo, L.H., 2020. Eco-Corona vs Protein Corona: Effects of Humic Substances on Corona Formation and Nanoplastic Particle Toxicity in Daphnia magna. Environ. Sci. Technol. 54, 8001–8009. https://doi.org/10.1021/acs.est.0c00615

Farrell, P., Nelson, K., 2013. Trophic level transfer of microplastic: Mytilus edulis (L.) to *Carcinus maenas* (L.). Environ. Pollut. 177, 1–3. https://doi.org/10.1016/J.ENVPOL.2013.01.046

Fernandes, D., Potrykus, J., Morsiani, C., Raldua, D., Lavado, R., Porte, C., 2002. The combined use of chemical and biochemical markers to assess water quality in two low-stream rivers (NE Spain). Environ. Res. 90, 169–178. https://doi.org/10.1006/enrs.2002.4390

Fernández-Cisnal, R., García-Sevillano, M.A., García-Barrera, T., Gómez-Ariza, J.L., Abril, N., 2018. Metabolomic alterations and oxidative stress are associated with environmental pollution in *Procambarus clarkii*. Aquat. Toxicol. 205, 76–88. https://doi.org/10.1016/j.aquatox.2018.10.005

Fernández-Cisnal, R., García-Sevillano, M.A., Gómez-Ariza, J.L., Pueyo, C., López-Barea, J., Abril, N., 2017. 2D-DIGE as a proteomic biomarker discovery tool in environmental studies with *Procambarus clarkii*. Sci. Total Environ. 584–585, 813–827. https://doi.org/10.1016/j.scitotenv.2017.01.125

Fernández Robledo, J.A., Yadavalli, R., Allam, B., Pales Espinosa, E., Gerdol, M., Greco, S., Stevick, R.J., Gómez-Chiarri, M., Zhang, Y., Heil, C.A., Tracy, A.N., Bishop-Bailey, D., Metzger, M.J., 2019. From the raw bar to the bench: Bivalves as models for human health. Dev. Comp. Immunol. https://doi.org/10.1016/j.dci.2018.11.020

Finnegan, A.M.D., Gouramanis, C., 2021. Projected plastic waste loss scenarios between 2000 and 2030 into the largest freshwater-lake system in Southeast Asia. Sci. Rep. 11, 3897. https://doi.org/10.1038/s41598-021-83064-9

Fogh Mortensen, L., Tange, I., Stenmarck, Å., Fråne, A., Nielsen, T., Boberg, N., Bauer, F.,

2021. Plastics, the circular economy and Europe′s environment - A priority for action, EEA Report. https://doi.org/10.2800/5847

Fox, J., Weisberg, S., 2019. An R Companion to Applied Regression, Third. ed. Sage, Thousand Oaks CA.

Frehland, S., Kaegi, R., Hufenus, R., Mitrano, D.M., 2020. Long-term assessment of nanoplastic particle and microplastic fiber flux through a pilot wastewater treatment plant using metal-doped plastics. Water Res. 182, 115860. https://doi.org/10.1016/j.watres.2020.115860

Frias, J.P.G.L., Nash, R., 2019. Microplastics: Finding a consensus on the definition. Mar. Pollut. Bull. 138, 145–147. https://doi.org/10.1016/j.marpolbul.2018.11.022

Fröhlich, E., Kueznik, T., Samberger, C., Roblegg, E., Wrighton, C., Pieber, T.R., 2010. Size-dependent effects of nanoparticles on the activity of cytochrome P450 isoenzymes. Toxicol. Appl. Pharmacol. 242, 326–332. https://doi.org/10.1016/j.taap.2009.11.002

Fu, L., Niu, B., Zhu, Z., Wu, S., Li, W., 2012. CD-HIT: Accelerated for clustering the next-generation sequencing data. Bioinformatics 28, 3150–3152. https://doi.org/10.1093/bioinformatics/bts565

Fusakio, M.E., Willy, J.A., Wang, Y., Mirek, E.T., Baghdadi, R.J.T.A., Adams, C.M., Anthony, T.G., Wek, R.C., 2016. Transcription factor ATF4 directs basal and stress-induced gene expression in the unfolded protein response and cholesterol metabolism in the liver. Mol. Biol. Cell 27, 1536–1551. https://doi.org/10.1091/mbc.E16-01-0039

Gabbott, S., Key, S., Russell, C., Yonan, Y., Zalasiewicz, J., 2020. The geography and geology of plastics, in: Plastic Waste and Recycling. Elsevier, pp. 33–63. https://doi.org/10.1016/b978-0-12-817880-5.00003-7

Gall, S.C., Thompson, R.C., 2015. The impact of debris on marine life. Mar. Pollut. Bull. 92, 170–179. https://doi.org/10.1016/j.marpolbul.2014.12.041

Galloway, T.S., Cole, M., Lewis, C., 2017. Interactions of microplastic debris throughout the marine ecosystem. Nat. Ecol. Evol. 1, 0116. https://doi.org/10.1038/s41559-017-0116

Galloway, T.S., Lewis, C.N., 2016. Marine microplastics spell big problems for future generations. Proc. Natl. Acad. Sci. U. S. A. 113, 2331–3. https://doi.org/10.1073/pnas.1600715113

Gambarini, V., Pantos, O., Kingsbury, J.M., Weaver, L., Handley, K.M., Lear, G., 2021. Phylogenetic Distribution of Plastic-Degrading Microorganisms. mSystems 6. https://doi.org/10.1128/msystems.01112-20

Gardon, T., Morvan, L., Huvet, A., Quillien, V., Soyez, C., Le Moullac, G., Le Luyer, J., 2020. Microplastics induce dose-specific transcriptomic disruptions in energy metabolism and immunity of the pearl oyster *Pinctada margaritifera*. Environ. Pollut. 266, 115180. https://doi.org/10.1016/j.envpol.2020.115180

Gaspar, T.R., Chi, R.J., Parrow, M.W., Ringwood, A.H., 2018. Cellular bioreactivity of micro- and nano-plastic particles in oysters. Front. Mar. Sci. 5, 345. https://doi.org/10.3389/fmars.2018.00345

Gellissen, G., Hennecke, R., Spindler, K.D., 1991. The site of synthesis of hemocyanin in the crayfish, *Astacus leptodactylus*. Experientia 47, 194–195.

https://doi.org/10.1007/BF01945425

GESAMP (IMO/FAO/UNESCO-IOC/UNIDO/WMO/IAEA/UN/UNEP/UNDP Joint Group of Experts on the Scientific Aspects of Marine Environmental Protection), 2016. Sources, fate and effects of microplastics in the marine environment: part two of a global assessment, Reports and Studies GESAMP. International maritime organization.

GESAMP (IMO/FAO/UNESCO-IOC/UNIDO/WMO/IAEA/UN/UNEP/UNDP Joint Group of Experts on the Scientific Aspects of Marine Environmental Protection), 2015. Sources, fate and effects of microplastics in the marine environment: a global assessment, Reports and Studies GESAMP. International maritime organization, London.

Gewert, B., Plassmann, M.M., Macleod, M., 2015. Pathways for degradation of plastic polymers floating in the marine environment. Environ. Sci. Process. Impacts. https://doi.org/10.1039/c5em00207a

Geyer, R., 2020. Production, use, and fate of synthetic polymers, in: Letcher, T.M. (Ed.), Plastic Waste and Recycling. Elsevier, pp. 13–32. https://doi.org/10.1016/b978-0-12-817880-5.00002-5

Geyer, R., Jambeck, J.R., Law, K.L., 2017. Production, use, and fate of all plastics ever made. Sci. Adv. 3, e1700782. https://doi.org/10.1126/sciadv.1700782

Gherardi, F., 2006. Crayfish invading Europe: The case study of *Procambarus clarkii*. Mar. Freshw. Behav. Physiol. https://doi.org/10.1080/10236240600869702

Gherardi, F., Barbaresi, S., Vaselli, O., Bencini, A., 2002. A comparison of trace metal accumulation in indigenous and alien freshwater macro-decapods. Mar. Freshw. Behav. Physiol. 35, 179–188. https://doi.org/10.1080/1023624021000014761

Giancotti, F.G., Ruoslahti, E., 1999. Integrin signaling. Science 285, 1028–1033. https://doi.org/10.1126/science.285.5430.1028

Gigault, J., El Hadri, H., Nguyen, B., Grassl, B., Rowenczyk, L., Tufenkji, N., Feng, S., Wiesner, M., 2021. Nanoplastics are neither microplastics nor engineered nanoparticles. Nat. Nanotechnol. https://doi.org/10.1038/s41565-021-00886-4

Gigault, J., Pedrono, B., Maxit, B., Ter Halle, A., 2016. Marine plastic litter: The unanalyzed nano-fraction. Environ. Sci. Nano 3, 346–350. https://doi.org/10.1039/c6en00008h

Gigault, J., Ter Halle, A., Baudrimont, M., Pascal, P.-Y., Gauffre, F., Phi, T.-L., El Hadri, H., Grassl, B., Reynaud, S., 2018. Current opinion: What is a nanoplastic? Environ. Pollut. 235, 1030–1034. https://doi.org/10.1016/J.ENVPOL.2018.01.024

Giglio, A., Manfrin, C., Zanetti, M., Aquiloni, L., Simeon, E., Bravin, M.K., Battistella, S., Giulianini, P.G., 2018. Effects of X-ray irradiation on haemocytes of *Procambarus clarkii* (Arthropoda: Decapoda) males. Eur. Zool. J. 85, 26–35. https://doi.org/10.1080/24750263.2017.1423119

Giulianini, P.G., Bierti, M., Lorenzon, S., Battistella, S., Ferrero, E.A., 2007. Ultrastructural and functional characterization of circulating hemocytes from the freshwater crayfish *Astacus leptodactylus*: Cell types and their role after in vivo artificial non-self challenge. Micron 38, 49–57. https://doi.org/10.1016/j.micron.2006.03.019

Gonçalves, C., Martins, M., Sobral, P., Costa, P.M., Costa, M.H., 2019. An assessment of the ability to ingest and excrete microplastics by filter-feeders: A case study with the

Mediterranean mussel. Environ. Pollut. 245, 600–606. https://doi.org/10.1016/j.envpol.2018.11.038

González-Baró, M.D.R., Pollero, R.J., 1993. Palmitic acid metabolism in hepatopancreas of the freshwater shrimp *Macrobrachium borellii*. Comp. Biochem. Physiol. -- Part B Biochem. 106, 71–75. https://doi.org/10.1016/0305-0491(93)90009-T

González-Fernández, C., Tallec, K., Le Goïc, N., Lambert, C., Soudant, P., Huvet, A., Suquet, M., Berchel, M., Paul-Pont, I., 2018. Cellular responses of Pacific oyster (*Crassostrea gigas*) gametes exposed in vitro to polystyrene nanoparticles. Chemosphere 208, 764–772. https://doi.org/10.1016/j.chemosphere.2018.06.039

González-Fernández, D., Cózar, A., Hanke, G., Viejo, J., Morales-Caselles, C., Bakiu, R., Barceló, D., Bessa, F., Bruge, A., Cabrera, M., Castro-Jiménez, J., Constant, M., Crosti, R., Galletti, Y., Kideys, A.E., Machitadze, N., Pereira de Brito, J., Pogojeva, M., Ratola, N., Rigueira, J., Rojo-Nieto, E., Savenko, O., Schöneich-Argent, R.I., Siedlewicz, G., Suaria, G., Tourgeli, M., 2021. Floating macrolitter leaked from Europe into the ocean. Nat. Sustain. 4, 474–483. https://doi.org/10.1038/s41893-021-00722-6

González-Soto, N., Hatfield, J., Katsumiti, A., Duroudier, N., Lacave, J.M., Bilbao, E., Orbea, A., Navarro, E., Cajaraville, M.P., 2019. Impacts of dietary exposure to different sized polystyrene microplastics alone and with sorbed benzo[a]pyrene on biomarkers and whole organism responses in mussels *Mytilus galloprovincialis*. Sci. Total Environ. 684, 548–566. https://doi.org/10.1016/j.scitotenv.2019.05.161

Goodwin, S., McPherson, J.D., Richard McCombie, W., 2016. Coming of age: ten years of next-generation sequencing technologies. Nat. Publ. Gr. https://doi.org/10.1038/nrg.2016.49

Goretti, E., Pallottini, M., Ricciarini, M.I., Selvaggi, R., Cappelletti, D., 2016. Heavy metals bioaccumulation in selected tissues of red swamp crayfish: An easy tool for monitoring environmental contamination levels. Sci. Total Environ. 559, 339–346. https://doi.org/10.1016/j.scitotenv.2016.03.169

Götze, S., Saborowski, R., Martínez-Cruz, O., Muhlia-Almazán, A., Sánchez-Paz, A., 2017. Proteasome properties of hemocytes differ between the whiteleg shrimp Penaeus vannamei and the brown shrimp *Crangon crangon* (Crustacea, Decapoda). Cell Stress Chaperones 22, 879–891. https://doi.org/10.1007/s12192-017-0819-4

Grabherr, M.G., Haas, B.J., Yassour, M., Levin, J.Z., Thompson, D.A., Amit, I., Adiconis, X., Fan, L., Raychowdhury, R., Zeng, Q., Chen, Z., Mauceli, E., Hacohen, N., Gnirke, A., Rhind, N., Di Palma, F., Birren, B.W., Nusbaum, C., Lindblad-Toh, K., Friedman, N., Regev, A., 2011. Full-length transcriptome assembly from RNA-Seq data without a reference genome. Nat. Biotechnol. 29, 644–652. https://doi.org/10.1038/nbt.1883

Gray, A.D., Weinstein, J.E., 2017. Size- and shape-dependent effects of microplastic particles on adult daggerblade grass shrimp (*Palaemonetes pugio*). Environ. Toxicol. Chem. 36, 3074–3080. https://doi.org/10.1002/etc.3881

Green, D.S., 2016. Effects of microplastics on European flat oysters, *Ostrea edulis* and their associated benthic communities. Environ. Pollut. 216, 95–103. https://doi.org/10.1016/j.envpol.2016.05.043

Green, D.S., Boots, B., O'Connor, N.E., Thompson, R., 2017. Microplastics Affect the Ecological Functioning of an Important Biogenic Habitat. Environ. Sci. Technol. 51, 68–

77. https://doi.org/10.1021/acs.est.6b04496

Green, D.S., Colgan, T.J., Thompson, R.C., Carolan, J.C., 2019. Exposure to microplastics reduces attachment strength and alters the haemolymph proteome of blue mussels (*Mytilus edulis*). Environ. Pollut. 246, 423–434. https://doi.org/10.1016/j.envpol.2018.12.017

Grune, T., 2000. Oxidative stress, aging and the proteasomal system. Biogerontology. https://doi.org/10.1023/A:1010037908060

Gu, W., Liu, S., Chen, L., Liu, Y., Gu, C., Ren, H.Q., Wu, B., 2020. Single-Cell RNA Sequencing Reveals Size-Dependent Effects of Polystyrene Microplastics on Immune and Secretory Cell Populations from Zebrafish Intestines. Environ. Sci. Technol. 54, 3417–3427. https://doi.org/10.1021/acs.est.9b06386

Gutiérrez-Aguilar, M., Baines, C.P., 2015. Structural mechanisms of cyclophilin D-dependent control of the mitochondrial permeability transition pore. Biochim. Biophys. Acta - Gen. Subj. https://doi.org/10.1016/j.bbagen.2014.11.009

Hamed, M., Soliman, H.A.M., Osman, A.G.M., Sayed, A.E.D.H., 2019. Assessment the effect of exposure to microplastics in Nile Tilapia (*Oreochromis niloticus*) early juvenile: I. blood biomarkers. Chemosphere 228, 345–350. https://doi.org/10.1016/j.chemosphere.2019.04.153

Hämer, J., Gutow, L., Köhler, A., Saborowski, R., 2014. Fate of Microplastics in the Marine Isopod *Idotea emarginata*. Environ. Sci. Technol. 48, 13451–13458. https://doi.org/10.1021/es501385y

Han, J., Won, E.J., Kang, H.M., Lee, M.C., Jeong, C.B., Kim, H.S., Hwang, D.S., Lee, J.S., 2017. Marine copepod cytochrome P450 genes and their applications for molecular ecotoxicological studies in response to oil pollution. Mar. Pollut. Bull. 124, 953–961. https://doi.org/10.1016/j.marpolbul.2016.09.048

Hansen, B.H., Altin, D., Vang, S.H., Nordtug, T., Olsen, A.J., 2008. Effects of naphthalene on gene transcription in *Calanus finmarchicus* (Crustacea: Copepoda). Aquat. Toxicol. 86, 157–165. https://doi.org/10.1016/j.aquatox.2007.10.009

Harding, H.P., Zhang, Y., Zeng, H., Novoa, I., Lu, P.D., Calfon, M., Sadri, N., Yun, C., Popko, B., Paules, R., Stojdl, D.F., Bell, J.C., Hettmann, T., Leiden, J.M., Ron, D., 2003. An integrated stress response regulates amino acid metabolism and resistance to oxidative stress. Mol. Cell 11, 619–633. https://doi.org/10.1016/S1097-2765(03)00105-9

Hassan, P.A., Rana, S., Verma, G., 2015. Making sense of Brownian motion: Colloid characterization by dynamic light scattering. Langmuir. https://doi.org/10.1021/la501789z

Heindler, F.M., Alajmi, F., Huerlimann, R., Zeng, C., Newman, S.J., Vamvounis, G., van Herwerden, L., 2017. Toxic effects of polyethylene terephthalate microparticles and Di(2-ethylhexyl)phthalate on the calanoid copepod, *Parvocalanus crassirostris*. Ecotoxicol. Environ. Saf. 141, 298–305. https://doi.org/10.1016/J.ECOENV.2017.03.029

Heinlaan, M., Kasemets, K., Aruoja, V., Blinova, I., Bondarenko, O., Lukjanova, A., Khosrovyan, A., Kurvet, I., Pullerits, M., Sihtmäe, M., Vasiliev, G., Vija, H., Kahru, A., 2020. Hazard evaluation of polystyrene nanoplastic with nine bioassays did not show particle-specific acute toxicity. Sci. Total Environ. 707. https://doi.org/10.1016/j.scitotenv.2019.136073

Hernandez, L.M., Xu, E.G., Larsson, H.C.E., Tahara, R., Maisuria, V.B., Tufenkji, N., 2019.

Plastic Teabags Release Billions of Microparticles and Nanoparticles into Tea. Environ. Sci. Technol. 53, 12300–12310. https://doi.org/10.1021/acs.est.9b02540

Hernandez, L.M., Yousefi, N., Tufenkji, N., 2017. Are there nanoplastics in your personal care products? Environ. Sci. Technol. Lett. 4, 280–285. https://doi.org/10.1021/acs.estlett.7b00187

Hobbs, H.H., Jass, J.P., Huner, J. V., 2008. A Review of Global Crayfish Introductions With Particular Emphasis On Two North American Species (Decapoda, Cambaridae). Crustaceana 56, 299–316. https://doi.org/10.1163/156854089x00275

Holcik, M., Sonenberg, N., 2005. Translational control in stress and apoptosis. Nat. Rev. Mol. Cell Biol. 6, 318-327. https://doi.org/10.1038/nrm1618

Homola, E., Chang, E.S., 1997. Distribution and regulation of esterases that hydrolyze methyl farnesoate in *Homarus americanus* and other crustaceans. Gen. Comp. Endocrinol. 106, 62–72. https://doi.org/10.1006/gcen.1996.6850

Horton, A.A., Svendsen, C., Williams, R.J., Spurgeon, D.J., Lahive, E., 2017a. Large microplastic particles in sediments of tributaries of the River Thames, UK – Abundance, sources and methods for effective quantification. Mar. Pollut. Bull. 114, 218–226. https://doi.org/10.1016/j.marpolbul.2016.09.004

Horton, A.A., Walton, A., Spurgeon, D.J., Lahive, E., Svendsen, C., 2017b. Microplastics in freshwater and terrestrial environments: Evaluating the current understanding to identify the knowledge gaps and future research priorities. Sci. Total Environ. 586, 127–141. https://doi.org/10.1016/J.SCITOTENV.2017.01.190

Hu, M., Palić, D., 2020. Micro- and nano-plastics activation of oxidative and inflammatory adverse outcome pathways. Redox Biol. 101620. https://doi.org/10.1016/j.redox.2020.101620

Hu, Q., Wang, H., He, C., Jin, Y., Fu, Z., 2020. Polystyrene nanoparticles trigger the activation of p38 MAPK and apoptosis via inducing oxidative stress in zebrafish and macrophage cells. Environ. Pollut. 116075. https://doi.org/10.1016/j.envpol.2020.116075

Huang, Y., Li, T., Jin, M., Yin, S., Hui, K.M., Ren, Q., 2017. Newly identified PcToll4 regulates antimicrobial peptide expression in intestine of red swamp crayfish *Procambarus clarkii*. Gene 610, 140–147. https://doi.org/10.1016/j.gene.2017.02.018

Huang, Y., Zhao, L.L., Feng, J.L., Zhu, H.X., Huang, X., Ren, Q., Wang, W., 2015. A novel integrin function in innate immunity from Chinese mitten crab (*Eriocheir sinensis*). Dev. Comp. Immunol. 52, 155–165. https://doi.org/10.1016/j.dci.2015.05.005

Hüffer, T., Praetorius, A., Wagner, S., Von Der Kammer, F., Hofmann, T., 2017. Microplastic Exposure Assessment in Aquatic Environments: Learning from Similarities and Differences to Engineered Nanoparticles. Environ. Sci. Technol. 51, 2499–2507. https://doi.org/10.1021/acs.est.6b04054

Hurley, R., Woodward, J., Rothwell, J.J., 2018. Microplastic contamination of river beds significantly reduced by catchment-wide flooding. Nat. Geosci. https://doi.org/10.1038/s41561-018-0080-1

Hurley, R.R., Nizzetto, L., 2018. Fate and occurrence of micro(nano)plastics in soils: Knowledge gaps and possible risks. Curr. Opin. Environ. Sci. Heal. https://doi.org/10.1016/j.coesh.2017.10.006

Imai, J., Maruya, M., Yashiroda, H., Yahara, I., Tanaka, K., 2003. The molecular chaperone Hsp90 plays a role in the assembly and maintenance of the 26S proteasome. EMBO J. 22, 3557–3567. https://doi.org/10.1093/emboj/cdg349

Ishwarya, R., Jayakumar, R., Abinaya, M., Govindarajan, M., Alharbi, N.S., Kadaikunnan, S., Khaled, J.M., Al-Anbr, M.N., Vaseeharan, B., 2019. Facile synthesis of haemocyanin-capped zinc oxide nanoparticles: Effect on growth performance, digestive-enzyme activity, and immune responses of *Penaeus semisulcatus*. Int. J. Biol. Macromol. 139, 688–696. https://doi.org/10.1016/j.ijbiomac.2019.07.216

Ishwarya, R., Vaseeharan, B., Subbaiah, S., Nazar, A.K., Govindarajan, M., Alharbi, N.S., Kadaikunnan, S., Khaled, J.M., Al-anbr, M.N., 2018. Sargassum wightii-synthesized ZnO nanoparticles – from antibacterial and insecticidal activity to immunostimulatory effects on the green tiger shrimp *Penaeus semisulcatus*. J. Photochem. Photobiol. B Biol. 183, 318–330. https://doi.org/10.1016/j.jphotobiol.2018.04.049

Isobe, A., Uchiyama-Matsumoto, K., Uchida, K., Tokai, T., 2017. Microplastics in the Southern Ocean. Mar. Pollut. Bull. 114, 623–626. https://doi.org/10.1016/j.marpolbul.2016.09.037

Jacquin, J., Cheng, J., Odobel, C., Pandin, C., Conan, P., Pujo-Pay, M., Barbe, V., Meistertzheim, A.L., Ghiglione, J.F., 2019. Microbial ecotoxicology of marine plastic debris: A review on colonization and biodegradation by the "plastisphere." Front. Microbiol. 10, 865. https://doi.org/10.3389/fmicb.2019.00865

Jaikumar, G., Brun, N.R., Vijver, M.G., Bosker, T., 2019. Reproductive toxicity of primary and secondary microplastics to three cladocerans during chronic exposure. Environ. Pollut. 249, 638–646. https://doi.org/10.1016/j.envpol.2019.03.085

Jambeck, J.R., Geyer, R., Wilcox, C., Siegler, T.R., Perryman, M., Andrady, A., Narayan, R., Law, K.L., 2015. Plastic waste inputs from land into the ocean. Science. 347, 768–71. https://doi.org/10.1126/science.1260352

Jamieson, A.J., Brooks, L.S.R., Reid, W.D.K., Piertney, S.B., Narayanaswamy, B.E., Linley, T.D., 2019. Microplastics and synthetic particles ingested by deep-sea amphipods in six of the deepest marine ecosystems on Earth. R. Soc. Open Sci. 6. https://doi.org/10.1098/rsos.180667

Jamil, M., Wang, W., Xu, M., Tu, J., 2015. Exploring the roles of basal transcription factor 3 in eukaryotic growth and development. Biotechnol. Genet. Eng. Rev. 31, 21–45. https://doi.org/10.1080/02648725.2015.1080064

Jancova, P., Anzenbacherova, E., Anzenbacher, P., 2010. Phase II drug metabolizing enzymes. Biomed. Pap. 154, 103–116. https://doi.org/10.5507/bp.2010.017

Jefferson, J.J., Leung, C.L., Liem, R.K.H., 2004. Plakins: Goliaths that link cell junctions and the cytoskeleton. Nat. Rev. Mol. Cell Biol. https://doi.org/10.1038/nrm1425

Jemec, A., Horvat, P., Kunej, U., Bele, M., Kržan, A., 2016. Uptake and effects of microplastic textile fibers on freshwater crustacean *Daphnia magna*. Environ. Pollut. 219, 201–209. https://doi.org/10.1016/j.envpol.2016.10.037

Jensen, L.E., Whitehead, A.S., 1998. Regulation of serum amyloid A protein expression during the acute-phase response. Biochem. J. https://doi.org/10.1042/bj3340489

Jeong, C.B., Kang, H.M., Byeon, E., Kim, M.S., Ha, S.Y., Kim, M., Jung, J.H., Lee, J.S., 2021. Phenotypic and transcriptomic responses of the rotifer *Brachionus koreanus* by single and

combined exposures to nano-sized microplastics and water-accommodated fractions of crude oil. J. Hazard. Mater. 416, 125703. https://doi.org/10.1016/j.jhazmat.2021.125703

Jeong, C.B., Kang, H.M., Lee, M.C., Kim, D.H., Han, J., Hwang, D.S., Souissi, S., Lee, S.J., Shin, K.H., Park, H.G., Lee, J.S., 2017. Adverse effects of microplastics and oxidative stress-induced MAPK/Nrf2 pathway-mediated defense mechanisms in the marine copepod *Paracyclopina nana*. Sci. Rep. 7. https://doi.org/10.1038/srep41323

Jeong, C.B., Kang, H.M., Lee, Y.H., Kim, M.S., Lee, Jin Sol, Seo, J.S., Wang, M., Lee, Jae Seong, 2018. Nanoplastic Ingestion Enhances Toxicity of Persistent Organic Pollutants (POPs) in the Monogonont Rotifer *Brachionus koreanus* via Multixenobiotic Resistance (MXR) Disruption. Environ. Sci. Technol. 52, 11411–11418. https://doi.org/10.1021/acs.est.8b03211

Jeong, C.B., Won, E.J., Kang, H.M., Lee, M.C., Hwang, D.S., Hwang, U.K., Zhou, B., Souissi, S., Lee, S.J., Lee, J.S., 2016. Microplastic Size-Dependent Toxicity, Oxidative Stress Induction, and p-JNK and p-p38 Activation in the Monogonont Rotifer (*Brachionus koreanus*). Environ. Sci. Technol. 50, 8849–8857. https://doi.org/10.1021/acs.est.6b01441

Jeong, J., Choi, J., 2019. Adverse outcome pathways potentially related to hazard identification of microplastics based on toxicity mechanisms. Chemosphere. https://doi.org/10.1016/j.chemosphere.2019.05.003

Jiao, T., Chu, X.H., Gao, Z.Q., Yang, T.T., Liu, Y., Yang, L., Zhang, D.Z., Wang, J.L., Tang, B.P., Wu, K., Liu, Q.N., Dai, L.S., 2019. New insight into the molecular basis of Fe (III) stress responses of *Procambarus clarkii* by transcriptome analysis. Ecotoxicol. Environ. Saf. 182. https://doi.org/10.1016/j.ecoenv.2019.109388

Jimenez-Gutierrez, S., Cadena-Caballero, C.E., Barrios-Hernandez, C., Perez-Gonzalez, R., Martinez-Perez, F., Jimenez-Gutierrez, L.R., 2019. Crustacean vitellogenin: A systematic and experimental analysis of their genes, genomes, mRNAs and proteins; and perspective to Next Generation Sequencing. Crustaceana 92, 1169–1205. https://doi.org/10.1163/15685403-00003930

Johnson, N.G., Burnett, L.E., Burnett, K.G., 2011. Properties of bacteria that trigger hemocytopenia in the Atlantic Blue Crab, *Callinectes sapidus*. Biol. Bull. 221, 164–175. https://doi.org/10.1086/BBLv221n2p164

Jones-Williams, K., Galloway, T., Cole, M., Stowasser, G., Waluda, C., Manno, C., 2020. Close encounters - microplastic availability to pelagic amphipods in sub-antarctic and antarctic surface waters. Environ. Int. 140, 105792. https://doi.org/10.1016/j.envint.2020.105792

Juarez-Moreno, K., Mejía-Ruiz, C.H., Díaz, F., Reyna-Verdugo, H., Re, A.D., Vazquez-Felix, E.F., Sánchez-Castrejón, E., Mota-Morales, J.D., Pestryakov, A., Bogdanchikova, N., 2017. Effect of silver nanoparticles on the metabolic rate, hematological response, and survival of juvenile white shrimp *Litopenaeus vannamei*. Chemosphere 169, 716–724. https://doi.org/10.1016/j.chemosphere.2016.11.054

Kandasamy, K., Alikunhi, N.M., Manickaswami, G., Nabikhan, A., Ayyavu, G., 2013. Synthesis of silver nanoparticles by coastal plant *Prosopis chilensis* (L.) and their efficacy in controlling vibriosis in shrimp *Penaeus monodon*. Appl. Nanosci. 3, 65–73. https://doi.org/10.1007/s13204-012-0064-1

Kane, I.A., Clare, M.A., Miramontes, E., Wogelius, R., Rothwell, J.J., Garreau, P., Pohl, F., 2020. Seafloor microplastic hotspots controlle by deep-sea circulation. Science (80-.).

368, 1140–1145. https://doi.org/10.1126/science.aba5899

Kelly, A., Lannuzel, D., Rodemann, T., Meiners, K.M., Auman, H.J., 2020. Microplastic contamination in east Antarctic sea ice. Mar. Pollut. Bull. 154, 111130. https://doi.org/10.1016/j.marpolbul.2020.111130

Klein, S., Dimzon, I.K., Eubeler, J., Knepper, T.P., 2018. Analysis, occurrence, and degradation of microplastics in the aqueous environment, in: Handbook of Environmental Chemistry. Springer Verlag, pp. 51–67. https://doi.org/10.1007/978-3-319-61615-5_3

Klein, S., Worch, E., Knepper, T.P., 2015. Occurrence and Spatial Distribution of Microplastics in River Shore Sediments of the Rhine-Main Area in Germany. Environ. Sci. Technol. https://doi.org/10.1021/acs.est.5b00492

Koelmans, A.A., Besseling, E., Foekema, E., Kooi, M., Mintenig, S., Ossendorp, B.C., Redondo-Hasselerharm, P.E., Verschoor, A., van Wezel, A.P., Scheffer, M., 2017a. Risks of Plastic Debris: Unravelling Fact, Opinion, Perception, and Belief. Environ. Sci. Technol. 51, 11513–11519. https://doi.org/10.1021/acs.est.7b02219

Koelmans, A.A., Besseling, E., Shim, W.J., 2015. Nanoplastics in the Aquatic Environment. Critical Review, in: Marine Anthropogenic Litter. Springer International Publishing, Cham, pp. 325–340. https://doi.org/10.1007/978-3-319-16510-3_12

Koelmans, A.A., Kooi, M., Law, K.L., Van Sebille, E., 2017b. All is not lost: Deriving a top-down mass budget of plastic at sea. Environ. Res. Lett. 12, 114028. https://doi.org/10.1088/1748-9326/aa9500

Kooi, M., Reisser, J., Slat, B., Ferrari, F.F., Schmid, M.S., Cunsolo, S., Brambini, R., Noble, K., Sirks, L.A., Linders, T.E.W., Schoeneich-Argent, R.I., Koelmans, A.A., 2016. The effect of particle properties on the depth profile of buoyant plastics in the ocean. Sci. Rep. 6, 1–10. https://doi.org/10.1038/srep33882

Kooi, M., Van Nes, E.H., Scheffer, M., Koelmans, A.A., 2017. Ups and Downs in the Ocean: Effects of Biofouling on Vertical Transport of Microplastics. Environ. Sci. Technol. 51, 7963–7971. https://doi.org/10.1021/acs.est.6b04702

Korez, Š., Gutow, L., Saborowski, R., 2020. Coping with the “dirt”: brown shrimp and the microplastic threat. Zoology 143, 125848. https://doi.org/10.1016/j.zool.2020.125848

Koster, J., Geerts, D., Favre, B., Borradori, L., Sonnenberg, A., 2003. Analysis of the interactions between BP180, BP230, plectin and the integrin α6β4 important for hemidesmosome assembly. J. Cell Sci. https://doi.org/10.1242/jcs.00241

Krause, S., Molari, M., Gorb, E. V., Gorb, S.N., Kossel, E., Haeckel, M., 2020. Persistence of plastic debris and its colonization by bacterial communities after two decades on the abyssal seafloor. Sci. Rep. 10, 1–15. https://doi.org/10.1038/s41598-020-66361-7

Kühn, S., van Franeker, J.A., 2020. Quantitative overview of marine debris ingested by marine megafauna. Mar. Pollut. Bull. https://doi.org/10.1016/j.marpolbul.2019.110858

Kuznetsova, A., Brockhoff, P.B., Christensen, R.H.B., 2017. lmerTest Package: Tests in Linear Mixed Effects Models . J. Stat. Softw. 82, 1–26. https://doi.org/10.18637/jss.v082.i13

Kwon, Y.T., Ciechanover, A., 2017. The Ubiquitin Code in the Ubiquitin-Proteasome System and Autophagy. Trends Biochem. Sci. https://doi.org/10.1016/j.tibs.2017.09.002

Lacerda, A.L. d. F., Rodrigues, L. dos S., van Sebille, E., Rodrigues, F.L., Ribeiro, L., Secchi,

E.R., Kessler, F., Proietti, M.C., 2019. Plastics in sea surface waters around the Antarctic Peninsula. Sci. Rep. 9, 1–12. https://doi.org/10.1038/s41598-019-40311-4

Lambert, S., Wagner, M., 2018. Microplastics are contaminants of emerging concern in freshwater environments: An overview, in: Handbook of Environmental Chemistry. Springer Verlag, pp. 1–23. https://doi.org/10.1007/978-3-319-61615-5_1

Lambert, S., Wagner, M., 2016. Characterisation of nanoplastics during the degradation of polystyrene. Chemosphere 145, 265–268. https://doi.org/10.1016/j.chemosphere.2015.11.078

Lan, J.F., Zhao, L.J., Wei, S., Wang, Y., Lin, L., Li, X.C., 2016. PcToll2 positively regulates the expression of antimicrobial peptides by promoting PcATF4 translocation into the nucleus. Fish Shellfish Immunol. 58, 59–66. https://doi.org/10.1016/j.fsi.2016.09.007

Lau, W.W.Y., Shiran, Y., Bailey, R.M., Cook, E., Stuchtey, M.R., Koskella, J., Velis, C.A., Godfrey, L., Boucher, J., Murphy, M.B., Thompson, R.C., Jankowska, E., Castillo, A.C., Pilditch, T.D., Dixon, B., Koerselman, L., Kosior, E., Favoino, E., Gutberlet, J., Baulch, S., Atreya, M.E., Fischer, D., He, K.K., Petit, M.M., Sumaila, U.R., Neil, E., Bernhofen, M. V., Lawrence, K., Palardy, J.E., 2020. Evaluating scenarios toward zero plastic pollution. Science (80-.). 369, 1455–1461. https://doi.org/10.1126/SCIENCE.ABA9475

Lear, G., Kingsbury, J.M., Franchini, S., Gambarini, V., Maday, S.D.M., Wallbank, J.A., Weaver, L., Pantos, O., 2021. Plastics and the microbiome: impacts and solutions. Environ. Microbiomes. https://doi.org/10.1186/s40793-020-00371-w

Lebreton, L.C.M., Greer, S.D., Borrero, J.C., 2012. Numerical modelling of floating debris in the world's oceans. Mar. Pollut. Bull. 64, 653–661. https://doi.org/10.1016/j.marpolbul.2011.10.027

Lebreton, L.C.M., Slat, B., Ferrari, F., Sainte-Rose, B., Aitken, J., Marthouse, R., Hajbane, S., Cunsolo, S., Schwarz, A., Levivier, A., Noble, K., Debeljak, P., Maral, H., Schoeneich-Argent, R., Brambini, R., Reisser, J., 2018. Evidence that the Great Pacific Garbage Patch is rapidly accumulating plastic. Sci. Rep. 8, 4666. https://doi.org/10.1038/s41598-018-22939-w

Lebreton, L.C.M., van der Zwet, J., Damsteeg, J.-W., Slat, B., Andrady, A., Reisser, J., 2017. River plastic emissions to the world's oceans. Nat. Commun. 8, 15611. https://doi.org/10.1038/ncomms15611

Lechner, A., Keckeis, H., Lumesberger-Loisl, F., Zens, B., Krusch, R., Tritthart, M., Glas, M., Schludermann, E., 2014. The Danube so colourful: A potpourri of plastic litter outnumbers fish larvae in Europe's second largest river. Environ. Pollut. 188, 177–181. https://doi.org/10.1016/j.envpol.2014.02.006

Lee, K.W., Shim, W.J., Kwon, O.Y., Kang, J.H., 2013. Size-dependent effects of micro polystyrene particles in the marine copepod *Tigriopus japonicus*. Environ. Sci. Technol. 47, 11278–11283. https://doi.org/10.1021/es401932b

Leist, M., Ghallab, A., Graepel, R., Marchan, R., Hassan, R., Bennekou, S.H., Limonciel, A., Vinken, M., Schildknecht, S., Waldmann, T., Danen, E., van Ravenzwaay, B., Kamp, H., Gardner, I., Godoy, P., Bois, F.Y., Braeuning, A., Reif, R., Oesch, F., Drasdo, D., Höhme, S., Schwarz, M., Hartung, T., Braunbeck, T., Beltman, J., Vrieling, H., Sanz, F., Forsby, A., Gadaleta, D., Fisher, C., Kelm, J., Fluri, D., Ecker, G., Zdrazil, B., Terron, A., Jennings, P., van der Burg, B., Dooley, S., Meijer, A.H., Willighagen, E., Martens, M.,

Evelo, C., Mombelli, E., Taboureau, O., Mantovani, A., Hardy, B., Koch, B., Escher, S., van Thriel, C., Cadenas, C., Kroese, D., van de Water, B., Hengstler, J.G., 2017. Adverse outcome pathways: opportunities, limitations and open questions. Arch. Toxicol. 91, 3477–3505. https://doi.org/10.1007/s00204-017-2045-3

LeMoine, C.M.R., Kelleher, B.M., Lagarde, R., Northam, C., Elebute, O.O., Cassone, B.J., 2018. Transcriptional effects of polyethylene microplastics ingestion in developing zebrafish (*Danio rerio*). Environ. Pollut. 243, 591–600. https://doi.org/10.1016/j.envpol.2018.08.084

Lenth, R. V., 2016. Least-squares means: The R package lsmeans. J. Stat. Softw. 69, 1–33. https://doi.org/10.18637/jss.v069.i01

Leslie, H.A., Brandsma, S.H., van Velzen, M.J.M., Vethaak, A.D., 2017. Microplastics en route: Field measurements in the Dutch river delta and Amsterdam canals, wastewater treatment plants, North Sea sediments and biota. Environ. Int. 101, 133–142. https://doi.org/10.1016/j.envint.2017.01.018

Li, F., Ni, M., Zhang, H., Wang, B., Xu, K., Tian, J., Hu, J., Shen, W., Li, B., 2015. Expression profile analysis of silkworm P450 family genes after phoxim induction. Pestic. Biochem. Physiol. 122, 103–109. https://doi.org/10.1016/j.pestbp.2014.12.013

Li, W., Godzik, A., 2006. Cd-hit: A fast program for clustering and comparing large sets of protein or nucleotide sequences. Bioinformatics 22, 1658–1659. https://doi.org/10.1093/bioinformatics/btl158

Li, Y., Liu, Z., Li, M., Jiang, Q., Wu, D., Huang, Y., Jiao, Y., Zhang, M., Zhao, Y., 2020a. Effects of nanoplastics on antioxidant and immune enzyme activities and related gene expression in juvenile *Macrobrachium nipponense*. J. Hazard. Mater. 398, 122990. https://doi.org/10.1016/j.jhazmat.2020.122990

Li, Y., Liu, Z., Yang, Y., Jiang, Q., Wu, D., Huang, Youhui, Jiao, Y., Chen, Q., Huang, Yinying, Zhao, Y., 2020b. Effects of nanoplastics on energy metabolism in the oriental river prawn (*Macrobrachium nipponense*). Environ. Pollut. 115890. https://doi.org/10.1016/j.envpol.2020.115890

Li, Z., Feng, C., Wu, Y., Guo, X., 2020. Impacts of nanoplastics on bivalve: Fluorescence tracing of organ accumulation, oxidative stress and damage. J. Hazard. Mater. 392, 122418. https://doi.org/10.1016/j.jhazmat.2020.122418

Liang, Z., Liu, R., Zhao, D., Wang, L., Sun, M., Wang, M., Song, L., 2016. Ammonia exposure induces oxidative stress, endoplasmic reticulum stress and apoptosis in hepatopancreas of pacific white shrimp (*Litopenaeus vannamei*). Fish Shellfish Immunol. 54, 523–528. https://doi.org/10.1016/j.fsi.2016.05.009

Limonta, G., Mancia, A., Benkhalqui, A., Bertolucci, C., Abelli, L., Fossi, M.C., Panti, C., 2019. Microplastics induce transcriptional changes, immune response and behavioral alterations in adult zebrafish. Sci. Rep. 9. https://doi.org/10.1038/s41598-019-52292-5

Lin, W., Jiang, R., Hu, S., Xiao, X., Wu, J., Wei, S., Xiong, Y., Ouyang, G., 2019. Investigating the toxicities of different functionalized polystyrene nanoplastics on *Daphnia magna*. Ecotoxicol. Environ. Saf. 180, 509–516. https://doi.org/10.1016/j.ecoenv.2019.05.036

Lin, Y.C., Chen, J.C., Chen, Y.Y., Liu, C.H., Cheng, W., Hsu, C.H., Tsui, W.C., 2013. Characterization of white shrimp *Litopenaeus vannamei* integrin β and its role in

immunomodulation by dsRNA-mediated gene silencing. Dev. Comp. Immunol. 40, 167–179. https://doi.org/10.1016/j.dci.2013.01.001

Lindstedt, G., Lindstedt, S., 1970. Cofactor requirements of gamma-butyrobetaine hydroxylase from rat liver. J. Biol. Chem. 245, 4178–4186.

Liu, L., Fokkink, R., Koelmans, A.A., 2016. Sorption of polycyclic aromatic hydrocarbons to polystyrene nanoplastic. Environ. Toxicol. Chem. 35, 1650–1655. https://doi.org/10.1002/etc.3311

Liu, W., Zhao, Y., Shi, Z., Li, Z., Liang, X., 2020. Ecotoxicoproteomic assessment of microplastics and plastic additives in aquatic organisms: A review. Comp. Biochem. Physiol. - Part D Genomics Proteomics 36, 100713. https://doi.org/10.1016/j.cbd.2020.100713

Liu, Z., Cai, M., Wu, D., Yu, P., Jiao, Y., Jiang, Q., Zhao, Y., 2020a. Effects of nanoplastics at predicted environmental concentration on *Daphnia pulex* after exposure through multiple generations. Environ. Pollut. 256, 113506. https://doi.org/10.1016/j.envpol.2019.113506

Liu, Z., Huang, Y., Jiao, Y., Chen, Q., Wu, D., Yu, P., Li, Y., Cai, M., Zhao, Y., 2020b. Polystyrene nanoplastic induces ROS production and affects the MAPK-HIF-1/NFkB-mediated antioxidant system in *Daphnia pulex*. Aquat. Toxicol. 220, 105420. https://doi.org/10.1016/j.aquatox.2020.105420

Liu, Z., Li, Y., Pérez, E., Jiang, Q., Chen, Q., Jiao, Y., Huang, Y., Yang, Y., Zhao, Y., 2021a. Polystyrene nanoplastic induces oxidative stress, immune defense, and glycometabolism change in *Daphnia pulex*: Application of transcriptome profiling in risk assessment of nanoplastics. J. Hazard. Mater. 402, 123778. https://doi.org/10.1016/j.jhazmat.2020.123778

Liu, Z., Li, Y., Sepúlveda, M.S., Jiang, Q., Jiao, Y., Chen, Q., Huang, Y., Tian, J., Zhao, Y., 2021b. Development of an adverse outcome pathway for nanoplastic toxicity in *Daphnia pulex* using proteomics. Sci. Total Environ. 766, 144249. https://doi.org/10.1016/j.scitotenv.2020.144249

Liu, Z., Yu, P., Cai, M., Wu, D., Zhang, M., Chen, M., Zhao, Y., 2019a. Effects of microplastics on the innate immunity and intestinal microflora of juvenile *Eriocheir sinensis*. Sci. Total Environ. 685, 836–846. https://doi.org/10.1016/j.scitotenv.2019.06.265

Liu, Z., Yu, P., Cai, M., Wu, D., Zhang, M., Huang, Y., Zhao, Y., 2019b. Polystyrene nanoplastic exposure induces immobilization, reproduction, and stress defense in the freshwater cladoceran *Daphnia pulex*. Chemosphere 215, 74–81. https://doi.org/10.1016/j.chemosphere.2018.09.176

Llorca, M., Vega-Herrera, A., Schirinzi, G., Savva, K., Abad, E., Farré, M., 2021. Screening of suspected micro(nano)plastics in the Ebro Delta (Mediterranean Sea). J. Hazard. Mater. 404, 124022. https://doi.org/10.1016/j.jhazmat.2020.124022

Lorenzon, S., 2005. Hyperglycemic stress response in Crustacea. Invertebr. Surviv. J. 2, 132–141.

Lorenzon, S., Edomi, P., Giulianini, P.G., Mettulio, R., Ferrero, E.A., 2004. Variation of crustacean hyperglycemic hormone (cHH) level in the eyestalk and haemolymph of the shrimp *Palaemon elegans* following stress. J. Exp. Biol. 207, 4205–4213. https://doi.org/10.1242/jeb.01264

Lorenzon, S., Giulianini, P.G., Libralato, S., Martinis, M., Ferrero, E.A., 2008. Stress effect of two different transport systems on the physiological profiles of the crab *Cancer pagurus*. Aquaculture 278, 156–163. https://doi.org/10.1016/j.aquaculture.2008.03.011

Lorenzon, S., Martinis, M., Ferrero, E.A., 2011. Ecological Relevance of Hemolymph Total Protein Concentration in Seven Unrelated Crustacean Species from Different Habitats Measured Predictively by a Density-Salinity Refractometer. J. Mar. Biol. 2011. https://doi.org/10.1155/2011/153654

Love, M.I., Huber, W., Anders, S., 2014. Moderated estimation of fold change and dispersion for RNA-seq data with DESeq2. Genome Biol. 15, 550. https://doi.org/10.1186/s13059-014-0550-8

Luan, L., Wang, X., Zheng, H., Liu, L., Luo, X., Li, F., 2019. Differential toxicity of functionalized polystyrene microplastics to clams (*Meretrix meretrix*) at three key development stages of life history. Mar. Pollut. Bull. 139, 346–354. https://doi.org/10.1016/j.marpolbul.2019.01.003

Luo, M., Yang, L., Wang, Z. ang, Zuo, H., Weng, S., He, J., Xu, X., 2019. A novel C-type lectin with microbiostatic and immune regulatory functions from *Litopenaeus vannamei*. Fish Shellfish Immunol. 93, 361–368. https://doi.org/10.1016/j.fsi.2019.07.047

Lushchak, V.I., 2011. Environmentally induced oxidative stress in aquatic animals. Aquat. Toxicol. https://doi.org/10.1016/j.aquatox.2010.10.006

Lusher, A., Hollman, P., Mandoza-Hill, J., 2017. Microplastics in fisheries and aquaculture: Status of knowledge on their occurrence and implications for aquatic organisms and food safety, FAO Fisheries and Aquaculture Technical Paper.

Lusher, A., Tirelli, V., O'Connor, I., Officer, R., 2015. Microplastics in Arctic polar waters: The first reported values of particles in surface and sub-surface samples. Sci. Rep. 5, 14947. https://doi.org/10.1038/srep14947

Lv, Weiwei, Zhou, W., Lu, S., Huang, W., Yuan, Q., Tian, M., Lv, Weiguang, He, D., 2019. Microplastic pollution in rice-fish co-culture system: A report of three farmland stations in Shanghai, China. Sci. Total Environ. 652, 1209–1218. https://doi.org/10.1016/J.SCITOTENV.2018.10.321

MacManes, M.D., 2018. The Oyster River Protocol: A multi-assembler and kmer approach for de novo transcriptome assembly. PeerJ 2018. https://doi.org/10.7717/peerj.5428

Magni, S., Della Torre, C., Garrone, G., D'Amato, A., Parenti, C.C., Binelli, A., 2019. First evidence of protein modulation by polystyrene microplastics in a freshwater biological model. Environ. Pollut. 250, 407–415. https://doi.org/10.1016/j.envpol.2019.04.088

Magni, S., Gagné, F., André, C., Della Torre, C., Auclair, J., Hanana, H., Parenti, C.C., Bonasoro, F., Binelli, A., 2018. Evaluation of uptake and chronic toxicity of virgin polystyrene microbeads in freshwater zebra mussel *Dreissena polymorpha* (Mollusca: Bivalvia). Sci. Total Environ. 631–632, 778–788. https://doi.org/10.1016/j.scitotenv.2018.03.075

Mak, C.W., Ching-Fong Yeung, K., Chan, K.M., 2019. Acute toxic effects of polyethylene microplastic on adult zebrafish. Ecotoxicol. Environ. Saf. 182, 109442. https://doi.org/10.1016/j.ecoenv.2019.109442

Manfrin, C., Pallavicini, A., Battistella, S., Lorenzon, S., Giulianini, P.G., 2016. Crustacean

Immunity, in: Lessons in Immunity. Elsevier, pp. 107–116. https://doi.org/10.1016/B978-0-12-803252-7.00008-4

Manfrin, C., Souty-Grosset, C., Anastácio, P.M., Reynolds, J., Giulianini, P.G., 2019. Detection and Control of Invasive Freshwater Crayfish: From Traditional to Innovative Methods. Diversity 11, 5. https://doi.org/10.3390/d11010005

Mani, T., Hauk, A., Walter, U., Burkhardt-Holm, P., 2015. Microplastics profile along the Rhine River. Sci. Rep. 5. https://doi.org/10.1038/srep17988

Mashek, D.G., Li, L.O., Coleman, R.A., 2007. Long-chain acyl-CoA synthetases and fatty acid channeling. Future Lipidol. https://doi.org/10.2217/17460875.2.4.465

McCarthy, D.J., Chen, Y., Smyth, G.K., 2012. Differential expression analysis of multifactor RNA-Seq experiments with respect to biological variation. Nucleic Acids Res. 40, 4288–4297. https://doi.org/10.1093/nar/gks042

Metzker, M.L., 2010. Sequencing technologies the next generation. Nat. Rev. Genet. https://doi.org/10.1038/nrg2626

Mitrano, D.M., Wick, P., Nowack, B., 2021. Placing nanoplastics in the context of global plastic pollution. Nat. Nanotechnol. https://doi.org/10.1038/s41565-021-00888-2

Morani, F., Doccini, S., Sirica, R., Paterno, M., Pezzini, F., Ricca, I., Simonati, A., Delledonne, M., Santorelli, F.M., 2019. Functional Transcriptome Analysis in ARSACS KO Cell Model Reveals a Role of Sacsin in Autophagy. Sci. Rep. https://doi.org/10.1038/s41598-019-48047-x

MSFD Technical Subgroup on Marine Litter, 2013. Guidance on Monitoring of Marine Litter in European Seas, JRC Scientific and Policy Reports. Luxembourg. https://doi.org/10.2788/99475

Munari, C., Infantini, V., Scoponi, M., Rastelli, E., Corinaldesi, C., Mistri, M., 2017. Microplastics in the sediments of Terra Nova Bay (Ross Sea, Antarctica). Mar. Pollut. Bull. 122, 161–165. https://doi.org/10.1016/j.marpolbul.2017.06.039

Muñoz-Gómez, S.A., Slamovits, C.H., Dacks, J.B., Wideman, J.G., 2015. The evolution of MICOS: Ancestral and derived functions and interactions. Commun. Integr. Biol. 8, 1–5. https://doi.org/10.1080/19420889.2015.1094593

Muralisankar, T., Bhavan, P.S., Radhakrishnan, S., Seenivasan, C., Manickam, N., Srinivasan, V., 2014. Dietary supplementation of zinc nanoparticles and its influence on biology, physiology and immune responses of the freshwater prawn, *Macrobrachium rosenbergii*. Biol. Trace Elem. Res. 160, 56–66. https://doi.org/10.1007/s12011-014-0026-4

Muralisankar, T., Bhavan, P.S., Radhakrishnan, S., Seenivasan, C., Srinivasan, V., 2016. The effect of copper nanoparticles supplementation on freshwater prawn *Macrobrachium rosenbergii* post larvae. J. Trace Elem. Med. Biol. 34, 39–49. https://doi.org/10.1016/j.jtemb.2015.12.003

Murray, F., Cowie, P.R., 2011. Plastic contamination in the decapod crustacean *Nephrops norvegicus* (Linnaeus, 1758). Mar. Pollut. Bull. 62, 1207–1217. https://doi.org/10.1016/j.marpolbul.2011.03.032

Nash, K.L., Cvitanovic, C., Fulton, E.A., Halpern, B.S., Milner-Gulland, E.J., Watson, R.A., Blanchard, J.L., 2017. Planetary boundaries for a blue planet. Nat. Ecol. Evol. 1, 1625–

1634. https://doi.org/10.1038/s41559-017-0319-z

Ng, E.L., Huerta Lwanga, E., Eldridge, S.M., Johnston, P., Hu, H.W., Geissen, V., Chen, D., 2018. An overview of microplastic and nanoplastic pollution in agroecosystems. Sci. Total Environ. https://doi.org/10.1016/j.scitotenv.2018.01.341

Nielsen, H., Tsirigos, K.D., Brunak, S., von Heijne, G., 2019. A Brief History of Protein Sorting Prediction. Protein J. https://doi.org/10.1007/s10930-019-09838-3

Obbard, R.W., 2018. Microplastics in Polar Regions: The role of long range transport. Curr. Opin. Environ. Sci. Heal. https://doi.org/10.1016/j.coesh.2017.10.004

Osuna-Jiménez, I., Abril, N., Vioque-Fernández, A., Gómez-Ariza, J.L., Prieto-Álamo, M.J., Pueyo, C., 2014. The environmental quality of Doñana surrounding areas affects the immune transcriptional profile of inhabitant crayfish *Procambarus clarkii*. Fish Shellfish Immunol. 40, 136–145. https://doi.org/10.1016/j.fsi.2014.06.031

Pang, M., Wang, Y., Tang, Y., Dai, J., Tong, J., Jin, G., 2021. Transcriptome sequencing and metabolite analysis reveal the toxic effects of nanoplastics on tilapia after exposure to polystyrene. Environ. Pollut. 277, 116860. https://doi.org/10.1016/j.envpol.2021.116860

Patro, R., Duggal, G., Love, M.I., Irizarry, R.A., Kingsford, C., 2017. Salmon provides fast and bias-aware quantification of transcript expression. Nat. Methods 14, 417–419. https://doi.org/10.1038/nmeth.4197

Pattarayingsakul, W., Pudgerd, A., Munkongwongsiri, N., Vanichviriyakit, R., Chaijarasphong, T., Thitamadee, S., Kruangkum, T., 2019. The gastric sieve of penaeid shrimp species is a sub-micrometer nutrient filter. J. Exp. Biol. 222. https://doi.org/10.1242/jeb.199638

Paul-Pont, I., Lacroix, C., González Fernández, C., Hégaret, H., Lambert, C., Le Goïc, N., Frère, L., Cassone, A.L., Sussarellu, R., Fabioux, C., Guyomarch, J., Albentosa, M., Huvet, A., Soudant, P., 2016. Exposure of marine mussels *Mytilus* spp. to polystyrene microplastics: Toxicity and influence on fluoranthene bioaccumulation. Environ. Pollut. 216, 724–737. https://doi.org/10.1016/j.envpol.2016.06.039

Pedersen, A.F., Gopalakrishnan, K., Boegehold, A.G., Peraino, N.J., Westrick, J.A., Kashian, D.R., 2020a. Microplastic ingestion by quagga mussels, *Dreissena bugensis*, and its effects on physiological processes. Environ. Pollut. 260, 113964. https://doi.org/10.1016/j.envpol.2020.113964

Pedersen, A.F., Meyer, D.N., Petriv, A.M. V., Soto, A.L., Shields, J.N., Akemann, C., Baker, B.B., Tsou, W.L., Zhang, Y., Baker, T.R., 2020b. Nanoplastics impact the zebrafish (*Danio rerio*) transcriptome: Associated developmental and neurobehavioral consequences. Environ. Pollut. 266, 115090. https://doi.org/10.1016/j.envpol.2020.115090

Peeken, I., Primpke, S., Beyer, B., Gütermann, J., Katlein, C., Krumpen, T., Bergmann, M., Hehemann, L., Gerdts, G., 2018. Arctic sea ice is an important temporal sink and means of transport for microplastic. Nat. Commun. 9, 1–12. https://doi.org/10.1038/s41467-018-03825-5

Pellon-Maison, M., Garcia, C.F., Cattaneo, E.R., Coleman, R.A., Gonzalez-Baro, M.R., 2009. *Macrobrachium borellii* hepatopancreas contains a mitochondrial glycerol-3-phosphate acyltransferase which initiates triacylglycerol biosynthesis. Lipids 44, 337–344. https://doi.org/10.1007/s11745-008-3275-1

Peruzza, L., Piazza, F., Manfrin, C., Bonzi, L., Battistella, S., Giulianini, P., 2015. Reproductive plasticity of a *Procambarus clarkii* population living 10°C below its thermal optimum. Aquat. Invasions 10, 199–208. https://doi.org/10.3391/ai.2015.10.2.08

Pevzner, P.A., Tang, H., Waterman, M.S., 2001. An Eulerian path approach to DNA fragment assembly. Proc. Natl. Acad. Sci. U. S. A. 98, 9748–9753. https://doi.org/10.1073/pnas.171285098

Piehl, S., Mitterwallner, V., Atwood, E.C., Bochow, M., Laforsch, C., 2019. Abundance and distribution of large microplastics (1–5 mm) within beach sediments at the Po River Delta, northeast Italy. Mar. Pollut. Bull. 149, 110515. https://doi.org/10.1016/j.marpolbul.2019.110515

Pinto da Costa, J., Reis, V., Paço, A., Costa, M., Duarte, A.C., Rocha-Santos, T., 2019. Micro(nano)plastics – Analytical challenges towards risk evaluation. TrAC Trends Anal. Chem. 111, 173–184. https://doi.org/10.1016/J.TRAC.2018.12.013

Pinto da Costa, J., Santos, P.S.M., Duarte, A.C., Rocha-Santos, T., 2016. (Nano)plastics in the environment - Sources, fates and effects. Sci. Total Environ. https://doi.org/10.1016/j.scitotenv.2016.05.041

Piovesan, A., Caracausi, M., Antonaros, F., Pelleri, M.C., Vitale, L., 2016. GeneBase 1.1: A tool to summarize data from NCBI gene datasets and its application to an update of human gene statistics. Database 2016. https://doi.org/10.1093/database/baw153

PlasticsEurope, 2020. Plastics – the Facts 2020 [WWW Document]. URL https://www.plasticseurope.org/it/resources/publications/4312-plastics-facts-2020 (accessed 12.16.20).

Porte, C., Escartín, E., 1998. Cytochrome P450 system in the hepatopancreas of the red swamp crayfish *Procambarus clarkii*: A field study. Comp. Biochem. Physiol. - C Pharmacol. Toxicol. Endocrinol. 121, 333–338. https://doi.org/10.1016/S0742-8413(98)10054-3

Prapavorarat, A., Pongsomboon, S., Tassanakajon, A., 2010. Identification of genes expressed in response to yellow head virus infection in the black tiger shrimp, *Penaeus monodon*, by suppression subtractive hybridization. Dev. Comp. Immunol. 34, 611–617. https://doi.org/10.1016/j.dci.2010.01.002

Prat, O., Degli-Esposti, D., 2019. New challenges: Omics technologies in ecotoxicology, in: Ecotoxicology: New Challenges and New Approaches. Elsevier, pp. 181–208. https://doi.org/10.1016/B978-1-78548-314-1.50006-7

Qin, Z., Babu, V.S., Wan, Q., Muhammad, A., Li, J., Lan, J., Lin, L., 2018. Antibacterial activity of hemocyanin from red swamp crayfish (*Procambarus clarkii*). Fish Shellfish Immunol. 75, 391–399. https://doi.org/10.1016/j.fsi.2018.02.010

Qu, F., Xiang, Z., Yu, Z., 2014. The first molluscan acute phase serum amyloid A (A-SAA) identified from oyster *Crassostrea hongkongensis*: Molecular cloning and functional characterization. Fish Shellfish Immunol. 39, 145–151. https://doi.org/10.1016/j.fsi.2014.05.013

R Core Team, 2020. R: A language and environment for statistical computing.

Radha, S., Mullainadhan, P., Arumugam, M., 2013. Detection of two distinct types of hemolymphatic prophenoloxidase and their differential responses in the black tiger shrimp, *Penaeus monodon*, upon infection by white spot syndrome virus. Aquaculture

376–379, 76–84. https://doi.org/10.1016/j.aquaculture.2012.11.017

Redondo-Hasselerharm, P.E., Falahudin, D., Peeters, E.T.H.M., Koelmans, A.A., 2018. Microplastic Effect Thresholds for Freshwater Benthic Macroinvertebrates. Environ. Sci. Technol. 52, 2278–2286. https://doi.org/10.1021/acs.est.7b05367

Reed, S., Clark, M., Thompson, R., Hughes, K.A., 2018. Microplastics in marine sediments near Rothera Research Station, Antarctica. Mar. Pollut. Bull. 133, 460–463. https://doi.org/10.1016/j.marpolbul.2018.05.068

Renner, G., Schmidt, T.C., Schram, J., 2018. Analytical methodologies for monitoring micro(nano)plastics: Which are fit for purpose? Curr. Opin. Environ. Sci. Heal. https://doi.org/10.1016/j.coesh.2017.11.001

Ribeiro, F., Garcia, A.R., Pereira, B.P., Fonseca, M., Mestre, N.C., Fonseca, T.G., Ilharco, L.M., Bebianno, M.J., 2017. Microplastics effects in *Scrobicularia plana*. Mar. Pollut. Bull. 122, 379–391. https://doi.org/10.1016/j.marpolbul.2017.06.078

Rist, S., Assidqi, K., Zamani, N.P., Appel, D., Perschke, M., Huhn, M., Lenz, M., 2016. Suspended micro-sized PVC particles impair the performance and decrease survival in the Asian green mussel *Perna viridis*. Mar. Pollut. Bull. 111, 213–220. https://doi.org/10.1016/j.marpolbul.2016.07.006

Rist, S., Baun, A., Almeda, R., Hartmann, N.B., 2019. Ingestion and effects of micro- and nanoplastics in blue mussel (*Mytilus edulis*) larvae. Mar. Pollut. Bull. 140, 423–430. https://doi.org/10.1016/j.marpolbul.2019.01.069

Robertson, G., Schein, J., Chiu, R., Corbett, R., Field, M., Jackman, S.D., Mungall, K., Lee, S., Okada, H.M., Qian, J.Q., Griffith, M., Raymond, A., Thiessen, N., Cezard, T., Butterfield, Y.S., Newsome, R., Chan, S.K., She, R., Varhol, R., Kamoh, B., Prabhu, A.L., Tam, A., Zhao, Y., Moore, R.A., Hirst, M., Marra, M.A., Jones, S.J.M., Hoodless, P.A., Birol, I., 2010. De novo assembly and analysis of RNA-seq data. Nat. Methods 7, 909–912. https://doi.org/10.1038/nmeth.1517

Robinson, M.D., McCarthy, D.J., Smyth, G.K., 2010. edgeR: A Bioconductor package for differential expression analysis of digital gene expression data. Bioinformatics 26, 139–140. https://doi.org/10.1093/bioinformatics/btp616

Rocha, T.L., Gomes, T., Sousa, V.S., Mestre, N.C., Bebianno, M.J., 2015. Ecotoxicological impact of engineered nanomaterials in bivalve molluscs: An overview. Mar. Environ. Res. 111, 74–88. https://doi.org/10.1016/j.marenvres.2015.06.013

Rochman, C.M., Browne, M.A., Halpern, B.S., Hentschel, B.T., Hoh, E., Karapanagioti, H.K., Rios-Mendoza, L.M., Takada, H., Teh, S., Thompson, R.C., 2013. Classify plastic waste as hazardous. Nature. https://doi.org/10.1038/494169a

Rochman, C.M., Browne, M.A., Underwood, A.J., Van Franeker, J.A., Thompson, R.C., Amaral-Zettler, L.A., 2016. The ecological impacts of marine debris: Unraveling the demonstrated evidence from what is perceived. Ecology 97, 302–312. https://doi.org/10.1890/14-2070.1

Rochman, C.M., Kurobe, T., Flores, I., Teh, S.J., 2014. Early warning signs of endocrine disruption in adult fish from the ingestion of polyethylene with and without sorbed chemical pollutants from the marine environment. Sci. Total Environ. 493, 656–661. https://doi.org/10.1016/j.scitotenv.2014.06.051

Rochman, C.M., Parnis, J.M., Browne, M.A., Serrato, S., Reiner, E.J., Robson, M., Young, T., Diamond, M.L., Teh, S.J., 2017. Direct and indirect effects of different types of microplastics on freshwater prey (*Corbicula fluminea*) and their predator (*Acipenser transmontanus*). PLoS One 12, e0187664. https://doi.org/10.1371/journal.pone.0187664

Rochman, C.M., Tahir, A., Williams, S.L., Baxa, D. V., Lam, R., Miller, J.T., Teh, F.C., Werorilangi, S., Teh, S.J., 2015. Anthropogenic debris in seafood: Plastic debris and fibers from textiles in fish and bivalves sold for human consumption. Sci. Rep. 5, 14340. https://doi.org/10.1038/srep14340

Rockström, J., Steffen, W., Noone, K., Persson, Å., Chapin, F.S., Lambin, E.F., Lenton, T.M., Scheffer, M., Folke, C., Schellnhuber, H.J., Nykvist, B., De Wit, C.A., Hughes, T., Van Der Leeuw, S., Rodhe, H., Sörlin, S., Snyder, P.K., Costanza, R., Svedin, U., Falkenmark, M., Karlberg, L., Corell, R.W., Fabry, V.J., Hansen, J., Walker, B., Liverman, D., Richardson, K., Crutzen, P., Foley, J.A., 2009. A safe operating space for humanity. Nature 461, 472–475. https://doi.org/10.1038/461472a

Rosa, M., Ward, J.E., Shumway, S.E., 2018. Selective Capture and Ingestion of Particles by Suspension-Feeding Bivalve Molluscs: A Review. J. Shellfish Res. https://doi.org/10.2983/035.037.0405

Rosa, R.D., Vergnes, A., de Lorgeril, J., Goncalves, P., Perazzolo, L.M., Sauné, L., Romestand, B., Fievet, J., Gueguen, Y., Bachère, E., Destoumieux-Garzón, D., 2013. Functional Divergence in Shrimp Anti-Lipopolysaccharide Factors (ALFs): From Recognition of Cell Wall Components to Antimicrobial Activity. PLoS One 8, e67937. https://doi.org/10.1371/journal.pone.0067937

Rowlands, E., Galloway, T., Manno, C., 2021. A Polar outlook: Potential interactions of micro- and nano-plastic with other anthropogenic stressors. Sci. Total Environ. https://doi.org/10.1016/j.scitotenv.2020.142379

Saborowski, R., Paulischkis, E., Gutow, L., 2019. How to get rid of ingested microplastic fibers? A straightforward approach of the Atlantic ditch shrimp *Palaemon varians*. Environ. Pollut. 254. https://doi.org/10.1016/j.envpol.2019.113068

Sanchez-Vidal, A., Thompson, R.C., Canals, M., De Haan, W.P., 2018. The imprint of microfibres in Southern European deep seas. PLoS One 13, e0207033. https://doi.org/10.1371/journal.pone.0207033

SAPEA Science Advice for Policy by European Academies, 2019. A Scientific Perspective on Microplastics in Nature and Society., Evidence Review Report. SAPEA, Berlin. https://doi.org/10.26356/microplastics

Sarasamma, S., Audira, G., Siregar, P., Malhotra, N., Lai, Y.H., Liang, S.T., Chen, J.R., Chen, K.H.C., Hsiao, C. Der, 2020. Nanoplastics cause neurobehavioral impairments, reproductive and oxidative damages, and biomarker responses in zebrafish: Throwing up alarms of wide spread health risk of exposure. Int. J. Mol. Sci. 21, 1410. https://doi.org/10.3390/ijms21041410

Sendra, M., Saco, A., Yeste, M.P., Romero, A., Novoa, B., Figueras, A., 2020. Nanoplastics: From tissue accumulation to cell translocation into *Mytilus galloprovincialis* hemocytes. resilience of immune cells exposed to nanoplastics and nanoplastics plus Vibrio splendidus combination. J. Hazard. Mater. 388, 121788. https://doi.org/10.1016/j.jhazmat.2019.121788

Sendra, M., Sparaventi, E., Novoa, B., Figueras, A., 2021. An overview of the internalization and effects of microplastics and nanoplastics as pollutants of emerging concern in bivalves. Sci. Total Environ. https://doi.org/10.1016/j.scitotenv.2020.142024

Senko, J., Nelms, S., Reavis, J., Witherington, B., Godley, B., Wallace, B., 2020. Understanding individual and population-level effects of plastic pollution on marine megafauna. Endanger. Species Res. 43, 234–252. https://doi.org/10.3354/esr01064

Seppey, M., Manni, M., Zdobnov, E.M., 2019. BUSCO: Assessing genome assembly and annotation completeness, in: Methods in Molecular Biology. Humana Press Inc., pp. 227–245. https://doi.org/10.1007/978-1-4939-9173-0_14

Setälä, O., Norkko, J., Lehtiniemi, M., 2016. Feeding type affects microplastic ingestion in a coastal invertebrate community. Mar. Pollut. Bull. 102, 95–101. https://doi.org/10.1016/J.MARPOLBUL.2015.11.053

Shaalan, M., Saleh, M., El-Mahdy, M., El-Matbouli, M., 2016. Recent progress in applications of nanoparticles in fish medicine: A review. Nanomedicine Nanotechnology, Biol. Med. https://doi.org/10.1016/j.nano.2015.11.005

Shang, F., Taylor, A., 2011. Ubiquitin-proteasome pathway and cellular responses to oxidative stress. Free Radic. Biol. Med. https://doi.org/10.1016/j.freeradbiomed.2011.03.031

Shen, H., Hu, Y., Ma, Y., Zhou, X., Xu, Z., Shui, Y., Li, C., Xu, P., Sun, X., 2014. In-depth transcriptome analysis of the red swamp crayfish *Procambarus clarkii*. PLoS One 9. https://doi.org/10.1371/journal.pone.0110548

Sighicelli, M., Pietrelli, L., Lecce, F., Iannilli, V., Falconieri, M., Coscia, L., Di Vito, S., Nuglio, S., Zampetti, G., 2018. Microplastic pollution in the surface waters of Italian Subalpine Lakes. Environ. Pollut. 236, 645–651. https://doi.org/10.1016/J.ENVPOL.2018.02.008

Silveyra, G.R., Silveyra, P., Vatnick, I., Medesani, D.A., Rodríguez, E.M., 2018. Effects of atrazine on vitellogenesis, steroid levels and lipid peroxidation, in female red swamp crayfish *Procambarus clarkii*. Aquat. Toxicol. 197, 136–142. https://doi.org/10.1016/j.aquatox.2018.02.017

Singh, N., Tiwari, E., Khandelwal, N., Darbha, G.K., 2019. Understanding the stability of nanoplastics in aqueous environments: Effect of ionic strength, temperature, dissolved organic matter, clay, and heavy metals. Environ. Sci. Nano 6, 2968–2976. https://doi.org/10.1039/c9en00557a

Sivaramasamy, E., Zhiwei, W., Li, F., Xiang, J., 2016. Enhancement of Vibriosis Resistance in *Litopenaeus vannamei* by Supplementation of Biomastered Silver Nanoparticles by *Bacillus subtilis*. J Nanomed Nanotechnol 7, 352. https://doi.org/10.4172/2157-7439.1000352

Smith, V.J., Dyrynda, E.A., 2015. Antimicrobial proteins: From old proteins, new tricks. Mol. Immunol. 68, 383–398. https://doi.org/10.1016/j.molimm.2015.08.009

Snape, J.R., Maund, S.J., Pickford, D.B., Hutchinson, T.H., 2004. Ecotoxicogenomics: The challenge of integrating genomics into aquatic and terrestrial ecotoxicology. Aquat. Toxicol. 67, 143–154. https://doi.org/10.1016/j.aquatox.2003.11.011

Snyder, M.J., 2000. Cytochrome P450 enzymes in aquatic invertebrates: Recent advances and future directions. Aquat. Toxicol. 48, 529–547. https://doi.org/10.1016/S0166-445X(00)00085-0

Sokolova, I.M., 2013. Energy-Limited Tolerance to Stress as a Conceptual Framework to Integrate the Effects of Multiple Stressors. Integr. Comp. Biol. 53, 597–608. https://doi.org/10.1093/icb/ict028

Song, Z., Yang, X., Chen, F., Zhao, F., Zhao, Y., Ruan, L., Wang, Y., Yang, Y., 2019. Fate and transport of nanoplastics in complex natural aquifer media: Effect of particle size and surface functionalization. Sci. Total Environ. 669, 120–128. https://doi.org/10.1016/j.scitotenv.2019.03.102

Souty-Grosset, C., Anastácio, P.M., Aquiloni, L., Banha, F., Choquer, J., Chucholl, C., Tricarico, E., 2016. The red swamp crayfish *Procambarus clarkii* in Europe: Impacts on aquatic ecosystems and human well-being. Limnologica. https://doi.org/10.1016/j.limno.2016.03.003

Staudinger, H., 1920. Über Polymerisation. Berichte der Dtsch. Chem. Gesellschaft (A B Ser. 53, 1073–1085. https://doi.org/10.1002/cber.19200530627

Stephens, B., Azimi, P., El Orch, Z., Ramos, T., 2013. Ultrafine particle emissions from desktop 3D printers. Atmos. Environ. 79, 334–339. https://doi.org/10.1016/j.atmosenv.2013.06.050

Strange, R.C., Spiteri, M.A., Ramachandran, S., Fryer, A.A., 2001. Glutathione-S-transferase family of enzymes. Mutat. Res. - Fundam. Mol. Mech. Mutagen. 482, 21–26. https://doi.org/10.1016/S0027-5107(01)00206-8

Suaria, G., Avio, C.G., Mineo, A., Lattin, G.L., Magaldi, M.G., Belmonte, G., Moore, C.J., Regoli, F., Aliani, S., 2016. The Mediterranean Plastic Soup: Synthetic polymers in Mediterranean surface waters. Sci. Rep. 6, 1–10. https://doi.org/10.1038/srep37551

Sun, B., Quan, H., Zhu, F., 2016. Dietary chitosan nanoparticles protect crayfish *Procambarus clarkii* against white spot syndrome virus (WSSV) infection. Fish Shellfish Immunol. 54, 241–246. https://doi.org/10.1016/j.fsi.2016.04.009

Sun, J.-J., Lan, J.-F., Zhao, X.-F., Vasta, G.R., Wang, J.-X., 2017. Binding of a C-type lectin's coiled-coil domain to the Domeless receptor directly activates the JAK/STAT pathway in the shrimp immune response to bacterial infection. PLOS Pathog. 13, e1006626. https://doi.org/10.1371/journal.ppat.1006626

Sussarellu, R., Suquet, M., Thomas, Y., Lambert, C., Fabioux, C., Pernet, M.E.J., Goïc, N. Le, Quillien, V., Mingant, C., Epelboin, Y., Corporeau, C., Guyomarch, J., Robbens, J., Paul-Pont, I., Soudant, P., Huvet, A., 2016. Oyster reproduction is affected by exposure to polystyrene microplastics. Proc. Natl. Acad. Sci. U. S. A. 113, 2430–2435. https://doi.org/10.1073/pnas.1519019113

Swain, P., Nayak, S.K., Sasmal, A., Behera, T., Barik, S.K., Swain, S.K., Mishra, S.S., Sen, A.K., Das, J.K., Jayasankar, P., 2014. Antimicrobial activity of metal based nanoparticles against microbes associated with diseases in aquaculture. World J. Microbiol. Biotechnol. 30, 2491–2502. https://doi.org/10.1007/s11274-014-1674-4

Taketomi, Y., Nishikawa, S., Koga, S., 1996. Testis and androgenic gland during development of external sexual characteristics of the crayfish *Procambarus clarkii*. J. Crustac. Biol. 16, 24–34. https://doi.org/10.1163/193724096X00243

Tallec, K., Blard, O., González-Fernández, C., Brotons, G., Berchel, M., Soudant, P., Huvet, A., Paul-Pont, I., 2019. Surface functionalization determines behavior of nanoplastic

solutions in model aquatic environments. Chemosphere 225, 639–646. https://doi.org/10.1016/j.chemosphere.2019.03.077

Tallec, K., Huvet, A., Di Poi, C., González-Fernández, C., Lambert, C., Petton, B., Le Goïc, N., Berchel, M., Soudant, P., Paul-Pont, I., 2018. Nanoplastics impaired oyster free living stages, gametes and embryos. Environ. Pollut. 242, 1226–1235. https://doi.org/10.1016/j.envpol.2018.08.020

Tao, T., Xie, X., Liu, M., Jiang, Q., Zhu, D., 2017. Cloning of two carboxylesterase cDNAs from the swimming crab *Portunus trituberculatus*: Molecular evidences for their putative roles in methyl farnesotae degradation. Comp. Biochem. Physiol. Part - B Biochem. Mol. Biol. 203, 100–107. https://doi.org/10.1016/j.cbpb.2016.10.001

Taylor, M.L., Gwinnett, C., Robinson, L.F., Woodall, L.C., 2016. Plastic microfibre ingestion by deep-sea organisms. Sci. Rep. 6. https://doi.org/10.1038/srep33997

Tello-Olea, M., Rosales-Mendoza, S., Campa-Córdova, A.I., Palestino, G., Luna-González, A., Reyes-Becerril, M., Velazquez, E., Hernandez-Adame, L., Angulo, C., 2019. Gold nanoparticles (AuNP) exert immunostimulatory and protective effects in shrimp (*Litopenaeus vannamei)* against Vibrio parahaemolyticus. Fish Shellfish Immunol. 84, 756–767. https://doi.org/10.1016/j.fsi.2018.10.056

Ter Halle, A., Jeanneau, L., Martignac, M., Jardé, E., Pedrono, B., Brach, L., Gigault, J., 2017. Nanoplastic in the North Atlantic Subtropical Gyre. Environ. Sci. Technol. 51, 13689–13697. https://doi.org/10.1021/acs.est.7b03667

Textile Exchanges, 2020. Preferred Fiber and Materials Market Report 2020 103.

Thompson, R.C., Olson, Y., Mitchell, R.P., Davis, A., Rowland, S.J., John, A.W.G., McGonigle, D., Russell, A.E., 2004. Lost at Sea: Where Is All the Plastic? Science (80-.). 304, 838. https://doi.org/10.1126/science.1094559

Tricarico, E., Bertocchi, S., Brusconi, S., Casalone, E., Gherardi, F., Giorgi, G., Mastromei, G., Parisi, G., 2008. Depuration of microcystin-LR from the red swamp crayfish *Procambarus clarkii* with assessment of its food quality. Aquaculture 285, 90–95. https://doi.org/10.1016/j.aquaculture.2008.08.003

Triebskorn, R., Braunbeck, T., Grummt, T., Hanslik, L., Huppertsberg, S., Jekel, M., Knepper, T.P., Krais, S., Müller, Y.K., Pittroff, M., Ruhl, A.S., Schmieg, H., Schür, C., Strobel, C., Wagner, M., Zumbülte, N., Köhler, H.R., 2019. Relevance of nano- and microplastics for freshwater ecosystems: A critical review. TrAC - Trends Anal. Chem. https://doi.org/10.1016/j.trac.2018.11.023

Van Cauwenberghe, L., Claessens, M., Vandegehuchte, M.B., Janssen, C.R., 2015. Microplastics are taken up by mussels (*Mytilus edulis*) and lugworms (*Arenicola marina*) living in natural habitats. Environ. Pollut. 199, 10–17. https://doi.org/10.1016/j.envpol.2015.01.008

Van Cauwenberghe, L., Vanreusel, A., Mees, J., Janssen, C.R., 2013. Microplastic pollution in deep-sea sediments. Environ. Pollut. 182, 495–499. https://doi.org/10.1016/j.envpol.2013.08.013

Varó, I., Perini, A., Torreblanca, A., Garcia, Y., Bergami, E., Vannuccini, M.L., Corsi, I., 2019. Time-dependent effects of polystyrene nanoparticles in brine shrimp *Artemia franciscana* at physiological, biochemical and molecular levels. Sci. Total Environ. 675, 570–580.

https://doi.org/10.1016/j.scitotenv.2019.04.157

Vaz, F.M., Van Gool, S., Ofman, R., Ijlst, L., Wanders, R.J.A., 1998. Carnitine biosynthesis: Identification of the cDNA encoding human γ-butyrobetaine hydroxylase. Biochem. Biophys. Res. Commun. 250, 506–510. https://doi.org/10.1006/bbrc.1998.9343

Veneman, W.J., Spaink, H.P., Brun, N.R., Bosker, T., Vijver, M.G., 2017. Pathway analysis of systemic transcriptome responses to injected polystyrene particles in zebrafish larvae. Aquat. Toxicol. 190, 112–120. https://doi.org/10.1016/j.aquatox.2017.06.014

Vert, M., Doi, Y., Hellwich, K.H., Hess, M., Hodge, P., Kubisa, P., Rinaudo, M., Schué, F., 2012. Terminology for biorelated polymers and applications (IUPAC recommendations 2012). Pure Appl. Chem. 84, 377–410. https://doi.org/10.1351/PAC-REC-10-12-04

Vianello, A., Jensen, R.L., Liu, L., Vollertsen, J., 2019. Simulating human exposure to indoor airborne microplastics using a Breathing Thermal Manikin. Sci. Rep. 9, 1–11. https://doi.org/10.1038/s41598-019-45054-w

Villarrubia-Gómez, P., Cornell, S.E., Fabres, J., 2018. Marine plastic pollution as a planetary boundary threat – The drifting piece in the sustainability puzzle. Mar. Policy 96, 213–220. https://doi.org/10.1016/j.marpol.2017.11.035

Vinken, M., 2019. Omics-based input and output in the development and use of adverse outcome pathways. Curr. Opin. Toxicol. https://doi.org/10.1016/j.cotox.2019.02.006

Vioque-Fernández, A., de Almeida, E.A., Ballesteros, J., García-Barrera, T., Gómez-Ariza, J.L., López-Barea, J., 2007a. Doñana National Park survey using crayfish (*Procambarus clarkii*) as bioindicator: Esterase inhibition and pollutant levels. Toxicol. Lett. 168, 260–268. https://doi.org/10.1016/j.toxlet.2006.10.023

Vioque-Fernández, A., de Almeida, E.A., López-Barea, J., 2007b. Esterases as pesticide biomarkers in crayfish (*Procambarus clarkii*, Crustacea): Tissue distribution, sensitivity to model compounds and recovery from inactivation. Comp. Biochem. Physiol. - C Toxicol. Pharmacol. 145, 404–412. https://doi.org/10.1016/j.cbpc.2007.01.006

Vlachogianni, T., Skocir, M., Constantin, P., Labbe, C., Orthodoxou, D., Pesmatzoglou, I., Scannella, D., Spika, M., Zissimopoulos, V., Scoullos, M., 2020. Plastic pollution on the Mediterranean coastline: Generating fit-for-purpose data to support decision-making via a participatory-science initiative. Sci. Total Environ. 711, 135058. https://doi.org/10.1016/j.scitotenv.2019.135058

Wagner, M., Scherer, C., Alvarez-Muñoz, D., Brennholt, N., Bourrain, X., Buchinger, S., Fries, E., Grosbois, C., Klasmeier, J., Marti, T., Rodriguez-Mozaz, S., Urbatzka, R., Vethaak, A.D., Winther-Nielsen, M., Reifferscheid, G., 2014. Microplastics in freshwater ecosystems: what we know and what we need to know. Environ. Sci. Eur. 26, 1–9. https://doi.org/10.1186/s12302-014-0012-7

Wahl, A., Le Juge, C., Davranche, M., El Hadri, H., Grassl, B., Reynaud, S., Gigault, J., 2021. Nanoplastic occurrence in a soil amended with plastic debris. Chemosphere 262, 127784. https://doi.org/10.1016/j.chemosphere.2020.127784

Wang, Jun, Li, Y., Lu, L., Zheng, M., Zhang, X., Tian, H., Wang, W., Ru, S., 2019. Polystyrene microplastics cause tissue damages, sex-specific reproductive disruption and transgenerational effects in marine medaka (*Oryzias melastigma*). Environ. Pollut. 254, 113024. https://doi.org/10.1016/j.envpol.2019.113024

Wang, Juan, Lv, Z., Lei, Z., Chen, Z., Lv, B., Yang, H., Wang, Z., Song, Q., 2019. Expression and functional analysis of cytochrome P450 genes in the wolf spider *Pardosa pseudoannulata* under cadmium stress. Ecotoxicol. Environ. Saf. 172, 19–25. https://doi.org/10.1016/j.ecoenv.2019.01.034

Wang, Q., Yu, X., Dou, L., Huang, X., Zhu, K., Guo, J., Yan, M., Wang, S., Man, Y., Tang, W., Shen, T., Li, J., 2019. MIR-154-5p functions as an important regulator of angiotensin II-mediated heart remodeling. Oxid. Med. Cell. Longev. 2019. https://doi.org/10.1155/2019/8768164

Wang, X.W., Zhang, H.W., Li, X., Zhao, X.F., Wang, J.X., 2011. Characterization of a C-type lectin (PcLec2) as an upstream detector in the prophenoloxidase activating system of red swamp crayfish. Fish Shellfish Immunol. 30, 241–247. https://doi.org/10.1016/j.fsi.2010.10.012

Wang, X.W., Zhao, X.F., Wang, J.X., 2014. C-type lectin binds to β-integrin to promote hemocytic phagocytosis in an invertebrate. J. Biol. Chem. 289, 2405–2414. https://doi.org/10.1074/jbc.M113.528885

Wang, Y., Guthrie, C., 1998. PRP16, a DEAH-box RNA helicase, is recruited to the spliceosome primarily via its nonconserved N-terminal domain. RNA 4, 1216–1229. https://doi.org/10.1017/S1355838298980992

Wang, Z., Gerstein, M., Snyder, M., 2009. RNA-Seq: A revolutionary tool for transcriptomics. Nat. Rev. Genet. https://doi.org/10.1038/nrg2484

Ward, J.E., Zhao, S., Holohan, B.A., Mladinich, K.M., Griffin, T.W., Wozniak, J., Shumway, S.E., 2019. Selective Ingestion and Egestion of Plastic Particles by the Blue Mussel (*Mytilus edulis*) and Eastern Oyster (*Crassostrea virginica*): Implications for Using Bivalves as Bioindicators of Microplastic Pollution. Environ. Sci. Technol. 53, 8776–8784. https://doi.org/10.1021/acs.est.9b02073

Watts, A.J.R., Urbina, M.A., Corr, S., Lewis, C., Galloway, T.S., 2015. Ingestion of Plastic Microfibers by the Crab *Carcinus maenas* and Its Effect on Food Consumption and Energy Balance. Environ. Sci. Technol. 49, 14597–14604. https://doi.org/10.1021/acs.est.5b04026

Watts, A.J.R., Urbina, M.A., Goodhead, R., Moger, J., Lewis, C., Galloway, T.S., 2016. Effect of Microplastic on the Gills of the Shore Crab *Carcinus maenas*. Environ. Sci. Technol. 50, 5364–5369. https://doi.org/10.1021/acs.est.6b01187

Webb, S., Gaw, S., Marsden, I.D., McRae, N.K., 2020. Biomarker responses in New Zealand green-lipped mussels *Perna canaliculus* exposed to microplastics and triclosan. Ecotoxicol. Environ. Saf. 201, 110871. https://doi.org/10.1016/j.ecoenv.2020.110871

Wei, K., Wei, Y., Song, C., 2020. The response of phenoloxidase to cadmium-disturbed hepatopancreatic immune-related molecules in freshwater crayfish *Procambarus clarkii*. Fish Shellfish Immunol. 99, 190–198. https://doi.org/10.1016/j.fsi.2020.02.012

Welden, N.A.C., Cowie, P.R., 2016. Long-term microplastic retention causes reduced body condition in the langoustine, *Nephrops norvegicus*. Environ. Pollut. 218, 895–900. https://doi.org/10.1016/j.envpol.2016.08.020

Woodall, L.C., Sanchez-Vidal, A., Canals, M., Paterson, G.L.J., Coppock, R., Sleight, V., Calafat, A., Rogers, A.D., Narayanaswamy, B.E., Thompson, R.C., 2014. The deep sea is

a major sink for microplastic debris. R. Soc. Open Sci. 1. https://doi.org/10.1098/rsos.140317

Woods, M.N., Stack, M.E., Fields, D.M., Shaw, S.D., Matrai, P.A., 2018. Microplastic fiber uptake, ingestion, and egestion rates in the blue mussel (*Mytilus edulis*). Mar. Pollut. Bull. 137, 638–645. https://doi.org/10.1016/j.marpolbul.2018.10.061

Wright, S.L., Rowe, D., Thompson, R.C., Galloway, T.S., 2013. Microplastic ingestion decreases energy reserves in marine worms. Curr. Biol. https://doi.org/10.1016/j.cub.2013.10.068

Wright, S.L., Ulke, J., Font, A., Chan, K.L.A., Kelly, F.J., 2020. Atmospheric microplastic deposition in an urban environment and an evaluation of transport. Environ. Int. 136, 105411. https://doi.org/10.1016/j.envint.2019.105411

Wu, A.R., Neff, N.F., Kalisky, T., Dalerba, P., Treutlein, B., Rothenberg, M.E., Mburu, F.M., Mantalas, G.L., Sim, S., Clarke, M.F., Quake, S.R., 2014. Quantitative assessment of single-cell RNA-sequencing methods. Nat. Methods 11, 41–46. https://doi.org/10.1038/nmeth.2694

Wu, D., Liu, Z., Cai, M., Jiao, Y., Li, Y., Chen, Q., Zhao, Y., 2019. Molecular characterisation of cytochrome P450 enzymes in waterflea (*Daphnia pulex*) and their expression regulation by polystyrene nanoplastics. Aquat. Toxicol. 217, 105350. https://doi.org/10.1016/j.aquatox.2019.105350

Xu, C., Li, E., Liu, Y., Wang, X., Qin, J.G., Chen, L., 2017. Comparative proteome analysis of the hepatopancreas from the Pacific white shrimp *Litopenaeus vannamei* under long-term low salinity stress. J. Proteomics 162, 1–10. https://doi.org/10.1016/j.jprot.2017.04.013

Xu, J.-D., Diao, M.-Q., Niu, G.-J., Wang, X.-W., Zhao, X.-F., Wang, J.-X., 2018. A Small GTPase, RhoA, Inhibits Bacterial Infection Through Integrin Mediated Phagocytosis in Invertebrates. Front. Immunol. 9, 1928. https://doi.org/10.3389/fimmu.2018.01928

Yan, L., Yang, P., Jiang, F., Cui, N., Ma, E., Qiao, C., Cui, F., 2012. Transcriptomic and phylogenetic analysis of *Culex pipiens quinquefasciatus* for three detoxification gene families. BMC Genomics 13, 609. https://doi.org/10.1186/1471-2164-13-609

Yang, L., Zhang, Y., Kang, S., Wang, Z., Wu, C., 2021. Microplastics in soil: A review on methods, occurrence, sources, and potential risk. Sci. Total Environ. https://doi.org/10.1016/j.scitotenv.2021.146546

Yoshida, S., Hiraga, K., Takehana, T., Taniguchi, I., Yamaji, H., Maeda, Y., Toyohara, K., Miyamoto, K., Kimura, Y., Oda, K., 2016. A bacterium that degrades and assimilates poly(ethylene terephthalate). Science (80-.). 351, 1196–1199. https://doi.org/10.1126/science.aad6359

Yu, J., Loh, K., Song, Z.Y., Yang, H.Q., Zhang, Y., Lin, S., 2018. Update on glycerol-3-phosphate acyltransferases: The roles in the development of insulin resistance. Nutr. Diabetes. https://doi.org/10.1038/s41387-018-0045-x

Yu, P., Liu, Z., Wu, D., Chen, M., Lv, W., Zhao, Y., 2018. Accumulation of polystyrene microplastics in juvenile *Eriocheir sinensis* and oxidative stress effects in the liver. Aquat. Toxicol. 200, 28–36. https://doi.org/10.1016/J.AQUATOX.2018.04.015

Zdobnov, E.M., Tegenfeldt, F., Kuznetsov, D., Waterhouse, R.M., Simao, F.A., Ioannidis, P., Seppey, M., Loetscher, A., Kriventseva, E. V., 2017. OrthoDB v9.1: Cataloging

evolutionary and functional annotations for animal, fungal, plant, archaeal, bacterial and viral orthologs. Nucleic Acids Res. 45, D744–D749. https://doi.org/10.1093/nar/gkw1119

Zettler, E.R., Mincer, T.J., Amaral-Zettler, L.A., 2013. Life in the "plastisphere": Microbial communities on plastic marine debris. Environ. Sci. Technol. 47, 7137–7146. https://doi.org/10.1021/es401288x

Zhang, C., Jeong, C.B., Lee, J.S., Wang, D., Wang, M., 2019. Transgenerational Proteome Plasticity in Resilience of a Marine Copepod in Response to Environmentally Relevant Concentrations of Microplastics. Environ. Sci. Technol. 53, 8426–8436. https://doi.org/10.1021/acs.est.9b02525

Zhang, D., Fraser, M.A., Huang, W., Ge, C., Wang, Y., Zhang, C., Guo, P., 2020. Microplastic pollution in water, sediment, and specific tissues of crayfish (*Procambarus clarkii*) within two different breeding modes in Jianli, Hubei province, China. Environ. Pollut. 115939. https://doi.org/10.1016/j.envpol.2020.115939

Zhang, H., Kuo, Y.Y., Gerecke, A.C., Wang, J., 2012. Co-release of hexabromocyclododecane (HBCD) and nano- and microparticles from thermal cutting of polystyrene foams. Environ. Sci. Technol. 46, 10990–10996. https://doi.org/10.1021/es302559v

Zhang, W., Liu, Z., Tang, S., Li, D., Jiang, Q., Zhang, T., 2020. Transcriptional response provides insights into the effect of chronic polystyrene nanoplastic exposure on *Daphnia pulex*. Chemosphere 238, 124563. https://doi.org/10.1016/J.CHEMOSPHERE.2019.124563

Zhang, X.-W., Ren, Q., Zhang, H.W., Wang, K.K., Wang, J.X., 2013. A C-type lectin could selectively facilitate bacteria clearance in red swamp crayfish, *Procambarus clarkii*. Fish Shellfish Immunol. 35, 1387–1394. https://doi.org/10.1016/j.fsi.2013.08.004

Zhang, X.-W., Wang, X.-W., Sun, C., Zhao, X.-F., Wang, J.-X., 2011. C-type lectin from red swamp crayfish *Procambarus clarkii* participates in cellular immune response. Arch. Insect Biochem. Physiol. 76, 168–184. https://doi.org/10.1002/arch.20416

Zhang, X.-W., Wang, Y., Wang, X.W., Wang, L., Mu, Y., Wang, J.X., 2016. A C-type lectin with an immunoglobulin-like domain promotes phagocytosis of hemocytes in crayfish *Procambarus clarkii*. Sci. Rep. 6, 1–12. https://doi.org/10.1038/srep29924

Zhang, Y., Wang, Leilei, Wang, Lingling, Wu, N., Zhou, Z., Song, L., 2012. An Integrin from Shrimp *Litopenaeus vannamei* Mediated Microbial Agglutination and Cell Proliferation. PLoS One 7, e40615. https://doi.org/10.1371/journal.pone.0040615

Zhang, Z., Schwartz, S., Wagner, L., Miller, W., 2000. A greedy algorithm for aligning DNA sequences. J. Comput. Biol. https://doi.org/10.1089/10665270050081478

Zhao, S., Ward, J.E., Danley, M., Mincer, T.J., 2018. Field-Based Evidence for Microplastic in Marine Aggregates and Mussels: Implications for Trophic Transfer. Environ. Sci. Technol. 52, 11038–11048. https://doi.org/10.1021/acs.est.8b03467

Zhao, W., Wang, L., Liu, M., Jiang, K., Wang, M., Yang, G., Qi, C., Wang, B., 2017. Transcriptome, antioxidant enzyme activity and histopathology analysis of hepatopancreas from the white shrimp *Litopenaeus vannamei* fed with aflatoxin B1(AFB1). Dev. Comp. Immunol. 74, 69–81. https://doi.org/10.1016/j.dci.2017.03.031

Zhao, Y., Bao, Z., Wan, Z., Fu, Z., Jin, Y., 2020. Polystyrene microplastic exposure disturbs hepatic glycolipid metabolism at the physiological, biochemical, and transcriptomic levels

in adult zebrafish. Sci. Total Environ. 710, 136279. https://doi.org/10.1016/j.scitotenv.2019.136279

Zheng, Y., Zhou, Z.-M., Min, X., Li, J.-M., Sha, J.-H., 2005. Identification and characterization of the BGR-like gene with a potential role in human testicular development/spermatogenesis. Asian J Androl 7. https://doi.org/10.1111/j.1745-7262.2005.00014.x

Ziajahromi, S., Kumar, A., Neale, P.A., Leusch, F.D.L., 2017. Impact of Microplastic Beads and Fibers on Waterflea (*Ceriodaphnia dubia*) Survival, Growth, and Reproduction: Implications of Single and Mixture Exposures. Environ. Sci. Technol. 51, 13397–13406. https://doi.org/10.1021/acs.est.7b03574

Zuur, A.F., Ieno, E.N., Walker, N.J., Saveliev, A.A., Smith, G.M., 2009. Mixed Effects Models and Extensions in Ecology with R, Journal of the Royal Statistical Society: Series A (Statistics in Society). Springer New York LLC. https://doi.org/10.1111/j.1467-985x.2010.00663_9.x

List of Figures

Figure 1:Effects of PS NP exposure on physiological parameters of *P. clarkii*. Data are presented for all individuals (N = 19) as mean + S.D., over all time points (T0, T24h, T48h, and T72h post-exposure). When mixed models revealed a statistical significance for sex, data are also showed for males (N=8) and females (N=11) separately. Asterisks represent significant differences between groups (*P<0.05). 24
Figure 2: Multidimensional scaling (MDS) plot of *P. clarkii* samples with total counts used as an expression value parameter. Distances correspond to leading log-fold-changes, i.e., the average (root-mean-square) of the largest absolute log-fold-changes, between each pair of samples. Different colors correspond to different experimental groups (Control, yellow; PS NP exposed, blue). Shapes define different groups of samples: hemocytes (Hem, circle), hepatopancreas of male specimens (Hep_M, empty triangle), and hepatopancreas of female specimens (Hep_F, full triangle). 27
Figure 3: Visual identification of DEGs (FDR ≤ 0.05 and |fold change| > 2) identified in *P. clarkii* exposed to PS NPs, relative to the controls, for each sample group analyzed: hemocytes (A, a), female hepatopancreas (B, b), and male hepatopancreas (C, c). The hierarchical clustering is based on Euclidean distance and complete linkage of normalized expression values (log CPM - counts per million -). Clustering indicates similar expression patterns among the samples of the control group (C, yellow) or nanoplastic-exposed group (NP, blue) (columns) and among genes (rows). Colors represent the normalized gene expression levels from light blue (low) to red (high). In the volcano plots, red (upregulation) and blue (downregulation) dots indicate DEG transcripts in the nanoplastic-exposed group, respectively, and dots in grey color show no significant differential expression. 28
Figure 4: Workflow of *M. galloprovincialis* transcriptome refinement. 50
Figure 5: Multidimensional scaling (MDS) plot of *M. galloprovincialis* samples with total counts used as expression value parameter. Distances correspond to leading log-fold-changes, i.e., the average (root-mean-square) of the largest absolute log-fold-changes, between each pair of samples. Abbreviations are as follows: NP, nanoplastic exposed group; C, control group. 53
Figure 6: A mean-difference plot (MD-plot) of expressed genes generated using EdgeR package. The scatter plot represents log2 fold changes (on the y-axis) versus the log2 mean of normalized counts (log2 count per million) (on the x-axis) of each expressed gene. DEGs are in red. 55

List of Tables

Table 1: Biometric data of *P. clarkii* individuals are presented as total wet weight and total length (TL). In addition, sex and reproductive stage of female individuals, as ovarian wet weight, gonadosomatic index (GSI) and ovarian maturation stage, and male individuals, as developmental stage, are indicated..... 22

Table 2: General information on RNA-Seq output and mapping rates for hemocytes and hepatopancreas libraries. 26

Table 3: General information on RNA-Seq output and read trimming and filtering results from MultiQC analysis. The percentage of retained reads are provided as compared to raw reads. Abbreviations are as follows: M – million; bp – base pairs. 51

Table 4: Summary of Illumina NovaSeq™ 6000 assembly and analysis of *M. galloprovincialis* trocophora larvae transcriptome..... 52

Table 5: Differentially expressed genes found in *M. galloprovincialis* trocophora larvae (N = 8) by EdgeR analysis, after exposure to 50 nm amino-modified polystyrene nanoparticles. Transcript name and length (in base pairs) are reported, together with the average values of expression given as Log_2 Counts PerMillion (CPM). Differential gene expression analysis results are provided as Log2 fold change and FDR p-value. When possible, a complete annotation is presented. 54

Table 6: Differentially expressed genes found in *M. galloprovincialis* trocophora larvae (N = 8) by DESeq2 analysis, after exposure to 50 nm amino-modified polystyrene nanoparticles. Transcript name and length (in base pairs) are reported, together with the average values of expression given as Base mean: the average of the normalized count values, dividing by size factors, taken over all samples. Differential gene expression analysis results are provided as Log2 fold change and FDR p-value. When possible, a complete annotation is presented. 54

Acknowledgments

My sincere and heartfelt thanks and appreciation go to my thesis advisor Prof. Piero Giulianini, who provided me with the guidance and counsel I needed to get through my PhD program. His willingness to engage in insightful scientific discussions and his patience have greatly helped me grow both as a person and as a professional over the past four years. I would like to thank him for always supporting me and giving me the freedom to pursue different projects and acquire new skills in various fields.

I am deeply grateful to Dr. Chiara Manfrin for her dedicated and invaluable teaching and guidance.

I would like to acknowledge all the professors and researchers of the Laboratory of Applied and Comparative Genomics of the University of Trieste. Prof. Alberto Pallavicini, Prof. Marco Gerdol, Prof. Fiorella Florian, Dr. Fabrizia Gionechetti and Dr. Valentina Torboli always kept the door open for me. They offered me constant support and precious scientific advice on experimental design and technical and laboratory methods.

A special mention goes to Samuele for guiding me (without much success!) through the magical world of bioinformatics. And for being a friend.

I profoundly thank my colleagues and friends, for sharing these incredible years with me and for making me feel at home in the stunning City of Wind.

I thank my family for all they have done and continue to do to support my curiosity.

Finally, I will be forever grateful to Matteo for the strength, perseverance, patience, and endless encouragement he has given me during this time.

Per aspera ad astra

List of scientific publications

Capanni, F., Greco, S., Tomasi, N., Giulianini, P.G., Manfrin, C., 2021. Orally administered nano-polystyrene caused vitellogenin alteration and oxidative stress in the red swamp crayfish (*Procambarus clarkii*). Sci. Total Environ. 791, 147984. https://doi.org/10.1016/j.scitotenv.2021.147984

Greco, S., D'Agostino, E., Manfrin, C., Gaetano, A.S., Furlanis, G., **Capanni, F.**, Santovito, G., Edomi, P., Giulianini, P.G., Gerdol, M., 2021. RNA-sequencing indicates high hemocyanin expression as a key strategy for cold adaptation in the Antarctic amphipod *Eusirus* cf. *giganteus* clade g3. BIOCELL. https://doi.org/10.32604/biocell.2021.016121

Rončević, T., Čikeš-Čulić, V., Maravić, A., **Capanni, F.**, Gerdol, M., Pacor, S., Tossi, A., Giulianini, P.G., Pallavicini, A., Manfrin, C., 2020. Identification and functional characterization of the astacidin family of proline-rich host defence peptides (PcAst) from the red swamp crayfish (*Procambarus clarkii*, Girard 1852). Dev. Comp. Immunol. 105. https://doi.org/10.1016/j.dci.2019.103574

Appendix

Supplementary material to Chapter 2

Table A1. Plasma glucose concentration (mg/dL) recorded in control and exposed groups of *P. clarkii* prior (T0) and 24h (T1), 48h (T2), and 72h (T3) after PS-NPs exposure. The number of samples analyzed, arithmetic mean, median, and range are reported for all specimens together as well as for males and females separately.

		Control				**Exposed**			
Time	*Sex*	*n*	*Mean (mg/dl)*	*Median (mg/dl)*	*Range (mg/dl)*	*n*	*Mean (mg/dl)*	*Median (mg/dl)*	*Range (mg/dl)*
T0	All	9	13.8	15.7	2.30 - 20.7	10	9.78	8.80	2.02 - 28.6
	Female	5	13.9	13.5	8.89 - 19.7	6	11.6	9.60	2.02 - 28.6
	Male	4	13.7	15.9	2.30 - 20.7	4	6.96	7.18	3.59 - 9.89
T1	All	8	8.56	7.66	3.27 - 16.2	9	7.40	4.38	1.10 - 17.5
	Female	4	12.3	12.1	8.81 - 16.2	6	7.42	6.46	1.50 - 16.5
	Male	4	4.77	4.65	3.27 - 6.52	3	7.35	3.41	1.10 - 17.5
T2	All	7	8.57	6.17	2.37 - 17.7	9	7.48	6.12	1.63 - 20.5
	Female	4	12.5	13.0	6.17 - 17.7	6	8.98	8.04	1.63 - 20.5
	Male	3	3.32	2.72	2.37 - 4.86	3	4.48	3.72	1.92 - 7.81
T3	All	9	9.44	7.74	3.91 - 16.1	9	7.41	7.88	1.01 - 15.4
	Female	5	10.6	14.1	4.44 - 14.7	6	8.69	9.58	1.01 - 15.4
	Male	4	8.00	5.95	3.91 - 16.1	3	4.87	3.77	2.96 - 7.88

Table A2. Final model estimates, 95% confidence intervals, p-values, and degree of freedom (df) for *P. clarkii* plasma glucose (mg/dL) data. The final model comprised Treatment (i.e., control or exposed) and Time (i.e., T0, T24h, T48h, T72h) as fixed factors and id nested in Trial as a random intercept. Residual variance (σ^2), the variance associated with the random factor (τ_{00} id:trial), and the Intraclass Correlation Coefficient (ICC) are reported. The number of specimens (id), trial and samples (observations) as well as marginal and conditional R^2 are indicated. Bold values denote statistical significance ($p < 0.05$).

Glucose model

Model = Glucose concentration ~ Time + Treatment + (1 | id:Trial)

Parameters	***Estimates***	***Conf. Int (95%)***	***P-value***	***df***
Intercept	12.84	9.21 − 16.46	**<0.001**	26.11
Time [24h]	-4.00	-6.76 − -1.24	**0.005**	48.59
Time [48h]	-3.55	-6.36 − -0.73	**0.015**	48.65
Time [72h]	-3.46	-6.17 − -0.75	**0.013**	48.37
Treatment [exp]	-2.13	-6.72 − 2.45	0.339	16.94

Random Effects

σ^2	16.62
τ_{00} id:trial	17.68
ICC	0.52
N id	19
N trial	4
Observations	70
Marginal R^2 / Conditional R^2	0.102 / 0.565

Table A3. Analysis of deviance table summary using type III Wald chi-squared test for linear mixed-effects model fit for *P. clarkii* plasma glucose concentration.

	χ^2	*df*	*P-value*
(Intercept)	52.98678	1	**3.36E-13**
Time	11.25126	3	**0.010442**
Treatment	0.967515	1	0.325301

Table A4. Total hemocytes ($\times 10^6$ cells/mL) recorded in the hemolymph of control and exposed groups of *P. clarkii* prior (T0) and 24h (T1), 48h (T2), and 72h (T3) after PS-NPs exposure. The number of samples analyzed, arithmetic mean, median, and range are reported for all specimens together as well as for males and females separately.

		Control				**Exposed**			
Time	*Sex*	*n*	*Mean (mg/dl)*	*Median (mg/dl)*	*Range (mg/dl)*	*n*	*Mean (mg/dl)*	*Median (mg/dl)*	*Range (mg/dl)*
T0	All	9	3.8	2.98	0.3 - 8.58	9	3.03	2.62	1.32 - 5.22
	Female	5	4.32	3.95	0.3 - 8.58	6	3.48	3.16	2.17 - 5.22
	Male	4	3.15	2.71	2.5 - 4.68	3	2.13	2.46	1.32 - 2.62
T1	All	8	5.55	4.9	3.92 - 7.87	10	4.61	4.65	2.98 - 6.29
	Female	5	5.62	5.1	3.92 - 7.87	6	4.76	5.1	3.27 - 5.62
	Male	3	5.42	4.71	4.22 - 7.34	4	4.38	4.14	2.98 - 6.29
T2	All	9	3.34	2.88	0.96 - 6.39	10	5.01	4.99	3.7 - 6.45
	Female	5	4.1	4.2	2.71 - 6.39	6	4.77	4.71	3.7 - 6.45
	Male	4	2.4	2.75	0.96 - 3.13	4	5.36	5.31	4.76 - 6.07
T3	All	8	4.27	4.52	1.43 - 6.46	10	3.58	3.51	0.5 - 6.71
	Female	5	3.79	4	1.43 - 5.43	6	2.71	2.94	0.5 - 4.22
	Male	3	5.05	6.18	2.52 - 6.46	4	4.87	5.1	2.59 - 6.71

Table A5. Final model estimates, 95% confidence intervals, p-values, and degree of freedom (df) for *P. clarkii* total hemocyte count (10^4 cells/mL) data. The final model comprised Treatment (i.e., control or exposed), Time (i.e., T0, T24h, T48h, T72h), and Sex (i.e., male or female) as fixed factors and id as a random intercept. Residual variance (σ^2), the variance associated with the random factor (τ_{00} id), and the Intraclass Correlation Coefficient (ICC) are reported. The number of specimens (id), trial and samples (observations) as well as marginal and conditional R^2 are indicated. Bold values denote statistical significance ($p < 0.05$).

Total hemocyte count model

Model = Cell count ~ Time + Treatment + Sex + (1 | id) + Treatment: Time + Time: Sex

Parameters	***Estimates***	***Conf. Int (95%)***	***P-value***	***df***
Intercept	434.37	312.98− 555.76	**<0.001**	60.67
Treatment [exp]	-87.89	-232.99− 57.20	0.23	60.71
Time [24h]	131.57	-37.30− 300.45	0.124	45.63
Time [48h]	-77.25	-244.97− 90.47	0.359	45.41
Time [72h]	-73.64	-242.51− 95.24	0.385	45.63
Sex [Male]	-122.53	-271.45− 26.39	0.105	60.75
Treatment [exp] : Time [24h]	-5.09	-207.01− 196.83	0.96	46.3
Treatment [exp] : Time [48h]	252.05	53.40− 450.70	**0.014**	45.79
Treatment [exp]: Time [72h]	14.09	-187.84− 216.01	0.889	46.3
Time [24h] : Sex [Male]	93	-113.73− 299.72	0.37	47.01
Time [48h] : Sex [Male]	71.47	-131.02− 273.95	0.481	46.09
Time [72h] : Sex [Male]	299.71	92.98− 506.43	**0.005**	47.01

Random Effects

σ^2	22223.81
τ_{00} id	1078.16
ICC	0.05
N id	19
Observations	73
Marginal R^2 / Conditional R^2	0.287 / 0.320

Table A6. Analysis of deviance table summary using type III Wald chi-squared test for linear mixed-effects model fit for *P. clarkii* total hemocyte count (10^4 cells/mL) data.

	χ^2	*df*	*P-value*
(Intercept)	51.28988	1	**7.97E-13**
Treatment	1.473015	1	0.224871
Time	8.183363	3	**0.04237**
Sex	2.721695	1	0.098993
Treatment:Time	9.771533	3	**0.020611**
Time:Sex	9.528768	3	**0.023027**

Table A7. Basal phenoloxidase (PO) enzyme activity (V_{max} abs/µL/min) recorded in the hemolymph of control and exposed groups of *P. clarkii* prior (T0) and 24h (T1), 48h (T2), and 72h (T3) after PS-NPs exposure. The number of samples analyzed, arithmetic mean, median, and range are reported for all specimens together as well as for males and females separately.

		Control				**Exposed**			
Time	*Sex*	*n*	*Mean (mg/dl)*	*Median (mg/dl)*	*Range (mg/dl)*	*n*	*Mean (mg/dl)*	*Median (mg/dl)*	*Range (mg/dl)*
T0	All	7	7.60e-04	1.09e-03	4.49e-05 - 1.35e-03	9	3.57e-04	2.02e-04	1.00e-50 - 8.54e-04
	Female	3	9.92e-04	1.19e-03	4.43e-04 - 1.35e-03	6	5.06e-04	5.29e-04	1.64e-04 - 8.54e-04
	Male	4	5.85e-04	6.04e-04	4.49e-05 - 1.09e-03	3	5.91e-05	2.40e-05	1.00e-50 - 1.53e-04
T1	All	6	6.68e-04	7.87e-04	1.03e-05 - 1.13e-03	9	3.57e-04	1.22e-04	2.54e-05 - 1.38e-03
	Female	3	6.22e-04	7.73e-04	2.93e-04 - 8.01e-04	5	3.77e-04	1.22e-04	8.58e-05 - 1.38e-03
	Male	3	7.13e-04	1.00e-03	1.03e-05 - 1.13e-03	4	3.32e-04	2.53e-04	2.54e-05 - 7.96e-04
T2	All	6	4.75e-04	3.97e-04	1.00e-50 - 1.16e-03	10	2.67e-04	1.13e-04	1.00e-50 - 1.29e-03
	Female	4	6.77e-04	6.56e-04	2.42e-04 - 1.16e-03	6	3.28e-04	1.47e-04	1.03e-04 - 1.29e-03
	Male	2	7.00e-05	7.00e-05	1.00e-50 - 1.40e-04	4	1.75e-04	4.86e-05	1.00e-50 - 6.02e-04
T3	All	9	4.75e-04	4.62e-04	1.00e-50 - 9.36e-04	10	2.32e-04	9.88e-05	1.00e-05 - 1.26e-03
	Female	5	5.15e-04	4.62e-04	2.35e-04 - 9.36e-04	6	2.83e-04	9.88e-05	4.46e-05 - 1.26e-03
	Male	4	4.24e-04	3.81e-04	1.00e-50 - 9.34e-04	4	1.54e-04	7.01e-05	1.00e-05 - 4.68e-04

Table A8. Final model estimates, 95% confidence intervals, p-values, and degree of freedom (df) for *P. clarkii* basal phenoloxidase (PO) enzyme activity (V_{max} abs/μL/min) data. The final model comprised Treatment (i.e., control or exposed) and Time (i.e., T0, T24h, T48h, T72h) as fixed factors and id nested in Trial as a random intercept. Residual variance (σ^2), the variance associated with the random factor (τ_{00} id), and the Intraclass Correlation Coefficient (ICC) are reported. The number of specimens (id), trial and samples (observations) as well as marginal and conditional R^2 are indicated. Bold values denote statistical significance ($p < 0.05$).

Basal phenoloxidase (PO) enzyme activity model

Model = PO V_{max} ~ Treatment + Time + (1 | id:Trial)

Parameters	***Estimates***	***Conf. Int (95%)***	***P-value***	***df***
Intercept	0.00071	0.00044 − 0.00099	**<0.001**	20.28
Treatment [exp]	-0.00028	-0.00065 − 0.00008	0.118	17.03
Time [24h]	-0.00009	-0.00021 − 0.00003	0.147	44.32
Time [48h]	-0.00016	-0.00028 − -0.00004	**0.01**	44.24
Time [72h]	-0.00022	-0.00033 − -0.00010	**<0.001**	44.43

Random Effects

σ^2	3.0e-08
τ_{00} id:Trial	1.3e-07
ICC	0.83
N id	19
N Trial	4
Observations	66
Marginal R^2 / Conditional R^2	0.143 / 0.856

Table A9. Analysis of deviance table summary using type III Wald chi-squared test for linear mixed-effects model fit for *P. clarkii* basal phenoloxidase (PO) enzyme activity (V_{max} abs/µL/min) data.

	χ^2	*df*	*P-value*
(Intercept)	29.60212582	1	**5.30E-08**
Treatment	2.704415287	1	0.100070766
Time	16.17362862	3	**0.00104472**

Table A10. Total phenoloxidase (proPO) enzyme activity (V_{max} abs/µL/min) recorded in the hemolymph of control and exposed groups of *P. clarkii* prior (T0) and 24h (T1), 48h (T2), and 72h (T3) after PS-NPs exposure. The number of samples analyzed, arithmetic mean, median, and range are reported for all specimens together as well as for males and females separately.

		Control				**Exposed**			
Time	*Sex*	*n*	*Mean (mg/dl)*	*Median (mg/dl)*	*Range (mg/dl)*	*n*	*Mean (mg/dl)*	*Median (mg/dl)*	*Range (mg/dl)*
T0	All	7	3.84e-03	4.01e-03	1.46e-03 - 5.72e-03	9	3.77e-03	4.26e-03	4.23e-04 - 6.06e-03
	Female	3	4.62e-03	5.16e-03	3.03e-03 - 5.66e-03	6	4.73e-03	4.80e-03	2.84e-03 - 6.06e-03
	Male	4	3.25e-03	2.92e-03	1.46e-03 - 5.72e-03	3	1.84e-03	1.84e-03	4.23e-04 - 3.26e-03
T1	All	6	3.15e-03	3.28e-03	9.65e-04 - 5.10e-03	8	3.29e-03	3.78e-03	5.02e-04 - 5.73e-03
	Female	3	3.03e-03	2.82e-03	2.44e-03 - 3.83e-03	5	4.16e-03	4.51e-03	2.10e-03 - 5.73e-03
	Male	3	3.27e-03	3.74e-03	9.65e-04 - 5.10e-03	3	1.84e-03	9.84e-04	5.02e-04 - 4.02e-03
T2	All	6	2.94e-03	3.24e-03	3.90e-04 - 4.72e-03	10	3.33e-03	4.03e-03	2.45e-04 - 5.21e-03
	Female	4	3.86e-03	3.90e-03	2.90e-03 - 4.72e-03	6	4.09e-03	4.37e-03	2.06e-03 - 5.21e-03
	Male	2	1.09e-03	1.09e-03	3.90e-04 - 1.80e-03	4	2.19e-03	2.23e-03	2.45e-04 - 4.06e-03
T3	All	9	3.28e-03	4.08e-03	2.58e-04 - 4.40e-03	10	2.88e-03	3.69e-03	2.85e-04 - 4.88e-03
	Female	5	4.00e-03	4.13e-03	3.28e-03 - 4.40e-03	6	3.75e-03	4.23e-03	1.05e-03 - 4.88e-03
	Male	4	2.38e-03	2.46e-03	2.58e-04 - 4.33e-03	4	1.58e-03	9.80e-04	2.85e-04 - 4.08e-03

Table A11. Final model estimates, 95% confidence intervals, p-values, and degree of freedom (df) for *P. clarkii* total phenoloxidase (proPO) enzyme activity (V_{max} abs/µL/min) data. The final model comprised Treatment (i.e., control or exposed), Time (i.e., T0, T24h, T48h, T72h), and Sex (i.e., male or female) as fixed factors and id nested in Trial as a random intercept. Residual variance (σ^2), the variance associated with the random factor (τ_{00} id), and the Intraclass Correlation Coefficient (ICC) are reported. The number of specimens (id), trial and samples (observations) as well as marginal and conditional R^2 are indicated. Bold values denote statistical significance ($p < 0.05$).

Total phenoloxidase (proPO) enzyme activity model

Model = proPO V_{max} ~ Treatment + Time + Sex + (1 | id:Trial)

Parameters	***Estimates***	***Conf. Int (95%)***	***P-value***	***df***
Intercept	0.00306	0.00179 − 0.00434	**<0.001**	17.207
Treatment [exp]	-0.00022	-0.00160 − 0.00115	0.736	16.0287
Time [24h]	-0.00059	-0.00099 − -0.00018	**0.006**	43.29419
Time [48h]	-0.00057	-0.00096 − -0.00018	**0.005**	43.16565
Time [72h]	-0.00088	-0.00125 − -0.00051	**<0.001**	43.31472
Sex [Female]	0.00173	0.00034 − 0.00312	**0.018**	15.97091
Random Effects				
σ^2	2.8e-07			
τ_{00} id:Trial	1.9e-06			
ICC	0.87			
N id	19			
N Trial	4			
Observations	65			
Marginal R^2 / Conditional R^2	0.276 / 0.906			

Table A12. Analysis of deviance table summary using type III Wald chi-squared test for linear mixed-effects model fit for *P. clarkii* total phenoloxidase (proPO) enzyme activity (V_{max} abs/μL/min) data.

	χ^2	*df*	*P-value*
(Intercept)	25.55109	1	**4.31E-07**
Treatment	0.117561	1	0.731695
Time	23.23165	3	**3.61E-05**
Sex	6.948969	1	**0.008387**

Table A13. Hemolymph total protein concentration (mg/mL) recorded in control and exposed groups of *P. clarkii* prior (T0) and 24h (T1), 48h (T2), and 72h (T3) after PS-NPs exposure. The number of samples analyzed, arithmetic mean, median, and range are reported for all specimens together as well as for males and females separately.

		Control				**Exposed**			
Time	*Sex*	*n*	*Mean (mg/dl)*	*Median (mg/dl)*	*Range (mg/dl)*	*n*	*Mean (mg/dl)*	*Median (mg/dl)*	*Range (mg/dl)*
T0	All	9	3.8	2.98	0.3 - 8.58	9	3.03	2.62	1.32 - 5.22
	Female	5	4.32	3.95	0.3 - 8.58	6	3.48	3.16	2.17 - 5.22
	Male	4	3.15	2.71	2.5 - 4.68	3	2.13	2.46	1.32 - 2.62
T1	All	8	5.55	4.9	3.92 - 7.87	10	4.61	4.65	2.98 - 6.29
	Female	5	5.62	5.1	3.92 - 7.87	6	4.76	5.1	3.27 - 5.62
	Male	3	5.42	4.71	4.22 - 7.34	4	4.38	4.14	2.98 - 6.29
T2	All	9	3.34	2.88	0.96 - 6.39	10	5.01	4.99	3.7 - 6.45
	Female	5	4.1	4.2	2.71 - 6.39	6	4.77	4.71	3.7 - 6.45
	Male	4	2.4	2.75	0.96 - 3.13	4	5.36	5.31	4.76 - 6.07
T3	All	8	4.27	4.52	1.43 - 6.46	10	3.58	3.51	0.5 - 6.71
	Female	5	3.79	4	1.43 - 5.43	6	2.71	2.94	0.5 - 4.22
	Male	3	5.05	6.18	2.52 - 6.46	4	4.87	5.1	2.59 - 6.71

Table A14. Final model estimates, 95% confidence intervals, p-values, and degree of freedom (df) for *P. clarkii* hemolymph total protein concentration (mg/mL) data. The final model comprised Treatment (i.e., control or exposed) and Time (i.e., T0, T24h, T48h, T72h) as fixed factors and id nested in Trial as a random intercept. Residual variance (σ^2), the variance associated with the random factor (τ_{00} id), and the Intraclass Correlation Coefficient (ICC) are reported. The number of specimens (id), trial and samples (observations) as well as marginal and conditional R^2 are indicated. Bold values denote statistical significance ($p < 0.05$).

Protein model

Model = Protein concentration ~ Treatment + Time + (1 | id:Trial)

Parameters	***Estimates***	***Conf. Int (95%)***	***P-value***	***df***
Intercept	79.3	61.78 − 96.9	**<0.001**	18.21395
Treatment [exp]	-12.7	-36.6 − 11.2	0.279	17.00569
Time [24h]	-9.68	-14.8 − -4.58	**<0.001**	52.00011
Time [48h]	-11.8	-17.1 − -6.54	**<0.001**	52.05441
Time [72h]	-7.33	-12.4 − -2.24	**0.006**	52.00011

Random Effects

σ^2	61.18
τ_{00} id:Trial	593.94
ICC	0.91
N id	19
N Trial	4
Observations	74
Marginal R^2 / Conditional R^2	0.087 / 0.915

Table A15. Analysis of deviance table summary using type III Wald chi-squared test for linear mixed-effects model fit for *P. clarkii* hemolymph total protein concentration (mg/mL) data.

	χ^2	*df*	*P-value*
(Intercept)	89.72535	1	**2.74E-21**
Treatment	1.250861	1	0.263388
Time	23.73083	3	**2.84E-05**

Table A16. Summary of the Illumina sequencing output and mapping results for both hemocytes and hepatopancreas samples. Hepatopancreas samples are further divided by sex.

	Raw reads		Clean reads						Mapped reads			
Sample	**Number of reads**	**Avg. length**	**Number of reads**	**% trimmed reads**	**Avg. length**	**% GC content**	**Q20**	**Q30**	**Number of reads**	**% mapped reads**	**Number of unique fragments**	**% unique fragm.**
Hemocytes												
C4	6,101,723	97.4	2,648,869	43	83.1	39.3	100	98.2	1,983,924	74.9	1,214,193	45.8
C5	6,268,749	97.7	2,848,390	45	83.1	39.7	100	98.4	2,024,977	71.1	1,175,033	41.3
C12	2,781,026	96.1	1,152,109	41	83.0	38.9	100	96.2	862,622	74.9	504,409	43.8
NP4	5,607,164	94.7	2,314,664	41	83.1	40.4	100	98.3	1,388,657	60.0	821,613	35.5
NP5	12,582,586	98.5	6,572,996	52	83.2	39.2	100	98.6	5,544,678	84.4	3,355,117	51.0
NP6	5,529,095	95.7	2,008,341	36	83.0	39.6	100	96.9	1,245,134	62.0	706,900	35.2
NP12	4,893,013	96.9	2,350,380	48	83.1	40.8	100	97.7	1,042,239	44.3	585,104	24.9
Hepatopancreas - Males												
C4	5,335,393	97.6	2,634,442	49	83.1	40.7	100	97.8	2,220,939	84.3	1,241,089	47.1
C5	6,401,138	96.5	2,948,895	46	83.1	41.0	100	98.6	2,580,737	87.5	1,338,894	45.4
C6	3,614,263	98.1	1,978,189	55	83.1	40.8	100	98.7	1,731,081	87.5	948,331	47.9
C12	5,613,931	97.3	2,868,308	51	83.1	40.9	100	98.2	2,589,481	90.3	1,244,427	43.4
NP4	3,691,222	98.1	1,869,460	51	83.2	40.6	100	98.3	1,631,393	87.3	907,900	48.6
NP5	4,627,742	98.5	2,216,628	48	83.2	41.8	100	98.6	1,876,254	84.6	1,021,665	46.1
NP6	3,458,483	98.5	1,505,409	44	83.2	41.3	100	98.4	1,278,780	84.9	709,533	47.1
Hepatopancreas - Females												

C1	2,263,861	98.5	1,078,492	48	83.2	41.6	100	98.6	803,927	74.5	423,483	39.3
C3	4,818,164	98.7	2,257,643	47	83.2	41.4	100	98.4	1,884,548	83.5	989,733	43.8
C7	4,764,297	98.2	2,182,412	46	83.2	40.8	100	98.6	1,910,347	87.5	964,645	44.2
C8	3,855,687	98.7	2,014,862	52	83.2	41.1	100	98.4	1,803,909	89.5	906,163	45.0
C9	4,697,853	98.4	2,503,551	53	83.2	40.7	100	98.7	2,107,157	84.2	1,123,755	44.9
NP1	4,999,908	97.3	2,599,179	52	83.2	41.4	100	98.1	2,274,664	87.5	1,214,290	46.7
NP2	2,620,065	97.7	1,219,606	47	83.2	41.5	100	98.4	991,914	81.3	553,111	45.4
NP3	4,093,795	98	2,016,745	49	83.2	41.7	100	98.5	1,718,094	85.2	972,384	48.2
NP7	6,189,626	98.5	3,295,916	53	83.2	41.6	100	98.4	2,828,340	85.8	1,549,736	47.0
NP8	5,376,232	94.2	2,125,766	40	83.0	41.2	100	96.8	1,761,564	82.9	907,454	42.7
NP9	5,994,807	98.4	3,255,879	54	83.2	41.0	100	98.2	2,772,984	85.2	1,390,914	42.7
Total sequences	126,179,823		60,467,131									
Total nucleotides	12,303,483,045		5,027,591,478									

Abbreviations: NP, nanoplastic; C: control; Q20 or Q30, percentage of bases with Phred quality score ≥ 20 or ≥ 30; % GC, percentage of G and C in clean bases.

Table A17. Differentially expressed genes found in *P. clarkii* hemocytes (N = 12), female hepatopancreas (N = 98), and male hepatopancreas (N = 32) after exposure to 100 nm polystyrene nanoparticles (72h). Transcript name and length (in base pairs) are reported, together with the average values of expression in control and exposed crayfish given in Transcripts Per Million (TPM). Differential gene expression analysis results are provided as Log_2 fold change and FDR p-value. Finally, when possible, a complete annotation is presented.

Accession ID at NCBI	Length (bp)	Avg TPM CTRL	Avg TPM EXP	Log_2 fc	FDR p-value	Description	Species	Total Score	Query Cover	E value	Ident (%)
Hemocytes											
Transcription and translation											
AGT03502.1	686	**6.0**	**111.3**	4.14	3.75E-04	transcription factor btf3	*Procambarus clarkii*	191	41%	9.00E-59	100
ACY66586.1	491	**436.8**	**1090.8**	5.64	1.45E-03	putative ribosomal protein S23e	*Scylla paramamosain*	290	87%	2.00E-98	99
XP_027208804.1	1957	**2.3**	**33.8**	6.9	2.42E-03	DNA ligase 1-like	*Penaeus vannamei*	169	15%	1.00E-43	77
XP_037774542.1	5585	**0.4**	**6.2**	4.92	0.02	pre-mRNA-splicing factor ATP-dependent RNA helicase PRP16-like	*Penaeus monodon*	1909	67%	0	83
Cytoskeleton											
XP_027225002.1	4894	**0.2**	**9.2**	6.44	0.01	dystonin-like	*Penaeus vannamei*	3326	99%	0	85
XP_037796207.1	2874	**1.3**	**19.7**	3.58	0.02	integrin beta-4-like	*Penaeus monodon*	259	26%	3.00E-75	62
Other											
XP_037783919.1	812	**43.5**	**0.0**	-9.54	0.05	V-type proton ATPase subunit G-like	*Penaeus monodon*	141	43%	2.00E-38	90
Not identified											
TRINITY_DN11849_c1_g1_i1	255	**2.7**	**487.7**	7.49	4.16E-10						
TRINITY_DN2373_c4_g1_i1	212	**2933.2**	**1167.6**	-11.04	1.23E-06						
NODE_70772_length_1083_cov_111.133929_g29064_i0	1083	**44.4**	**117.2**	-7.33	5.77E-05						
TRINITY_DN43718_c0_g3_i1	1001	**16.8**	**37.0**	6.74	2.86E-03						
NODE_94972_length_754_cov_5.620029_g43074_i0	754	**113.2**	**0.0**	-10.62	0.02						
Hepatopancreas - Females											
Vitellogenin											
AKN79738.1	922	**638.8**	**21.5**	-5.83	1.39E-08	vitellogenin	*Procambarus clarkii*	139	27%	7.00E-33	74
AAX94762.1	245	**65.8**	**3.1**	-5.03	5.23E-03	vitellogenin	*Portunus trituberculatus*	122	99%	2.00E-30	67

AAG17936.1	1275	**38.9**	**3.5**	-3.37	0.02	vitellogenin	*Cherax quadricarinatus*	418	100%	9.00E-128	52
AAG17936.1	4875	**1313.9**	**127.3**	-3.25	0.04	vitellogenin	*Cherax quadricarinatus*	1155	53%	0	63
Lipid metabolism and energy balance											
XP_027228007.1	2141	**41.4**	**5.3**	-3.21	1.01E-05	phosphomethylethanolamine N-methyltransferase-like isoform X1	*Penaeus vannamei*	649	66%	0	63
XP_027219820.1	2357	**9.4**	**63.2**	2.75	1.68E-03	organic cation transporter protein-like	*Penaeus vannamei*	127	24%	2.00E-19	38
MPC49412.1	1898	**61.8**	**8.1**	-2.69	0.01	Glycerol-3-phosphate acyltransferase 3	*Portunus trituberculatus*	526	68%	3.00E-179	68
XP_027211881.1	2516	**3.5**	**20.9**	2.74	0.02	gamma-butyrobetaine dioxygenase-like isoform X2	*Penaeus vannamei*	391	51%	7.00E-124	46
MPC31419.1	952	**628.0**	**106.0**	-2.52	0.03	Long-chain-fatty-acid--CoA ligase ACSBG2	*Portunus trituberculatus*	52.4	7%	0.002	96
Detoxification											
XP_027234090.1	3060	**2.4**	**46.8**	4.26	3.69E-05	probable cytochrome P450 49a1	*Penaeus vannamei*	462	49%	1.00E-148	45
Protein degradation											
XP_027225483.1	2366	**5.8**	**34.7**	3.05	5.04E-04	aminopeptidase N-like	*Penaeus vannamei*	1007	88%	0	70
XP_027209244.1	3009	**3.5**	**21.1**	2.52	1.30E-03	E3 ubiquitin-protein ligase TRIM11-like isoform X4	*Penaeus vannamei*	153	23%	3.00E-37	37
MPC48613.1	4560	**5.9**	**37.1**	2.66	0.01	putative ubiquitin carboxyl-terminal hydrolase 50	*Portunus trituberculatus*	102	18%	2.00E-18	28
ROT70691.1	3765	**9.4**	**42.1**	2.19	0.03	putative E3 ubiquitin-protein ligase TRIM32	*Penaeus vannamei*	244	41%	1.00E-66	30
O75832.1	2243	**20.6**	**121.6**	2.59	0.04	26S proteasome non-ATPase regulatory subunit 10	*Homo sapiens*	83.6	20%	8.00E-17	32
ROT70691.1	1204	**1.4**	**8.2**	2.98	0.05	putative E3 ubiquitin-protein ligase TRIM32	*Penaeus vannamei*	122	85%	1.00E-26	26
Transcription and translation											
MPC11420.1	386	**0.0**	**231.2**	11.18	6.08E-04	60S ribosomal protein L11	*Portunus trituberculatus*	186	71%	1.00E-57	95
XP_027212794.1	5638	**4.3**	**0.3**	-4.33	2.45E-03	serine/arginine repetitive matrix protein 1-like isoform X3	*Penaeus vannamei*	281	9%	1.00E-17	80
ROT70837.1	6533	**0.7**	**5.6**	2.78	3.55E-03	RNA helicase	*Penaeus vannamei*	1204	41%	0	66

						ATP-dependent RNA helicase					
MPC52676.1	7478	**0.1**	**1.9**	4.95	4.30E-03	DEAH12, chloroplastic	*Portunus trituberculatus*	1789	66%	0	51
						NFX1-type zinc finger-containing					
XP_027214614.1	7276	**2.5**	**16.9**	2.53	0.02	protein 1-like	*Penaeus vannamei*	2172	84%	0	55
XP_027211664.1	1991	**2.0**	**13.8**	3.13	0.03	la-related protein 6-like	*Penaeus vannamei*	348	61%	2.00E-109	53
						DNA-directed RNA polymerases I, II,					
Q9VC49.1	2685	**2.1**	**13.2**	3.49	0.03	and III subunit RPABC5	*Drosophila melanogaster*	136	7%	4.00E-37	99
WP_140073957.1	718	**117.8**	**245.7**	5.08	0.04	60S ribosomal protein L22	*Vibrio parahaemolyticus*	157	40%	1.00E-44	96
XP_027238282.1	528	**348.7**	**1360.3**	3.85	0.04	40S ribosomal protein S23	*Penaeus vannamei*	287	81%	2.00E-97	98
Acute-phase response											
XP_022321638.1	888	**0.5**	**30.1**	5.04	2.38E-03	serum amyloid A-5 protein-like	*Crassostrea virginica*	154	33%	7.00E-43	78
AXR98477.1	1495	**4.2**	**33.2**	5.54	0.01	activating transcription factor 4	*Procambarus clarkii*	796	87%	0	98
KU680800.1	1532	**0.6**	**8.3**	3.81	0.03	anti-lipopolysaccharide factor ALF9	*Procambarus clarkii*	97.1	5%	3.00E-15	88
						hemocyte homeostasis-associated					
ADN43413.1	2921	**1.4**	**10.9**	2.54	0.04	protein	*Pacifastacus leniusculus*	158	9%	1.00E-41	81
Oxidative stress											
						Peptidyl-prolyl cis-trans isomerase F,					
MPC10804.1	11584	**5.5**	**26.2**	2.34	5.56E-03	mitochondrial	*Portunus trituberculatus*	353	14%	3.00E-97	38
XP_027216449.1	13988	**1.7**	**7.6**	2.12	0.01	sacsin-like	*Penaeus vannamei*	3333	90%	0	44
XP_027216449.1	2508	**7.1**	**29.5**	2.04	0.01	sacsin-like	*Penaeus vannamei*	347	62%	9.00E-98	41
MPC26348.1	1321	**9.2**	**0.9**	-4.12	0.02	MICOS complex subunit mic25-a	*Portunus trituberculatus*	281	50%	2.00E-57	69
XP_027233397.1	1785	**11.6**	**1.5**	-2.95	0.05	arylsulfatase B-like	*Penaeus vannamei*	203	21%	1.00E-53	73
Hemocyanin and pseudohemocyanins											
P80096.1	282	**24.6**	**330.4**	4.06	0.02	Hemocyanin C chain	*Panulirus interruptus*	39.7	24%	0.001	74
Q6KF82.1	656	**0.0**	**29.1**	8.86	0.03	Pseudohemocyanin-1	*Homarus americanus*	46.2	10%	9.00E-05	79
AGT03503.1	291	**190.3**	**1029.6**	3.26	0.03	hemocyanin	*Procambarus clarkii*	60.1	28%	3.00E-09	100
Other											
XP_027217599.1	2463	**1.2**	**22.2**	5.81	6.08E-04	suppressor protein SRP40-like	*Penaeus vannamei*	62.4	22%	4.00E-06	26
AAD38027.1	1543	**8.0**	**77.3**	3.45	6.32E-04	beta 1,4-endoglucanase	*Cherax quadricarinatus*	410	66%	2.00E-135	66
AVD68958.1	395	**68.6**	**8.1**	-4.84	4.25E-03	obstructor F	*Cherax quadricarinatus*	132	84%	6.00E-36	54

XP_027213332.1	1374	**14.8**	**0.5**	-4.37	8.71E-03	glutamate receptor ionotropic, kainate 3-like	*Penaeus vannamei*	108	13%	2.00E-21	79
XP_027236915.1	1024	**37.2**	**20.7**	-3.38	0.02	oplophorus-luciferin 2-monooxygenase non-catalytic subunit-like	*Penaeus vannamei*	244	58%	2.00E-54	59
KAF0294794.1	1180	**9.9**	**110.4**	2.63	0.03	obstructor-E	*Amphibalanus amphitrite*	154	13%	4.00E-04	41
XP_027213291.1	1783	**112.5**	**549.9**	2.22	0.04	von Willebrand factor A domain-containing protein 7-like	*Penaeus vannamei*	271	46%	1.00E-44	37
XP_014685031.1	2359	**0.3**	**3.8**	3.66	0.04	PREDICTED: myosin light chain kinase, smooth muscle isoform X2	*Equus asinus*	374	15%	7.00E-15	47
XP_027217049.	6973	**2.2**	**0.0**	-8.22	0.04	flocculation protein FLO11-like isoform X1	*Penaeus vannamei*	831	41%	0	59
ROT64831.1	1446	**3.0**	**16.4**	3.85	0.05	putative CAP-Gly domain-containing linker protein 1 isoform X2	*Penaeus vannamei*	249	71%	6.00E-71	48
Not identified											
NODE_27147_length_2256_cov_54.437074_g13621_i1	2256	**1.0**	**24.3**	4.79	5.32E-11	No hit found					
XP_027229494.1	769	**1.2**	**150.6**	6.67	2.32E-08	uncharacterized protein LOC113821215	*Penaeus vannamei*	126	55%	3.00E-32	48
TRINITY_DN197820_c0_g1_i1	533	**97.1**	**0.3**	-7.35	9.71E-07	No hit found					
MPC08673.1	532	**145.9**	**9.1**	-3.74	3.69E-05	hypothetical protein	*Portunus trituberculatus*	72.4	43%	7.00E-12	47
MPC83951.1	279	**74.1**	**2.8**	-4.48	3.69E-05	hypothetical protein	*Portunus trituberculatus*	44.7	46%	0.008	40
TRINITY_DN53081_c0_g1_i1	234	**32.4**	**336.6**	4.54	3.69E-05	No hit found					
MPC73073.1	818	**4.2**	**51.6**	3.55	9.62E-05	hypothetical protein	*Portunus trituberculatus*	431	91%	2.00E-146	80
TRINITY_DN78095_c0_g1_i1	263	**405.3**	**37.3**	-3.18	9.62E-05	No hit found					
NODE_48627_length_1284_cov_98.054516_g28902_i0	1284	**20.2**	**1.5**	-4.32	1.11E-04	No hit found					
NODE_82748_length_893_cov_19.072127_g35682_i0	893	**27.5**	**130.3**	3.77	6.27E-04	No hit found					
S7272653	3183	**0.9**	**6.9**	3.3	6.88E-04	No hit found					
S6931545	655	**188.8**	**1370.2**	3.13	6.92E-04	No hit found					
MPC73073.1	2345	**1.0**	**11.4**	3.4	7.20E-04	hypothetical protein	*Portunus trituberculatus*	914	71%	0	79
NODE_52153_length_1190_cov_3.679295_g31386_i0	1190	**0.7**	**12.5**	4.05	8.58E-04	No hit found					
NODE_56057_length_1098_cov_667.389262_g24792_i1	1098	**206.7**	**21.9**	-3.02	1.29E-03	No hit found					
XP_027229494.1	895	**18.1**	**242.4**	3.89	3.53E-03	uncharacterized protein LOC113821215	*Penaeus vannamei*	103	49%	6.00E-23	46

XP_027214904.1	2405	**2.4**	**20.0**	3.13	3.93E-03	uncharacterized protein LOC113807818	*Penaeus vannamei*	270	33%	7.00E-79	49
MPC73073.1	2392	**5.1**	**34.0**	2.63	4.21E-03	hypothetical protein	*Portunus trituberculatus*	654	68%	0	60
NODE_90428_length_800_cov_297.558621_g40259_i0	800	**54.2**	**423.1**	2.72	4.91E-03	No hit found					
NODE_23167_length_2559_cov_114.326677_g12882_i0	2559	**1.4**	**11.1**	3.3	5.56E-03	No hit found					
TRINITY_DN6724_c1_g2_i1	229	**365.5**	**1145.4**	4.35	5.56E-03	No hit found					
R7059274	1686	**3.0**	**23.2**	3.05	5.99E-03	No hit found					
XP_027214622.1	2892	**260.0**	**2392.8**	3.65	6.36E-03	uncharacterized protein LOC113807540	*Penaeus vannamei*	358	52%	1.00E-108	39
R7104463	1567	**1.5**	**12.0**	3.07	7.59E-03	No hit found					
XP_027229494.1	1930	**15.8**	**144.2**	3.58	7.89E-03	uncharacterized protein LOC113821215	*Penaeus vannamei*	114	22%	3.00E-25	41
TRINITY_DN11362_c0_g3_i1	311	**1.1**	**52.7**	4.63	8.71E-03	No hit found					
R7004140	1849	**34.3**	**216.4**	2.72	9.36E-03	No hit found					
CDN41090.1	1672	**27.2**	**11.6**	-4.06	0.01	hypothetical protein BN871_AB_00880	*Paenibacillus sp. P22*	198	37%	1.00E-36	47
TRINITY_DN10824_c0_g2_i1	1587	**1.0**	**7.1**	3.21	0.01	No hit found					
TRINITY_DN2586_c0_g1_i1	1771	**22.4**	**3.3**	-2.9	0.01	No hit found					
TRINITY_DN31437_c2_g1_i2	207	**21.2**	**198.4**	5.22	0.01	No hit found					
NODE_117970_length_513_cov_251.713974_g88113_i0	513	**8.9**	**76.5**	3.14	0.02	No hit found					
NODE_23325_length_3097_cov_575.675050_g8166_i2	3097	**5.9**	**0.9**	-3.04	0.02	No hit found					
NODE_76596_length_980_cov_41.053039_g24662_i1	980	**8.0**	**92.7**	3.58	0.02	No hit found					
XP_022039188.1	884	**15.6**	**1.1**	-3.23	0.03	uncharacterized protein LOC110941822	*Helianthus annuus*	767	18%	3.00E-05	49
NODE_99096_length_716_cov_19.092044_g28299_i2	716	**15.7**	**0.1**	-6.52	0.03	No hit found					
R6999074	366	**0.0**	**533.2**	7.37	0.03	No hit found					
S6945940	862	**80.0**	**21.9**	-1.89	0.03	No hit found					
TRINITY_DN339059_c0_g1_i1	544	**21.3**	**1.1**	-3.91	0.03	No hit found					
XP_027235202.1	3737	**13.2**	**48.9**	2.02	0.04	uncharacterized protein LOC113826500	*Penaeus vannamei*	153	22%	3.00E-36	38
MPC34733.1	259	**54.4**	**224.1**	2.46	0.04	hypothetical protein	*Portunus trituberculatus*	41.2	47%	0.044	59
NODE_103412_length_682_cov_5.500824_g48640_i0	682	**62.6**	**13.2**	-2.19	0.04	No hit found					
NODE_26569_length_2829_cov_158.452796_g9616_i2	2829	**4.9**	**0.7**	-2.87	0.04	No hit found					
NODE_28518_length_2164_cov_367.324324_g16010_i0	2164	**3.6**	**16.5**	2.13	0.04	No hit found					
NODE_502969_length_209_cov_1.283582_g435863_i0	209	**0.4**	**35.9**	6.18	0.04	No hit found					

NODE_8232_length_4733_cov_29.782599_g4636_i0	4733	**22.9**	**5.7**	-1.94	0.04	No hit found					
R7035709	497	**122.6**	**50.1**	-4.26	0.04	No hit found					
S7197024	388	**0.0**	**33.2**	8.57	0.04	No hit found					
TRINITY_DN59791_c0_g1_i1	353	**1.0**	**20.7**	4.77	0.04	No hit found					
R7035758	3506	**17.7**	**3.4**	-2.23	0.05	No hit found					
S5322937	351	**41.6**	**5.5**	-4.02	0.05	No hit found					
Hepatopancreas - Males											
Detoxification											
XP_027227890.1	2713	**1.9**	**13.9**	5.6	8.09E-04	carboxylesterase 4A-like	*Penaeus vannamei*	803	69%	0	63
XP_027237166.1	1064	**16.2**	**45.5**	4.05	1.54E-03	thiopurine S-methyltransferase-like	*Penaeus vannamei*	209	49%	6.00E-62	56
XP_027234090.1	3060	**71.3**	**3.9**	-5.04	0.02	probable cytochrome P450 49a1	*Penaeus vannamei*	462	49%	1.00E-148	45
WP_140073978.1	875	**3.6**	**30.6**	2.91	0.03	glutathione S-transferase	*Vibrio parahaemolyticus*	99.8	36%	3.00E-21	56
Acute-phase response											
ADW08727.1	501	**5.1**	**60.3**	2.88	9.41E-03	C-type lectin-2	*Penaeus vannamei*	188	82%	4.00E-58	62
KU680795.1	3313	**1.2**	**7.8**	6.31	1.42E-03	anti-lipopolysaccharide factor ALF4	*Procambarus clarkii*	113	2%	6.00E-20	95
XP_027213496.1	1396	**9.5**	**31.9**	2.38	0.03	macrophage mannose receptor 1-like	*Penaeus vannamei*	365	50%	1.00E-81	54
Oxydative stress											
NWH79191.1	612	**70.1**	**154.7**	6.94	6.08E-08	AT5G2 synthase	*Piaya cayana*	62.8	14%	2.00E-09	100
AXR98457.1	1109	**133.0**	**30.9**	-2.6	0.05	heat shock protein 90 kDa	*Procambarus clarkii*	439	57%	1.00E-145	100
Lipid metabolism and energy balance											
ADP05225.1	961	**128.2**	**946.5**	4.16	1.18E-06	fatty acid-binding protein 1	*Eriocheir sinensis*	137	40%	2.00E-36	57
XP_019490731.1	397	**5.6**	**123.3**	7.94	1.59E-04	PREDICTED: digestive cysteine proteinase 3-like	*Hipposideros armiger*	49.3	16%	0.001	100
Transcription and translation											
ROT72679.1	695	**3.7**	**137.3**	5.2	1.77E-05	putative 60S ribosomal protein L18a-like	*Penaeus vannamei*	305	75%	3.00E-102	82
XP_027235487.1	721	**41.6**	**326.1**	3.71	8.63E-04	40S ribosomal protein S15Aa	*Penaeus vannamei*	257	54%	2.00E-84	94
XP_027210150.1	484	**6.4**	**59.0**	3.98	1.42E-03	RNA-binding protein squid-like isoform X1	*Penaeus vannamei*	48.9	22%	0.003	72

						transcription activator BRG1-like					
XP_027237837.1	1426	**11.5**	**1.0**	-4.02	4.57E-03	isoform X3	*Penaeus vannamei*	639	88%	0	83
Hemocyanin and pseudohemocyanins											
AFP23115.1	2598	**96.0**	**210.9**	3.9	1.99E-05	hemocyanin	*Cherax quadricarinatus*	1086	74%	0	80
Q6KF81.1	279	**21214.8**	**651.6**	-6.01	0.02	Pseudohemocyanin-2	*Homarus americanus*	44.7	25%	0.012	76
AFP23115.1	2322	**1.7**	**7.7**	3.94	0.02	hemocyanin	*Cherax quadricarinatus*	1049	83%	0	76
AFP23115.1	1300	**39.7**	**84.9**	2.67	0.04	hemocyanin	*Cherax quadricarinatus*	457	65%	3.00E-152	76
Other											
AYM45055.1	427	**16.1**	**303.2**	5.76	9.29E-11	putative endo-beta-1,4-mannase	*Gecarcoidea natalis*	63.5	24%	1.00E-08	83
AVD68958.1	395	**53.3**	**179.2**	3.91	7.26E-04	obstructor F	*Cherax quadricarinatus*	132	84%	6.00E-36	54
						LOW QUALITY PROTEIN: sodium					
XP_027226707.1	1337	**0.2**	**13.2**	5.27	1.90E-03	channel protein 60E-like	*Penaeus vannamei*	682	99%	0	75
Not identified											
XP_027229494.1	769	**1843.8**	**17.8**	-7.54	1.77E-05	uncharacterized protein LOC113821215	*Penaeus vannamei*	126	55%	3.00E-32	48
						uncharacterized protein LOC113810864					
XP_027218307.1	2234	**8.5**	**53.7**	8.5	1.19E-04	isoform X1	*Penaeus vannamei*	138	27%	2.00E-29	36
TRINITY_DN4790_c1_g1_i1	276	**21.8**	**116.0**	4.26	1.42E-03	No hit found					
R6997553	279	**393.9**	**1146.4**	12.55	1.49E-03	No hit found					
TRINITY_DN20048_c3_g2_i1	621	**7.5**	**28.3**	4.63	1.79E-03	No hit found					
TRINITY_DN11350_c0_g1_i1	374	**15.5**	**105.1**	2.67	6.07E-03	No hit found					
J7094195	357	**463.6**	**3021.8**	4.8	0.02	No hit found					
NODE_68088_length_892_cov_486.414576_g43566_i0	892	**10.9**	**70.6**	3.15	0.02	No hit found					
TRINITY_DN1960_c0_g1_i3	340	**49.4**	**7.6**	-3.38	0.03	No hit found					
TRINITY_DN2373_c4_g1_i1	212	**72.3**	**1.5**	-6.11	0.03	No hit found					

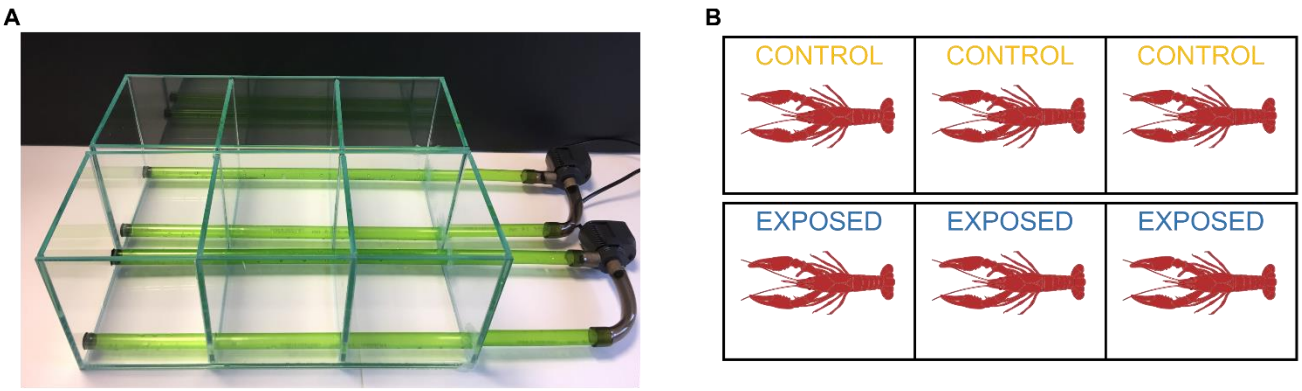

Figure A1. Experimental tanks (A) and a summary diagram of the experimental design (B).

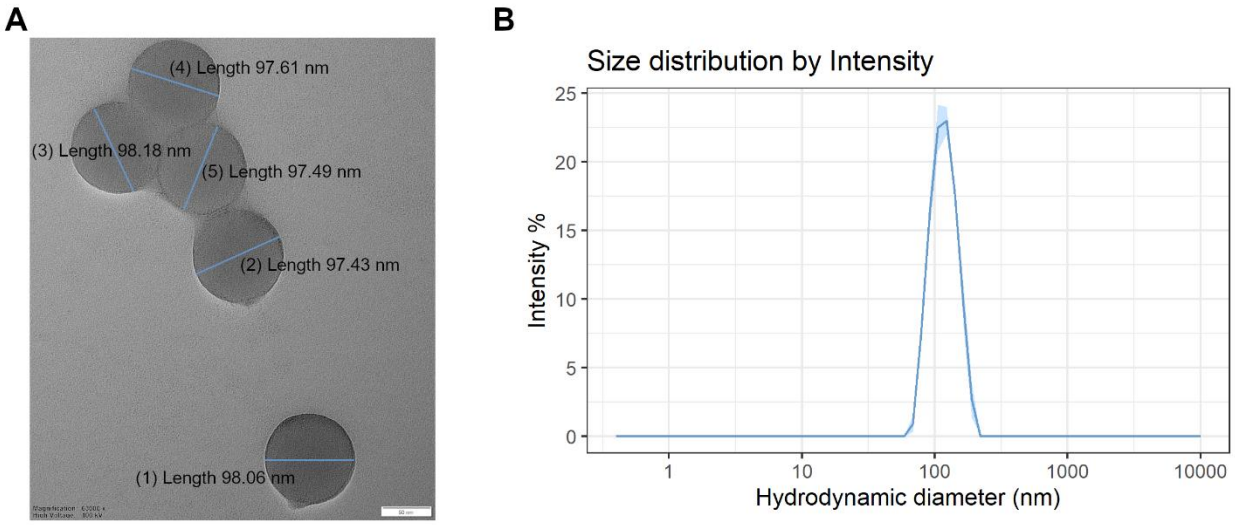

Figure A2. Transmission electron microscopy of pristine NPs in MilliQ water (A) (Scale bar = 50 nm). Dynamic light scattering analysis of NP particles (B). Intensity-weighted particle size distribution is reported as the average value of three measurements (blue line) and standard deviation interval (light blue area) for suspensions in MilliQ water at a concentration of 2 mg/L.

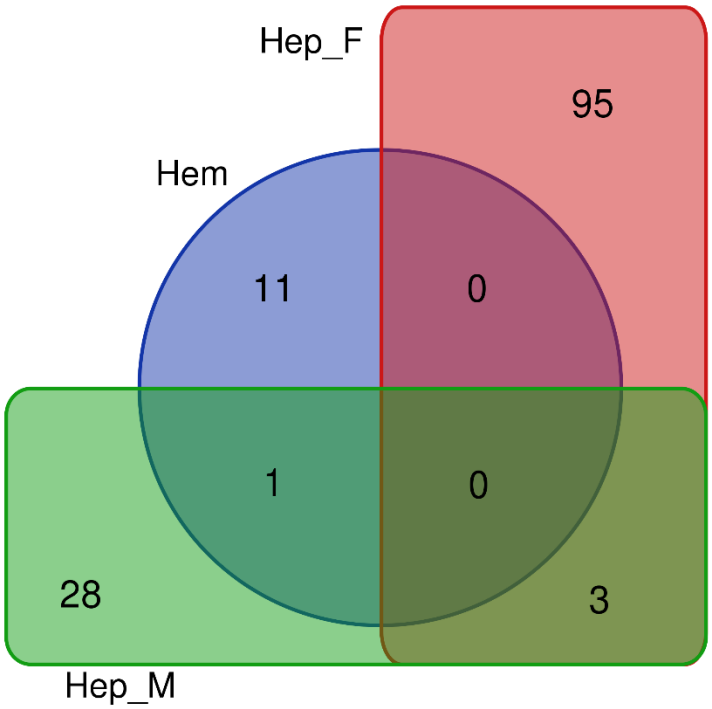

Figure A3. Venn diagram summarizing the overlap between differentially expressed genes in the three groups of samples analyzed: Hem = male hemocytes; Hep_M = male hepatopancreas; Hep_F = female hepatopancreas.

Supplementary material to Chapter 3

Table B1. Summary of the Illumina sequencing output and mapping results for *Mytilus galloprovincialis* trocophora larvae.

	Ra reads		Trimmed reads						Filtered reads		Mapped reads
Sample	**No. read pairs (M)**	**Avg. length**	**Number of reads (M)**	**Avg. length**	**% GC content**	**Q20**	**Q30**	**% retained sequences**	**Number of reads (M)**	**% retained sequences**	**% mapped reads**
C1	31.82	147	30.80	126	40.7	96.2	90.2	96.8	25.61	83.2	69.9
C2	40.50	149	39.60	127	40.7	96.4	90.7	97.8	32.41	81.9	69.6
C3	57.60	149	56.15	127	40.5	96.3	90.5	97.5	46.09	82.1	69.4
C4	19.86	146	18.94	126	42.6	96.6	91	95.4	14.76	78.0	64.3
NP1	58.60	148	56.79	126	42.3	96.7	91.2	96.9	43.95	77.4	65.1
NP2	30.62	148	29.79	126	41.1	96.3	90.4	97.3	24.56	82.5	69.6
NP3	43.61	133.5	36.66	123	42.0	96.3	90.6	84.1	31.11	84.9	69.0
NP4	167.07	147	160.68	126.5	40.5	96.3	90.3	96.2	134.41	83.7	71.0

Abbreviations: NP, nanoplastic-exposed group; C: control group; M: million; Q20 or Q30, percentage of bases with Phred quality score ≥ 20 or ≥ 30; % GC, percentage of G and C in clean bases.

Table B2: Comparison of putative transcriptomes assembly statistics.

Length filtering	Percentile	No. sequences	C	F	M	Total annotated seq. (No.)	Annotated seq. (%)	UniProtKB annotated seq. (No.)	Avg Length discarded (bp)	Median length discarded (bp)
Not filtered	0	292234	92.1	7.3	0.6	88970	30.4	63768		
	1	232542	92.1	7.2	0.7	64675	27.8	41750	234.7	216
	2	201003	92	7	1	59323	29.5	38067	240.29	221
	3	175477	92	6.9	1.1	55008	31.3	35277	247.13	227
	4	153690	91.9	6.5	1.6	51362	33.4	33118	254.34	233
	5	134499	91.8	6.4	1.8	47823	35.6	31087	262.34	238
	6	117527	91.6	6.2	2.2	44501	37.9	29221	270.79	243
	7	102204	91.6	5.7	2.7	41245	40.4	27395	280.22	248
	8	88445	90.7	5.1	4.2	37898	42.8	25482	290.66	253
	9	76060	89.8	5.2	5	34636	45.5	23610	302.17	258
	10	65340	88.6	4.9	6.5	31705	48.5	21956	313.63	262
Filtered > 250 bp	0	189022	92.1	7.2	0.7	63760	33.7	43164		
	1	164809	92	7	1	54114	32.8	34807	310.6	277
	2	150224	91.9	6.9	1.2	50924	33.9	32609	312.03	283
	3	138149	91.9	6.6	1.5	48420	35.0	31098	316.23	287
	4	127384	91.9	6.4	1.7	46183	36.3	29820	321.86	293
	5	117887	91.6	6.3	2.1	44230	37.5	28767	327.24	297
	6	109116	91.5	6.3	2.2	42280	38.7	27665	333.49	302
	7	101087	91.5	5.9	2.6	40491	40.1	26688	340.12	306
	8	95573	91.2	5.5	3.3	38702	40.5	25671	347.36	311
	9	86537	90.7	5.2	4.1	36931	42.7	24688	355.06	315
	10	80056	90.3	5.3	4.4	35276	44.1	23723	362.82	320

Abbreviations: bp: base pairs; C: Complete BUSCOs; F: Fragmented BUSCOs; M: Missing BUSCO